INTERAGENCY REPORT: ASTROGEOLOGY 59

GEOLOGIC MAPS AND TERRAIN ANALYSIS DATA FOR VIKING MARS '75 LANDING SITES CONSIDERED IN DECEMBER 1972

By

Harold Masursky and Mary H. Strobell

With geologic maps and terrain analysis data by:
M. H. Carr, G. W. Colton, C. A. Hodges, Harold Masursky, J. F. McCauley
C. E. Mayer, D. J. Milton, H. J. Moore, E. C. Morris, T. A. Mutch,
J. T. O'Connor, R. J. Pike, R. S. Saunders, D. H. Scott,
D. E. Stuart-Alexander, N. J. Trask, A. S. Walker, M. N. West,
and D. E. Wilhelms

Prepared under NASA contract L-55232

CONTENTS

	Page
Introduction	1
Section I. Geologic Maps	
Index map of Viking 75 landing sites	3
Quadrangle maps - scale 1:5,000,000	
Amazonis	5
Lunae Palus	7
Oxia Palus	9
Amenthes	11
Memnonia	13
Margaritifer Sinus	15
Mare Tyrrhenum	17
Aeolis	19
Landing site maps - scale 1:1,000,000 and 1:250,000	
Eumenides region, site 1	21
Chryse region, site 3	25
Uraniae region, site 4	29
Candor region, site 5	33
Amazonis region, site 7	37
Zephyria region, site 8	41
Memnonia region, site 9	45
Aquae Apollinares region, site 10	49
Hesperia ("Dandelion") region, site 12	53
Appendix I. Viking site selection rationale	54
Section II. Terrain Analysis Data	
Part 1. Slope analysis of the Martial equatorial belt at 30km resolution, by Richard J. Pike	55
Part 2. Infrared characterization of Martian surface, by Joseph T. O'Connor	62
Part 3. Fine-scale topography and near-surface materials of Mars by Henry J. Moore	65
Part 4. Correlations of selected B-frame photographs with Haystack radar data, 1971, by Carroll A. Hodges	71
Part 5. Summary of elevation data on candidate landing sites	72

ILLUSTRATIONS

		Page
Section II, Part 1		
Figure 1.	Index map of topographic profiles showing seven classes of terrain roughness	57
2.	Scatter diagram of terrain profiles	58
3.	Representative topographic profiles of Mars	58
4.	Relation between slope angle and slope length for three planets	58
Section II, Part 2		
Figure 1.	Minnaert plots of Martian infrared reflectivities for various geologic units	64
2.	Minnaert plots of Martian infrared reflectivity of selected terrestrial materials	64
Section II, Part 3		
Figure 1.	Slope-frequency distributions with estimated algebraic standard deviations of 2, 3, 4, 6, 8, and 10 degrees	68
2.	Probability of success or failure as a function of estimated algebraic standard deviation of slope	68
3.	Penetration of Viking Lander in lunar nominal soil	68
4.	Correlation of Mars radar rms slope with the various Martian terrain units	69
5.	Correlation of Mars radar dielectric constant values with the various Martian terrain units	69
Section II, Part 1		
Table 1.	Martian slope statistics at 30 km resolution	59
2.	Summary data on seven relative-roughness classes of Martian terrain	61
3.	Distribution of dispersion coefficient for slopes from 104 Martian topographic profiles	61
Section II, Part 2		
Table 1.	Infrared reflectivity properties for Martian geologic units and terrestrial laboratory materials	64
Section II, Part 3		
Table 1.	Haystack radar estimates of Viking Landing Sites	70

INTRODUCTION

This report presents a brief recapitulation of the work done prior to December 1972 by members of the Branch of Astrogeologic Studies in support of the project, Viking Site Investigations, funded by NASA's Viking Project Office, Langley Research Center, Hampton, Virginia, under NASA Contract L-55232, project chief, Harold Masursky.

G. W. Colton, C. A. Hodges, Harold Masursky, J. F. McCauley, C. E. Meyer, D. J. Milton, E. C. Morris, D. H. Scott, D. E. Stuart-Alexander, N. J. Trask, A. S. Walker, M. N. West, and D. E. Wilhelms of the Geological Survey, T. A. Mutch of Brown University, and R. S. Saunders of Jet Propulsion Laboratory, compiled geologic maps; H. J. Moore, J. T. O'Connor and R. J. Pike of the Geological Survey prepared terrain analyses data. Jet Propulsion Laboratory's Image Processing Laboratory prepared rectified and scaled (R&S) photographs which were used by the Geological Survey's Cartography Unit, under the direction of R. M. Batson, to prepare photomosaics. The Geological Survey's Illustrations unit, under the direction of J. W. VanDivier, and its drafting unit, under the direction of R. D. Carroll then completed these base maps and drafted the geologic maps.

The bulk of the report (Section I) consists of geologic maps prepared of nine of the candidate landing sites. Each map has an explanation showing the geologic/terrain units recognized and mapped, and most have brief geologic summaries of the geologic evolution of the site. Eight are quadrangle maps, scale 1:5 million; nine of the maps are at 1:1 million scale; and eight are at scale 1:250,000. Section II contains brief resumes of work done on remote sensing data and slope analysis pertinent to evaluating and comparing the terrain properties of the various sites.

Work done during the sixties on the Moon on projects Ranger, Surveyor, Lunar Orbiter, and Apollo proved that topographic and geologic maps are valuable both as an aid in site selection and, later as a tool during the mission operations stage, and the post-mission data reduction and analysis stages. The Viking Project Office, recognizing a need for similar maps for the Viking Mars landings, asked the Geological Survey to prepare cartographic and geologic maps and terrain analysis data to aid in site selection for the 1976 Mars landings.

Under the chairmanship of Harold Masursky, the team of geologists listed above selected several areas which were available to the spacecraft, safe for the lander, and scientifically interesting. Maps of eight quadrangles, at a scale of 1:5,000,000, which included these areas, were compiled by September 1972. From these maps and other data, ten preliminary candidate sites were selected by the Viking Landing Site Working Group and the Science Steering Group. Two of these sites, 2 and 6, were subsequently dropped from consideration and no site maps were prepared of them.

In late October geologists were assigned to prepare maps of the eight remaining sites at a scale of 1:1,000,000 which included the possible landing ellipses. Early in November another site, Hesperia (informally called "the Dandelion" during the Mariner mission) was added and a 1:1,000,000 scale map was prepared of the site. By mid-November, work was started on geologic maps, at a scale of 1:250,000, of small areas where high resolution Mariner 9 photographs had been taken within the 1:1 million scale maps and which included the selected landing ellipses. Site 12, Hesperia, was dropped, and no larger scale map of the area was prepared.

All the geologic and photobase maps were prepared, and two "scenarios" designating proposed prime and backup landing sites, were developed by discussions among the mappers. The maps and "scenarios" were presented by Harold Masursky at the Orlando meeting of the Landing Site Working Group held on December 4, 1972. H. J. Moore and M. H. Carr of the Geological Survey also served on the Working Group. The Working Group approved the choice of Chryse (Site 3) as the prime site for the A mission and tentatively chose Memnonia (Site 9) as the prime B site.

At this meeting the Landing Site Working Group and Science Steering Group recognized the possibility that concentrations of organic material and possible life forms might be found at the margins of the ice cap or in the intermediate latitudes where atmospheric water is at its maximum during the season when Viking will land on Mars. An additional group of candidate sites in these regions were chosen by the Working Group and Science Steering Group; these sites will be discussed in Interagency Report 60. Later the necessity for a "super safe" site was recognized--that is, one with Mariner 9 photographic coverage and recent (1971 or later) radar coverage. These sites were tentatively selected and detailed radar coverage during 1975-1976 was planned. These sites will be described in a later report.

Geologic maps and the accompanying photomosaics of the two sites favored by the Geological Survey, Chryse (Site 3) and Aquae Appolinares (Site 10) were placed on open file by the Geological Survey on January 29, 1973 ("open file" indicates that maps are available for examination at certain government facilities and copies can be ordered). Other maps prepared for this initial work on candidate Viking Landing Sites, including Memnonia (Site 9), the Science Steering Group's initial choice for the prime B site, were open-filed by the Survey on November 12, 1973; semi-controlled mosaics and individual photographs accompanying the geologic maps were open-filed at the same time.

Geologists who prepared the maps in this report were working against very tight deadlines, so the maps were not thoroughly edited. Therefore some minor discrepancies occur between the maps and their accompanying texts. Since the maps have been reduced for this report, the scale bar on each map represents the reduced, rather than the original scales (1:5 million, 1:1 million, and 1:250,000) are shown in the explanatory material.

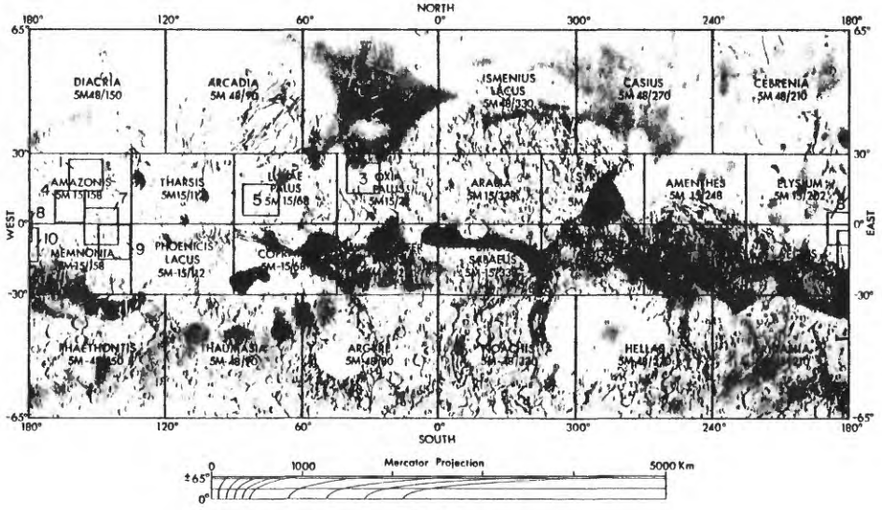

MARS

FIGURE 1 - INDEX MAP OF VIKING '75 LANDING SITES

PRELIMINARY GEOLOGIC MAP OF THE AMAZONIS QUADRANGLE
(MC-8) OF MARS

By Elliot C. Morris

September 1972

EXPLANATION

vs
Volcanic shield

The flank deposits of the very large constructional feature, Nix Olympica. This material forms rough concave slopes that become convex near the summit. The shield is capped by a caldera. The surface of the unit is made up of many narrow elongate ridges, roughly radial to the central caldera. A peripheral escarpment surrounds the unit at its outer edge.

sp
Smooth plains

The most extensive unit is the smooth plains. At A-camera resolution the unit shows little or no textural detail except for a few small craters and complex light and dark streaks, many of which appear to emanate from craters. The unit generally lies in large depressions and appears to overlap and bury some older units.

Spr, Smooth plains, ridged: A subunit, showing multiple lobate scarps, furrows and ridges; the furrows and ridges appear somewhat subdued in A-camera pictures.

gt
Grooved terrain

The unit surrounds Nix Olympica and appears to be related to this large volcanic shield. The grooved terrain consists largely of closely spaced low ridges and intervening linear troughs, apparently faulted along arcuate fractures and tilted gently to northeast. The ridges and troughs become more subdued westward and appear to be buried by the smooth plains unit (unit sp).

mc
Moderately cratered terrain

Contains widely spaced craters not exceeding 100 km in diameter; intercrater areas are undulating and non-distinctive.

kt
Knobby terrain

Knobby terrain consists of closely packed, small, sharp-appearing peaks. Some peaks are embayed by plains material and others are superposed on the plains. Some knobby terrain forms circular pattern which suggest buried rim deposits of old craters.

Craters

c_2
Younger craters

Younger craters are characterized principally by the preservation of a surrounding ejecta blanket. Small craters whose ejecta blankets are not recognizable at the map resolution are indicated as c_2 in order to show frequency of craters on the smooth plains unit.

c_1
Older craters

Older craters are severely degraded, lack recognizable ejecta blankets, and are generally shallower than c_2 craters.

AMAZONIS QUADRANGLE OF MARS
SCALE 1:5,000,000
BY E. C. MORRIS

EXPLANATION

- sp — Smooth plains material
- spr — Smooth plains material, ridged
- ce — Crater ejecta
- c_2 — Younger crater material
- vs — Volcanic shield material
- gt — Grooved material
- c_1 — Older crater material
- mc — Moderately cratered material
- kt — Knobby material

Contact
dashed where approximate

Fault

Graben

Scarp

Ridge

30° 0° 0 500 1000 km

SCALE 1:10,000,000 AT 0° LATITUDE
MERCATOR PROJECTION

PRELIMINARY GEOLOGIC MAP OF THE LUNAE PALUS QUADRANGLE
(MC-10) OF MARS
By Daniel J. Milton
September 1972

EXPLANATION

Volcanic dome
Large construct with single summit caldera.

P_4

Youngest plains and channels of aqueous erosion. Probably primarily aggradational. B-frames near channel junction show smooth surface with wind streaks.

P_3

Pediplain

Surface of planation. Probably primarily denudational, at least in the west. B-frame near 17°N, 76°W shows wind-etched, jointed bedrock.

P_2

Modified volcanic plains

B-frames show multiple surfaces separated by low scarps with angular digitations. Probably a series of volcanic flows eroded so as to destroy most old craters (10-km range) visible in volcanic plains. A primarily erosional topography, with bedrock control by the volcanic flows has been produced. Local relief probably greater than volcanic plain.

P_1

Volcanic plains

B-frames show mare-like ridges. Topography appears to consist of primary volcanic forms and superposed impact craters not greatly modified by erosion. May be lunar mare-like surface with some sort of regolith.

C_2

Modified cratered terrain

Large craters are generally level-rimmed. Intercrater areas may be occupied by younger deposits (volcanic?) and some craters may be collapse features over the site of buried impact craters.

C_1

Cratered terrain

Abundant rough-rimmed craters in the 50-km diameter range. Probably equivalent to the cratered lunar terra.

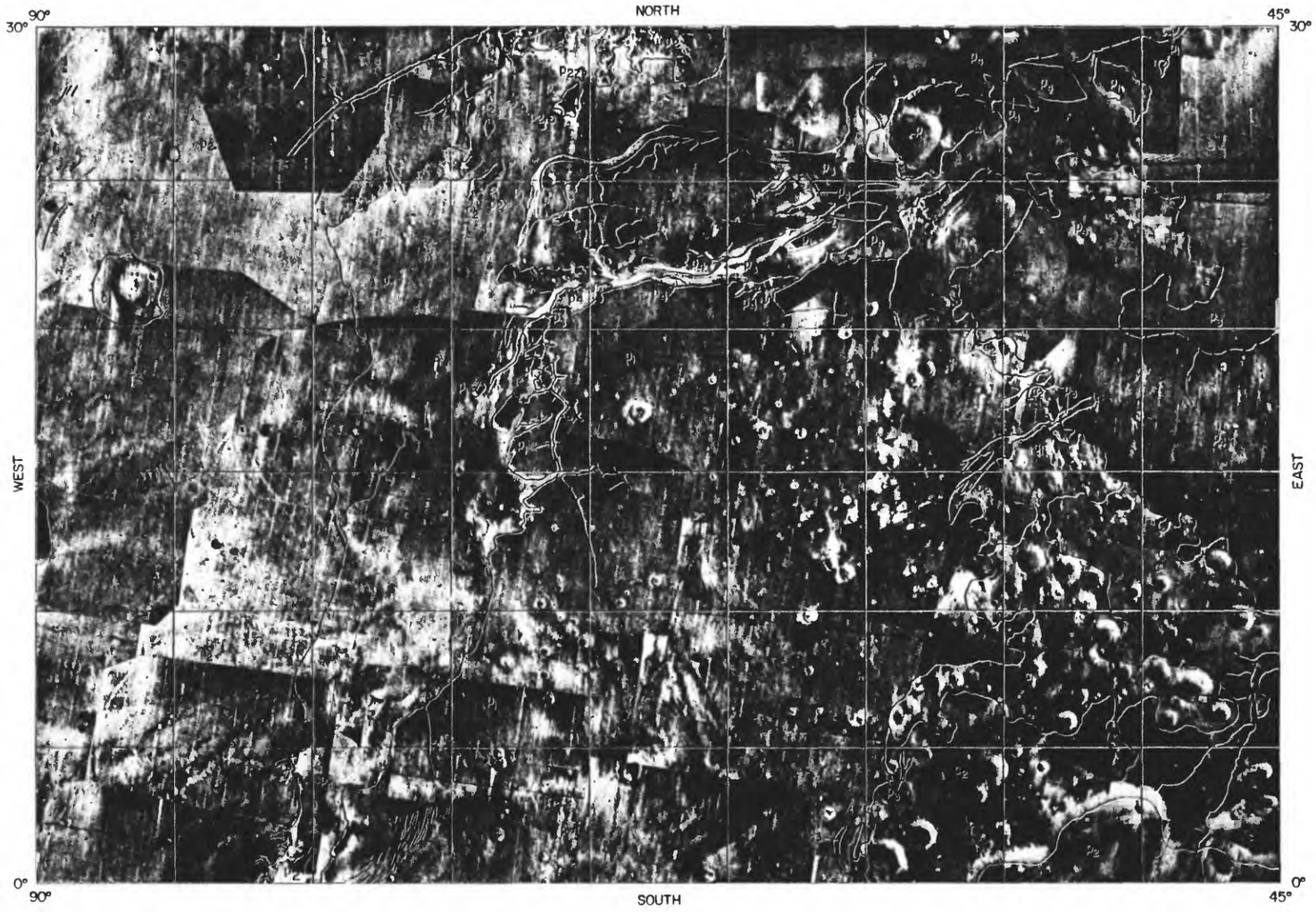

30° 0 500 1000 km
0°

SCALE 1:10,000,000 AT 0° LATITUDE

MERCATOR PROJECTION

LUNAE PALUS QUADRANGLE OF MARS

SCALE 1:5,000,000

BY D.J. MILTON

EXPLANATION

vd	Volcanic dome
p_4	Youngest plain (mostly gradational) and aqueous channels
p_3	Plain (primarily erosional and deposional forms)
p_2	Plain (primarily eroded volcanic? forms)
p_1	Plain (volcanic forms mostly preserved)
c_2	Cratered terrain, modified by volcanics (?)
c_1	Cratered terrain

Contact

Fault

Scarp

Lineament

PRELIMINARY GEOLOGIC MAP OF THE OXIA PALUS QUADRANGLE
(MC-11) OF MARS
By Don E. Wilhelms and John F. McCauley
September 1972

GEOLOGIC HISTORY AND STRATIGRAPHY

Geologic history began with a Moon-like episode of impact that produced craters and, at least in other regions, basins (units c_1 and dc). These impact materials were then partly or completely covered by layered deposits that form a plateau (unit pl). The plateau materials were subsequently fractured and rifted apart as part of the tensional episode that created the huge Martian canyon system. Accompanying or following this disruption, water in massive amounts was apparently released from the plateau materials, especially those which became chaotically broken up and rotated (unit ch and possibly unit h). This suggests that the plateau materials either included layers of ice or were permeated by ice. The resulting flood or floods eroded channels and carried away the fractured and chaotic plateau materials (and materials of old craters covered by and interbedded with them). Sediment from the muddy flood waters was deposited in the channels and at their mouths (units cb_1, cb_2, and cs). Some of these sediments reached the northwestern part of the quadrangle, either to become or to merge with the extensive plains deposits there (units sp and hp).

Channeling and sedimentation apparently occurred repeatedly. At least two episodes are indicated by the transection of a discontinuous and apparently older set of braided channel deposits (cb_1) by a fresher, continuous, and apparently younger set that occurs in the deepest channels (unit cb_2). Moreover, each of these braided units probably includes sediments of several ages. A third channel unit, which is smooth or shows only traces of braids at A-frame resolution, is younger than either of the braided units, though perhaps it is a facies of them that is only marginally younger. The hummocky unit (h) may be an old chaotic unit that formed during an earlier episode of rifting and flooding. Traces of layers with suggestions of braided channel morphology are present in the plateau materials. This complexity suggests that water-laid sediment could be the dominant material in this part of Mars.

PROPOSED LANDING SITES

This history suggests that the Viking landings should take place on the channel deposits, which are the most likely to contain water and therefore to support life. As the braided deposits are both too rough and too small in area, the smooth channel deposits (unit cs) should be the landing target. No one area of these deposits is geologically preferred over the others; operational factors can select the exact landing area.

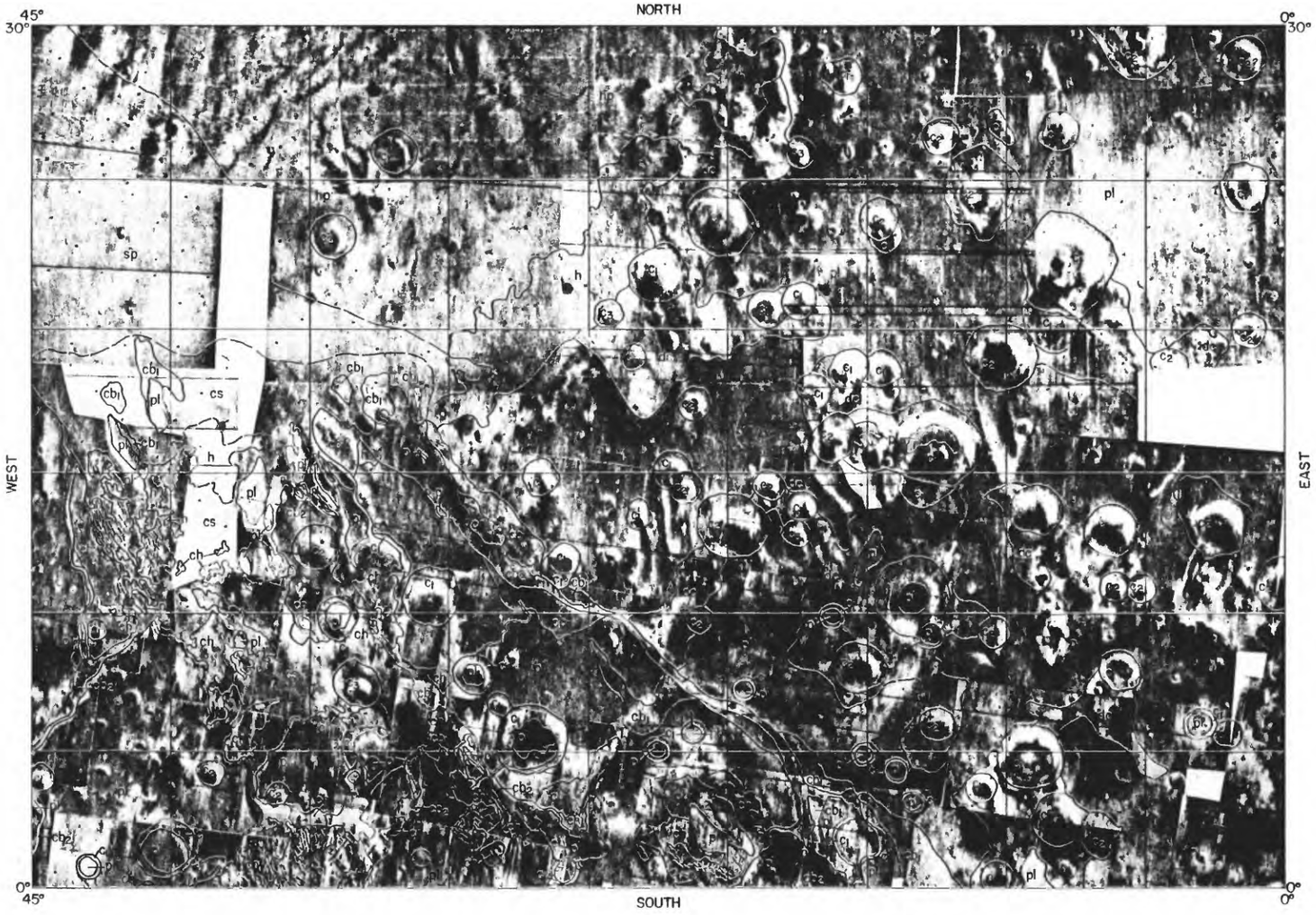

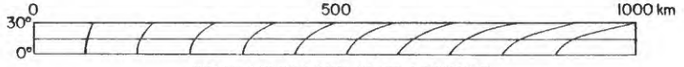

SCALE 1:10,000,000 AT 0° LATITUDE
MERCATOR PROJECTION

OXIA PALUS QUADRANGLE MARS
Scale 1:5,000,000
DON E. WILHELMS AND JOHN F. McCAULEY

EXPLANATION

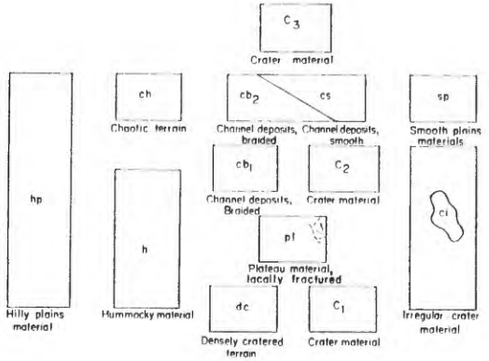

Contact
Dashed where very approximate

Narrow fracture

Narrow channel

PRELIMINARY GEOLOGIC MAP OF THE AMENTHES QUADRANGLE
(MC-14) OF MARS
By Desiree E. Stuart-Alexander
September 1972

GEOLOGY

Quadrangle MC-14 borders the Libya basin on the west and the higher Elysium plains on the east. Several material units can be defined, but the relative ages of several of these are still quite tentative. The mountainous material (unit mt) is interpreted as being related to the formation of the Libya basin and analogous to the rugged mountains that form the outer ring of lunar basins. The lower, lineated terrain (unit l) may be a less rugged, more highly sculptured facies of the mountains or else it may be a degraded, and therefore younger, version of the mountains. The belt of parallel grabens occurs in or near the lineated unit and is essentially concentric to the basin. Therefore the grabens are interpreted as being related to the basin, even though their present expression is relatively young, since they cut some terrain that is clearly post basin. The moderately cratered terrain (unit c) is an enigmatic unit because its craters all appear to be more subdued and therefore older than those that are superposed on the mountainous material. Yet the cratered terrain embays and fills some of the intermountain areas, suggesting that the cratered terrain is younger than the rugged mountains. If this relation is true, then the craters are being subdued by some type of depositional material that is covering the region and giving a spurious age to the craters. In contrast, the hummocky material (unit h) is an erosional unit that appears to be formed by degradation of the lineated and cratered units, and possibly also by materials derived from the mountainous terrain. Scattered throughout all units are areas of valley fill called plains material (unit p). The main distinction between this material and the cratered plains (unit pc) is that the latter seems to be more highly cratered and to have more remnants of hummocky terrain. In the remainder of the quadrangle, essentially the northern half, the author feels that the ground was not being seen. However, it was evident that there are some valleys and plateaus (unit vp), even though their surface roughness could not be ascertained. Also, the uncolored area, mapped with a question mark, seems to be primarily plains materials of varying types. Some of the extended mission B-frames show areas that resemble giant mud cracks; others are very smooth; still others are highly textured on a relatively fine scale. Craters are relatively scarce. This area is interpreted as mainly alluvial plains.

EXPLANATION

p
Plains
Relatively smooth valley fills.

?
Plains of various sorts
Probably only minor areas are really smooth; small, scattered craters visible.

pc
Cratered plains
More highly cratered than other plains units; scattered small hummocks and minor areas of other textures.

vp
Light valley and dark plateaus
Surface textures uncertain.

c
Cratered terrain
Most intercrater areas are irregularly textured.

h
Hummocky or pimply terrain
Grades into lineated terrain.

lt
Lineated terrain
Textured; positive relief with incipient gullying.

mt
Mountains
Forms scattered large, rugged hills. Related in position to Libya basin.

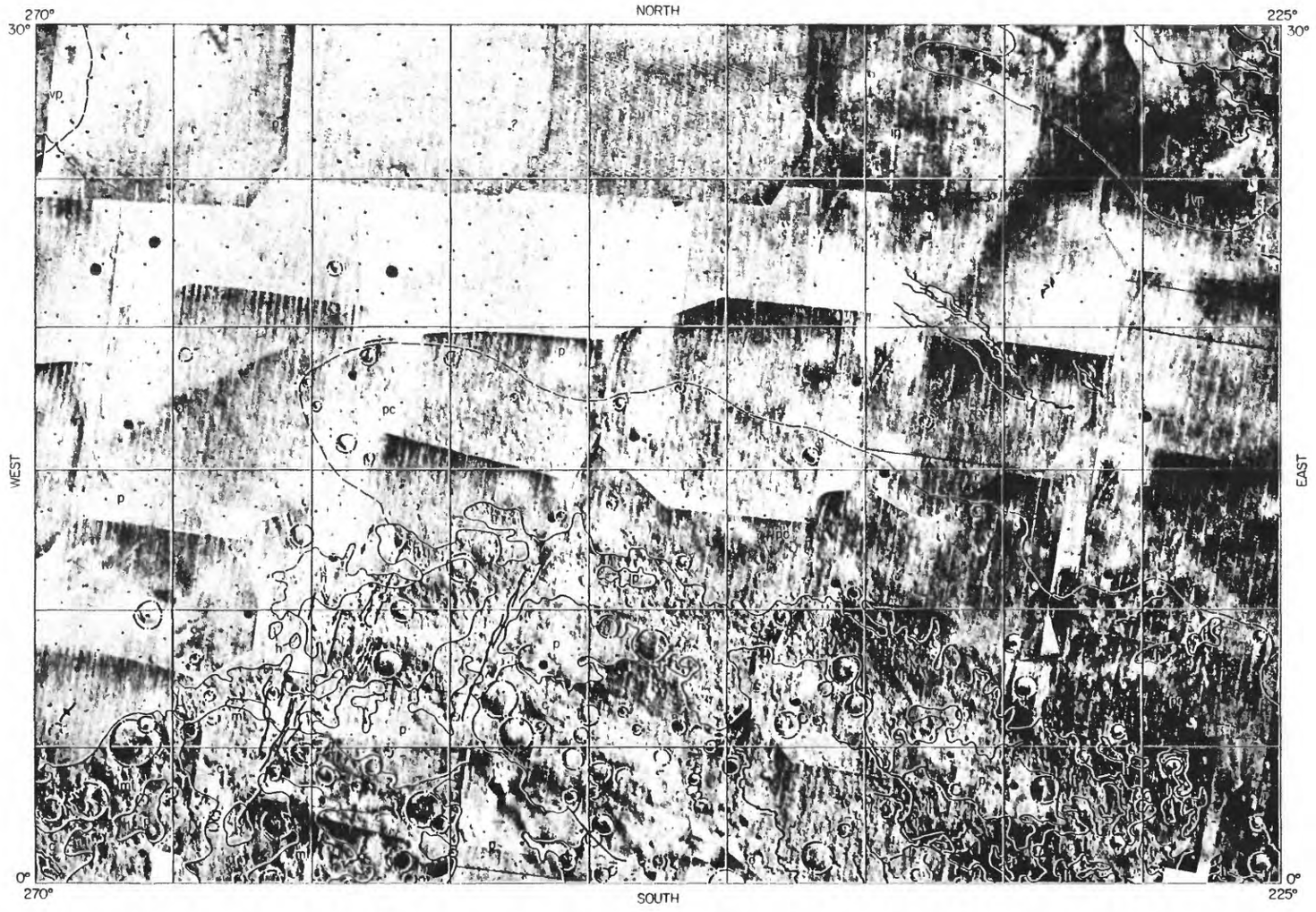

30° 0 500 1000 km
0°

SCALE 1:10,000,000 AT 0° LATITUDE
MERCATOR PROJECTION

AMENTHES QUADRANGLE, MARS

SCALE 1:5,000,000

BY DESIREE E. STUART-ALEXANDER

EXPLANATION

- vp — Valleys and plateaus
- ? — Uncertain plains
- p — Plains
- pc — Plains, cratered
- c — Cratered terrain
- h — Hummocky
- l — Lineated
- mt — Mountainous

Contact
dashed where approximate

Fault

Graben

Scarp

Ridge

Buried rim crest

 (no of page 12)

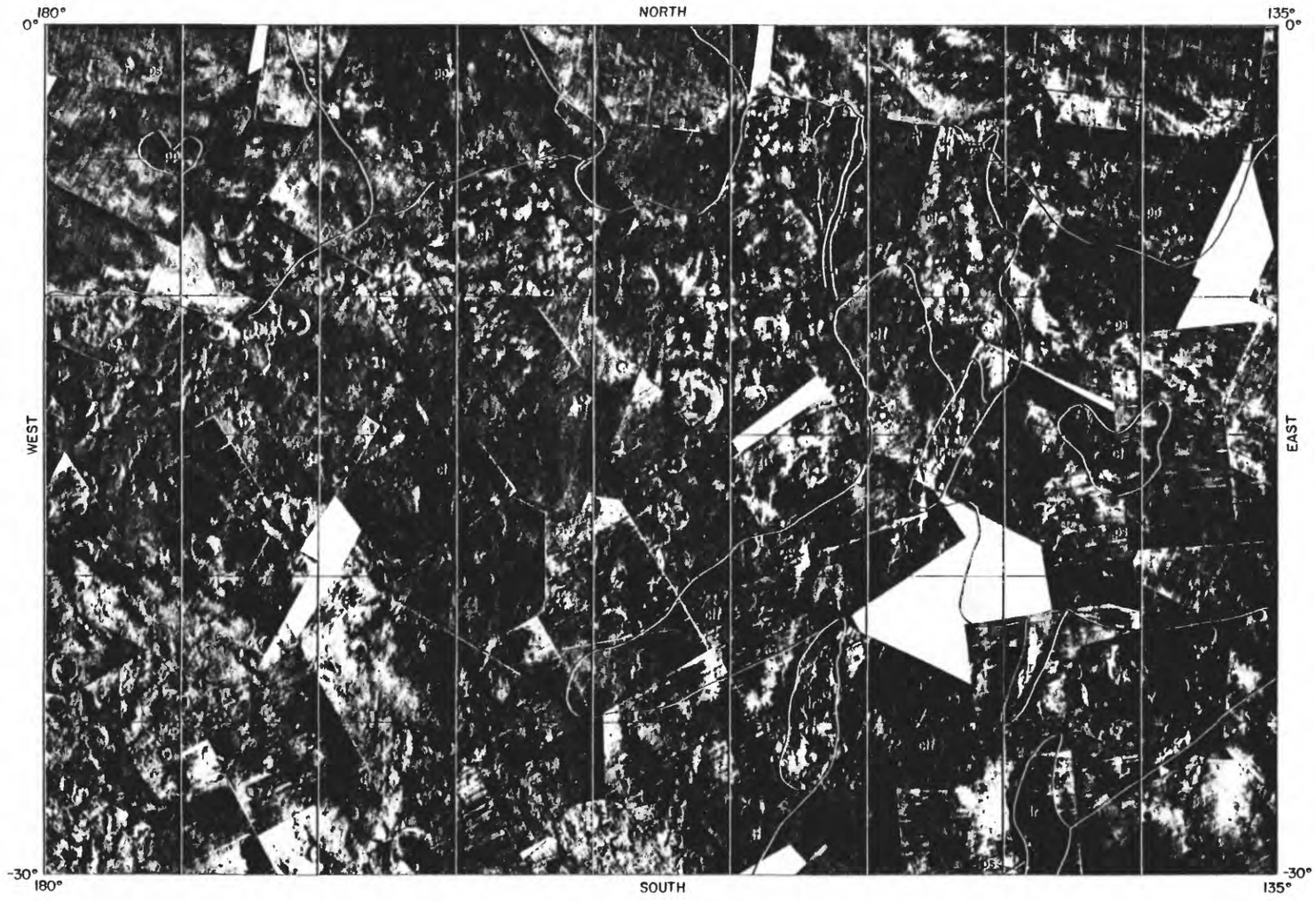

MEMNONIA QUADRANGLE MARS

Scale 1:5,000,000

T. MUTCH

EXPLANATION

ctf	Flat cratered terrain
ct	Cratered terrain
ir	Irregular terrain
ps	Smooth plains
pp	Patterned plains

Contact

Trough

0°
-30°
0
500
1000 km

SCALE 1:10,000,000 AT 0° LATITUDE
MERCATOR PROJECTION

PRELIMINARY GEOLOGIC MAP OF THE MARGARITIFER SINUS QUADRANGLE (MC-19) OF MARS

By R. Steven Saunders

September 1972

INTRODUCTION

This is a generalized geologic map of the Margaritifer Sinus quadrangle, MC-19, prepared in support of Viking landing site selection. The quadrangle contains some extremely rugged, scarp-bounded terrain photographed by the Mariner Mars 1969 mission and termed chaotic terrain by the MM 69 Television Experiment Team. The rest of the quadrangle is in a moderately cratered region. Much of the intercrater terrain is relatively smooth and planar at A-frame resolution (<1 km). This map utilizes the geologic unit terminology adopted for the "Preliminary Geologic Map of the Equatorial Region of Mars" prepared by John F. McCauley (McCauley and others, 1972). An important source used in the compilation of the present map was the report of the Viking Data Analysis Team containing topographic, radar, and terrain data.

PROPOSED LANDING SITE

A candidate landing site in this quadrangle was selected in the moderately cratered region centered at 13°S and 33°W. The geologic interest here is the possibility of sampling a region of Mars underlain by ancient crustal materials. The proposed site is near a large expanse of "chaotic terrain," an extremely rugged surface of unknown origin. Many of the largest sinuous channels on Mars appear to originate in chaotic terrain suggesting, if the channels are fluvial, that ground water or ice may play a role in the formation of chaotic terrain. The implication is that, at present, the most favorable site for a continuing source of moisture is in those areas bounding the chaotic terrain, particularly the smooth floors adjacent to the scarp walls.

A corollary to the ground water or permafrost model for chaotic terrain formation is that the wettest period in Martian history antedates the major volcanic episodes. The volcanics are not channeled or furrowed as is the cratered terrain. Volcanic action may melt large quantities of ice in the regolith and, if enough water is released, create a temporary humid condition; however, most of the water on Mars must have been released and trapped out at an early time. Thus (1) the most ancient rocks may record events or even life dating back to a more humid period shortly after accretion, and (2) the most ancient rocks are more likely to contain trapped ice than are the younger volcanic materials and therefore may be continually releasing water.

EXPLANATION

mc

Moderately cratered terrain

Contains superposed craters whose rim materials extend outward for 200 km or more. Intercrater areas are smooth at A-frame resolution (1-3 km). Unit contains abundant scarps, ridges, grabens, and sinuous channels. Also contains eroded remnants of ancient craters (unit mt) and eroded or obscured "ghost" craters. Interpretation: Complex regolith 1 km or more thick, mantled by eolian deposits, with local fluvial and volcanic deposits.

mt

Mountainous terrain

Generally linear subdued massifs, typically 20 by 100 km. Interpretation: Most are probably eroded remnants of destroyed crater rims.

ch

Channel and canyon deposits

Smooth to rugged, intricately channeled material of canyon floors and large sinuous channels. Smooth appearance may be in part owing to surface obscuration near end of dust storm. Interpretation: Alluvial deposits in surface drainage channels. Some appear to be fluvial streams whereas others may result from sudden release of ground water.

ct

Chaotic terrain

Rugged to rounded hills on canyon floors, and fault-bounded angular blocks in scarp-bounded depressions. The material classified as chaotic terrain is structurally gradational with cratered terrain (unit mc) where faulting and slumping have resulted in reorientation of individual blocks of adjoining cratered terrain. Interpretation: Produced by tectonic activity such as the formation of broad graben. Permafrost removal may account for the apparently continual mass wasting at the margins of the chaotic terrain.

c

Crater materials

Material within raised part of crater rim. Includes rim, wall, and floor materials. Interpretation: By analogy with the Moon, most are inferred to be of impact origin.

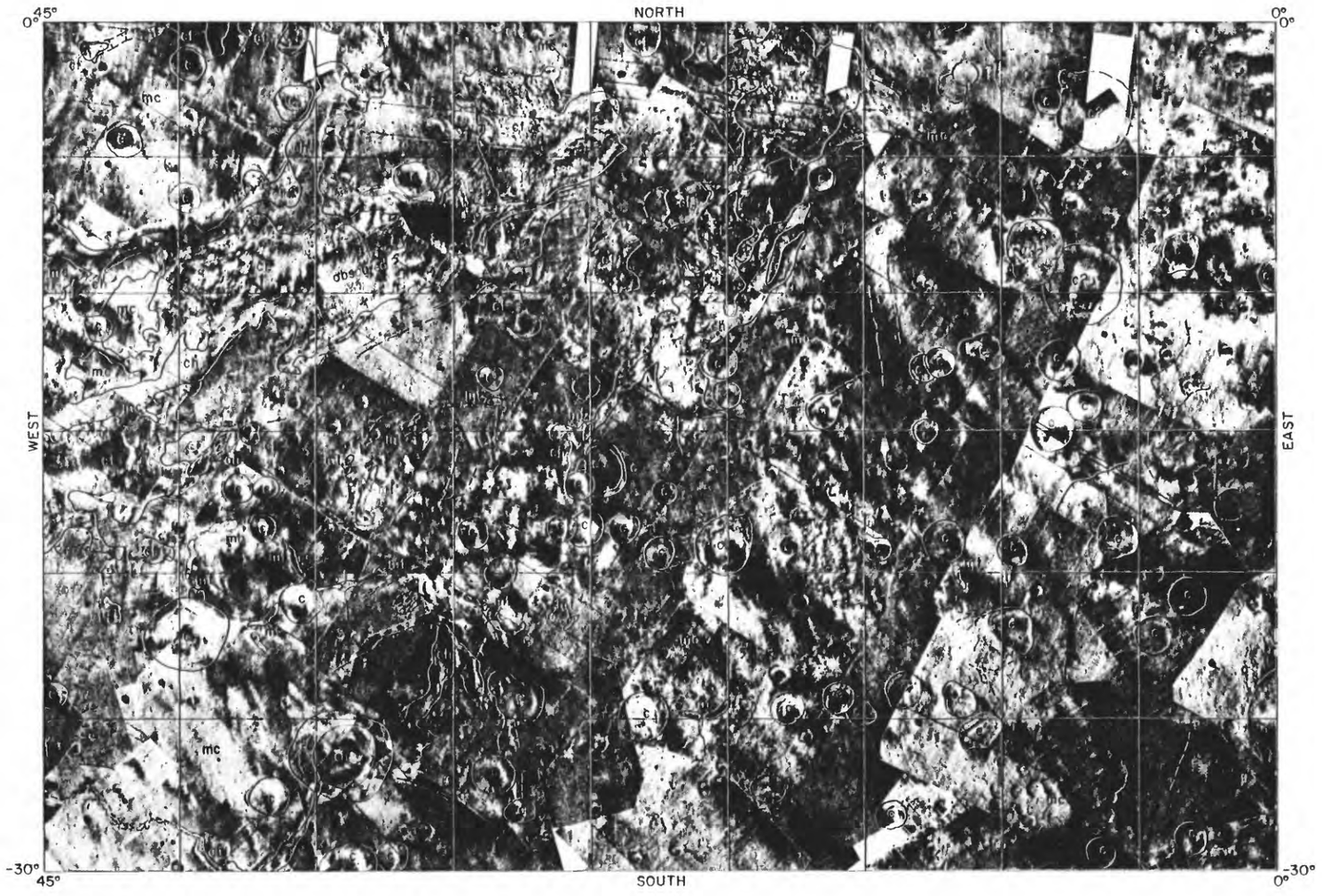

0° / -30° 0 500 1000 km

SCALE 1:10,000,000 AT 0° LATITUDE
MERCATOR PROJECTION

MARGARITIFER SINUS QUADRANGLE, MARS

SCALE 1:5,000,000

BY R.S. SAUNDERS

EXPLANATION

mc — Moderately cratered terrain

mt — Mountainous terrain

ch — Channel and canyon deposits

ct — Chaotic terrain

c — Crater materials

Contact

Graben

Scarp, hatchures point downslope

Narrow fracture

Buried crater rim crest

PRELIMINARY GEOLOGIC MAP OF THE MARE TYRRHENUM QUADRANGLE (MC-22) OF MARS

By Michael H. Carr

September 1972

EXPLANATION

vd
Volcanic dome

Roughly circular feature with central depression and radial ridge, channels, and graben. Strongly radial texture fades out into surrounding terrain. Central pit has linear extensions to southwest.

pl
Ridges and plains

Sparsely cratered plains with numerous low elongate ridges. Resembles lunar maria. Craters generally restricted to smaller size (*20 km) with fresh appearance.

Cratered terrain

Five facies recognized according to extent by which the terrain has been modified by tectonic and erosional processes. Different cratered units probably have no stratigraphic significance, except possibly in the case of cs, which may be partly blanketed by a unit younger than the rest of the cratered terrain.

cs, Cratered terrain, smooth: Numerous large craters (>50 km). Intercrater areas smooth or only sparsely gullied. Craters generally rimless depressions.

cg, Cratered terrain, gullied: Numerous large craters have closely spaced gullies in intercrater areas and on crater flanks.

cl, Cratered terrain, lineated: Numerous large craters. Strong linear texture that results from fractures mostly parallel to the cratered terrain/plains boundary.

cm, Cratered terrain, mountainous: Cratered terrain modified by formation of closely spaced isolated hills. Forms a continuous unit around the southern rim of the Libya basin. Probably ejecta from Libya basin.

cf, Cratered terrain, fractured: Cratered terrain modified by numerous closely spaced fractures trending mainly NW-SE and NNE-SSW. Fractures appear to be emphasized by erosion, particularly where adjacent to unit fs.

ps
smooth plain

Sparsely cratered plain. Occurs widely to the north and south of the map area; also locally within craters. Probably windblown dust.

c
Cratered deposits

Crater deposits mapped only where crater materials are distinguishable from surrounding materials. Where crater is simple rimless depression, crater rim is indicated but no separate crater material mapped.

vc
Volcanic channels

Channels formed by lava on the flanks of a volcanic dome.

ch
Channel deposits

Deposits within long, slightly sinuous channel-like feature in the northeast corner of the map area. Probably water deposited sediments.

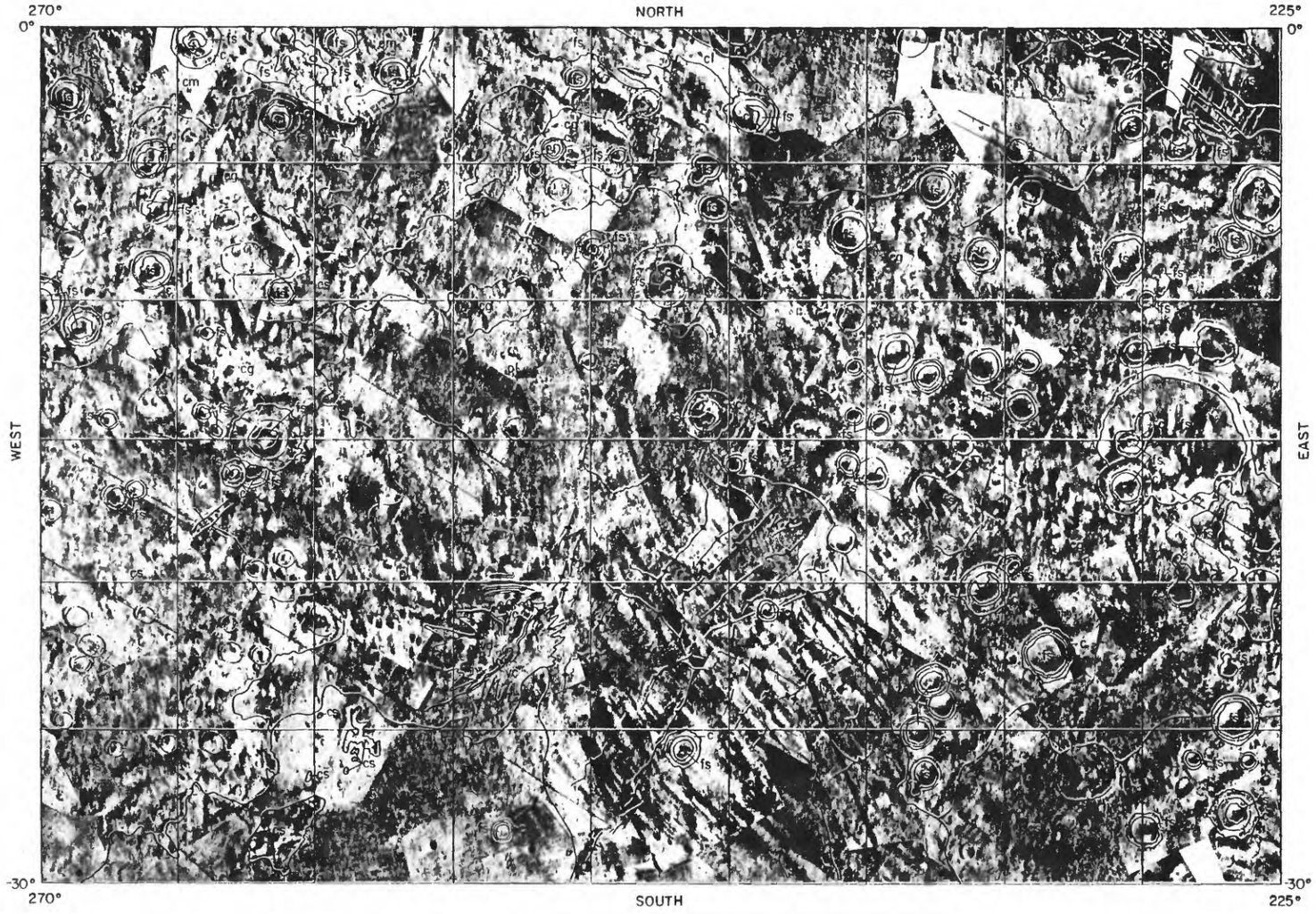

0° -30° 0 500 1000 km

SCALE 1:10,000,000 AT 0° LATITUDE
MERCATOR PROJECTION

MARE TYRRHENUM QUADRANGLE, MARS

SCALE 1:5,000,000

BY M.H. CARR

EXPLANATION

fs — Smooth floor

vd — Volcanic dome

vc — Volcanic channels

pl — Ridged plains

ch — Channel deposits

c — Crater deposits

cs | cg | cl | cm | cf

cs - Cratered terrain, smooth
cg - Cratered terrain, gullied
cl - Cratered terrain, lineated
cm - Cratered terrain, mountainous
cf - Cratered terrain, fractured

Contact
dashed where approximate

Fault

Graben

Scarp

Ridge

Buried rim crest

PRELIMINARY GEOLOGIC MAP OF THE AEOLIS QUADRANGLE (MC-23) OF MARS

By Mareta N. West

September 1972

EXPLANATION

Crater materials

c_5

Material of craters having deep interiors, sharp elevated rim crests, and rough rims. Most have central peaks; the largest has resolvable secondary craters.

c_4

Similar to c_5 but more subdued.

c_3

Bowl-shaped; gently sloping floors.

c_2

Shallow, flat-floored; rim crest subdued but higher than surrounding area.

c_1

Shallow, flat-floored, very subdued; some incomplete or indistinct; some rims appear to be level with surrounding terrain.

cp

Central peaks on floors of some c_3, c_4, and c_5 craters.

df

Dark floor material in craters of various apparent ages.

cc

Material of composite crater.

vc

Material of volcanic crater.

dm

Volcanic flow adjacent to volcanic crater.

ch

Material of crater chain.

Regional materials

p

Plains material

Nondistinctive material forming relatively level to rolling plains.

chl

Channel material

Material of sinuous depressions.

ft

Furrowed terrain

Material of numerous small linear to sinuous depressions; most furrows rimless, many sub-parallel.

rp

Rolling plains

Nondistinctive material differs texturally from, and appears rougher than, unit p.

cht

Chaotic terrain

Material of large, angular fractured blocks.

lt

Lineated terrain

Material of series of plateaus and troughs.

kt

Knobby terrain

Elongate to rounded hills, closely spaced to widespread.

mt

Mountainous terrain

Material of large multi-peaked mountains.

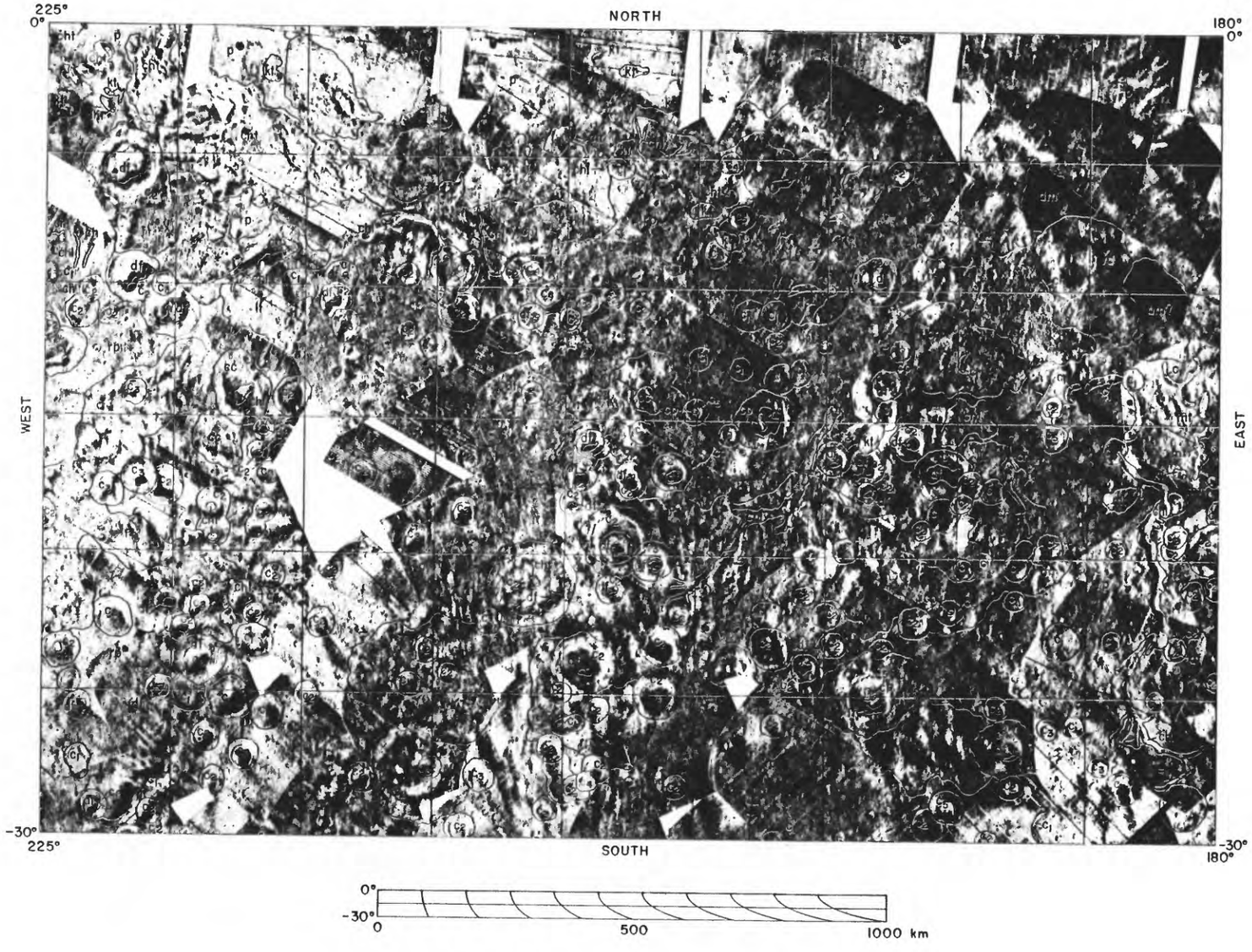
225°
0°
NORTH
180°
0°
WEST
EAST
-30°
225°
SOUTH
180°
-30°
0°
-30°
0
500
1000 km

CANDIDATE VIKING LANDING SITE I
EUMENIDES (21°N, 157°W)
1:1,000,000
By Desiree E. Stuart-Alexander

The proposed Eumenides landing site for Viking seems to be a low, planar area. It is bounded on the east by grooved terrain (gt) that forms the outermost apron around Nix Olympica and on the west (just off the map area) by low knobby terrain. Except for a few craters, there is no relief in the landing area at the A-frame scale of resolution. In general, craters are sparse throughout the area, and none of them appear sharp. Assuming that the general paucity of craters implies a relatively young surface, and that at least some craters should be very fresh in appearance, it is suggested that either there is still dust in the atmosphere, partially obscuring vision, or the craters are being prematurely aged. A likely candidate for the latter is wind erosion and/or deposition.

Possible surface materials at the nominal site are either alluvial or eolian fill; unfortunately, no diagnostic fine features are visible in the A-frames that cover the site or in the B-frames. If finely grooved terrain west of the landing site is the result of wind ablation, then the landing site might consist of fine-grained loess. However, to the east, geographically closer to the landing site, the knobby terrain is thought to be the result of alluvial erosion and of a different origin than the grooved terrain. This suggests that alluvial fill lies close to the surface of the plains. One B-frame located just north of the map area (DAS 8082973) also shows some very fine-scale knobby terrain and minor chaotic terrain.

EXPLANATION

c
4
c p
3
c lc hc Plains
2
c gt kt
1
Craters Grooved terrain Knobby terrain

Craters: Listed in order of increasing sharpness, with 1 the most subdued (and therefore interpreted as older) and 4 the sharpest. None are very sharp. Only impact-generated characteristics were observed. The largest crater (28 km wide) has been subdivided into an outermost lobate facies (unit lc) and an inner hummocky facies (unit hc). Unit lc could be observed only on the B-frames.

Plains: Featureless except for some few widely dispersed small craters. Believed to be a planar surface. Interpreted as either alluvial or eolian surface deposits.

Grooved terrain: Multiple fine grooves. Surrounds most of Nix Olympica. Interpreted as wind eroded surface, probably on volcanic materials.

Knobby terrain: Small knobby hills. Visible on one B-frame only.

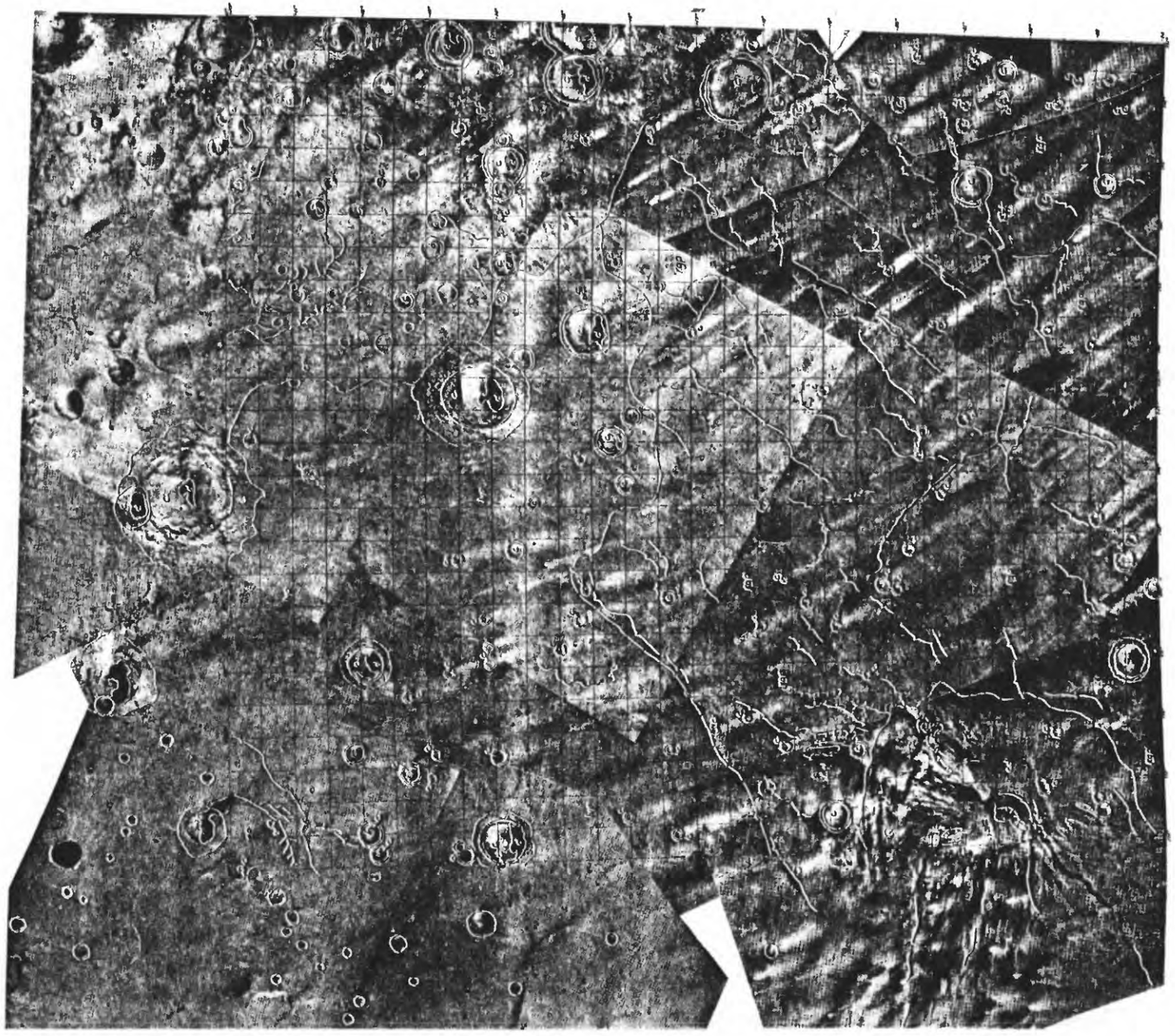

0 50 100 200 km
TRANSVERSE MERCATOR PROJECTION
SCALE 1:4000,000

SITE I EUMENIDES
Scale 1:1,000,000
D E STUART-ALEXANDER

EXPLANATION

C_5			sp	
C_4			Smooth plains	
C_3				
C_2	lc	hc	gl	kl
C_1	Lineated crater material	Hummock crater material	Grooved terrain	Knobby terrain
Craters				

——?——
Contact
Dashed where indefinite or extrapolated

CANDIDATE VIKING LANDING SITE I
EUMENIDES (21°N, 157°W)
1:250,000
By David H. Scott

The site is about 1,000 km west of Nix Olympica and lies within smooth plains (sp) material at both A-camera (southwest half of ellipse) and B-camera (northeast half) resolution. An elevation of -4.1 km is indicated by the preliminary elevation contour map. Several small (1-2 km) subdued craters are clearly visible indicating the absence of atmospheric dust. The featureless terrain and subdued crater morphologies are suggestive of an eolian blanket. Bedrock exposures are probably rare except around the large (28 km) crater near the northeast end of the landing ellipse where partly buried ejecta fragments may be abundant.

Landing hazards are minor; rms slopes are mostly low. An acceptable dielectric constant and slope (3.04°, 4.03°) were obtained in smooth plains material near the southwestern part of the ellipse but outside of the mapped area. The area does not have a high scientific interest because of the inferred thick, ubiquitous eolian cover. Movement of the ellipse center about 1° to the southwest is recommended to avoid rough crater rim material.

EXPLANATION

sp
Smooth plains material

Characteristics
Flat, featureless plains at A- and B-camera resolution. Low density of craters; all appear subdued. Craters as small as 1 km diameter clearly visible; wind plumes absent.

Interpretation
Eolian material, relatively thick, as no subjacent textural features revealed.

c cr crr cw cp
Crater materials

Characteristics
c, crater material, undivided. Craters too small for subdivision of units.
cr, crater rim material. Rough, hummocky, concave upward near rim crest.
crr, crater rim material, radial. Smooth, lobate scarps facing away from crater.
cw, crater wall material. Smooth, bright to rough and terraced.
cp, crater peak material. Large hills and ridges within central part of crater.

Interpretation
Crater morphologies indicate impact origins. Absence of radial lineaments in unit crr attributed to eolian blanket and(or) wind erosion.

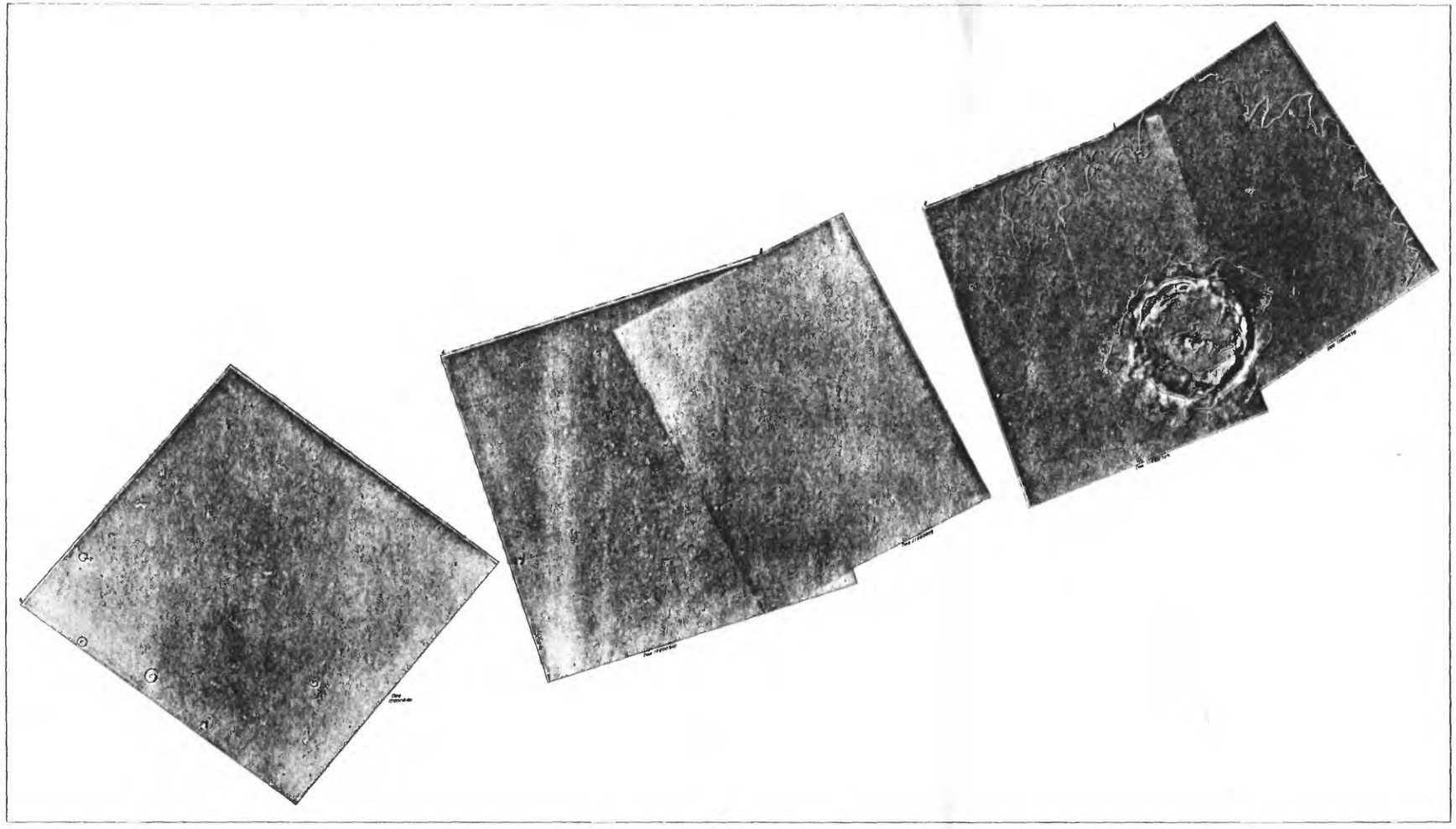

VIKING SITE 1
EUMENIDES 21° N, 157°
by
D. H. Scott

EXPLANATION

sp	- Smooth plains material
c	- Crater material
cr	- Crater rim material, rough
crr	- Crater rim material, smooth
cw	- Crater wall material
cp	- Crater peak material

SYMBOLS

Contact
Dashed where uncertain

Fault
Ball on low side

Scarp
Barb points downslope

CANDIDATE VIKING LANDING SITE 3
CHRYSE (19.5°N, 34.0°W)
1:1,000,000
By Newell J. Trask

Viking landing site 3, Chryse, is located at 19.5°N, 34.0°W at the mouth of several well-developed channels which connect to the equatorial rift valley system 1,600 km to the southwest.

The southern half of the map area consists mostly of deeply dissected plateau deposits, possibly silicic volcanic deposits which in places have broken into chaotic terrain. Material from the dissected plateau and chaotic deposits was apparently swept northward along well-defined channels to a low area of only slight relief. The landing ellipse lies in this low area.

The low-lying area consists of three main units with poorly defined boundaries. Close to the edges of the plateaus are deposits mapped as northward extensions of the channel deposits. These adjoin areas to the north mapped as light plains with no visible relief. North and northeast of the light plains are areas mapped as rolling terrain. They have lower albedo than the smooth plains and contain very low relief hills, scarps and ridges, and well-defined lineaments.

Considerations of Martian atmospheric dynamics suggest that the surface is everywhere partially covered by aeolian deposits. These may be thicker in the areas of the smooth plains. In the areas mapped as channel deposits there is a possibility of fluvial material mixed with surficial eolian material if indeed the well-developed channels have been carved by running water. Eolian deposits are probably thinner on the rolling terrain where subjacent, probably fractured, bedrock shows more clearly. The landing ellipse lies on both the channel deposits and the smooth plains unit. A few small outliers of the plateau deposits are also present within the ellipse.

EXPLANATION

Crater materials

c_1

Characteristics
Large craters (>20 km) with flat floors and subdued rims.
Interpretation
Impact craters, oldest.

c_2

Characteristics
Large craters (>20 km) with flat floors and rim deposits extending away from crests. Small craters (<20 km) slightly subdued.
Interpretation
Impact craters, intermediate age.

c_3

Characteristics
Small craters (<20 km) with relatively sharp rims.
Interpretation
Impact craters, relatively young.

vc
Volcanic craters

Characteristics
Craters centered atop low domes. Surrounded by dark plains.
Interpretation
Source vents for dark plains materials.

pl
Plateau deposits

Characteristics
Nearly level, elevated, flat-topped terrain. Superposed craters more abundant than on smooth plains; less abundant than on typical cratered terrain. Albedo lower than that of smooth plains.
Interpretation
Older wind or stream deposits now forming mesas and plateaus. May include some volcanic flows.

cht
Chaotic terrain

Characteristics
Long narrow mesas and plateaus, closely spaced.
Interpretation
Structurally dislocated, collapsed, and partly eroded plateau deposits.

kt
Knobby terrain

Characteristics
Subcircular, closely spaced hills, 2-5 km across.
Interpretation
Structurally dislocated and eroded plateau deposits.

rt
Rolling terrain

Characteristics
Very low relief, smooth hills about 10 km across. Some low relief scarps and ridges. Weak to moderately strong ENE trending lineaments. Albedo lower than that of smooth plains.
Interpretation
Wind eroded older terrain with a veneer of wind-blown deposits.

bsp
Bright smooth plains

Characteristics
Level, featureless, slightly raised above surroundings. Albedo slightly higher than that of smooth plains.
Interpretation
Older wind or stream deposits now forming low terraces "downstream" from small mesas.

sp
Smooth plains

Characteristics
Craters superposed on flat, featureless plane. Albedo high.
Interpretation
Windblown deposits. Areas mapped may contain some haze.

dp
Dark plains

Characteristics
Low albedo, level. No superposed craters.
Interpretation
Pyroclastic deposits.

ch
Channel deposits

Characteristics
Occupy troughs between elevated plateaus. Low scarps and swells and faint lineations are parallel to channel direction.
Interpretation
Surficial windblown deposits; may overlie water-laid deposits.

d
Dark materials

Characteristics
Irregular patches of low albedo. No intrinsic relief.
Interpretation
Windblown materials, possibly windblown volcanic ash.

l
Light materials

Characteristics
Plumose streaks occurring to leeward of small craters.
Interpretation
Windblown deposits.

CANDIDATE VIKING LANDING SITE 3
CHRYSE (19.5° N, 34.0° W)
1:1,000,000
by
Newell J. Trask

EXPLANATION

- c_1 - Crater materials
- d - Dark materials
- l - Light materials
- c_2 - Crater materials
- sp - Smooth plains
- rl - Rolling terrain
- bsp - Bright smooth plains
- cht - Chaotic terrain
- ch - Channel deposits
- dp - Dark plains
- vc - Volcanic craters
- c_3 - Crater materials
- pl - Plateau deposits
- kl - Knobby terrain

SYMBOLS

Contact

Lineament

Buried crater rim

VIKING LANDING SITE 3
CHRYSE (19.5°N, 34°W)
1:250,000
By Harold Masursky and George W. Colton

The landing site in the Chryse lowlands is in an area where the largest group of "stream" channels on Mars debouche.

If the channels are fluviatile, part of the site is underlain by smooth channel deposits that are marked by bright lineaments on Mariner 9 narrow angle pictures. These form piedmont alluvial fans or bajada deposits as in terrestrial deserts. Most of the remainder of the area is underlain by smooth plains deposits. These are essentially featureless on Mariner 9 wide angle pictures, but are interpreted to be windlaid deposits from nearby narrow angle pictures where crater plumes are prominently displayed. Reasoning from terrestrial analogy, the eolian deposits may be composed of linear and transverse dunes on the tens to hundreds of metres scale. These dunes may be covered with ripples on the centimetre scale. The channel deposits may be slightly rolling terrain with small channels and low interfluves on the tens of metres scale.

Basaltic lava flows may underlie the channel and smooth plains deposits, and basaltic ejecta may surround the impact craters in the area. Outliers of plateau deposits project through the plains deposits and may be composed of more silicic lava flows and volcaniclastic "continental" rocks. Sedimentary debris from these rocks probably makes up the bulk of the channel deposits. The eolian deposits may be silicic silt (60 percent silica according to Hanel's analysis of the airborne dust) derived from impact ejecta and wind and water-laid sediments.

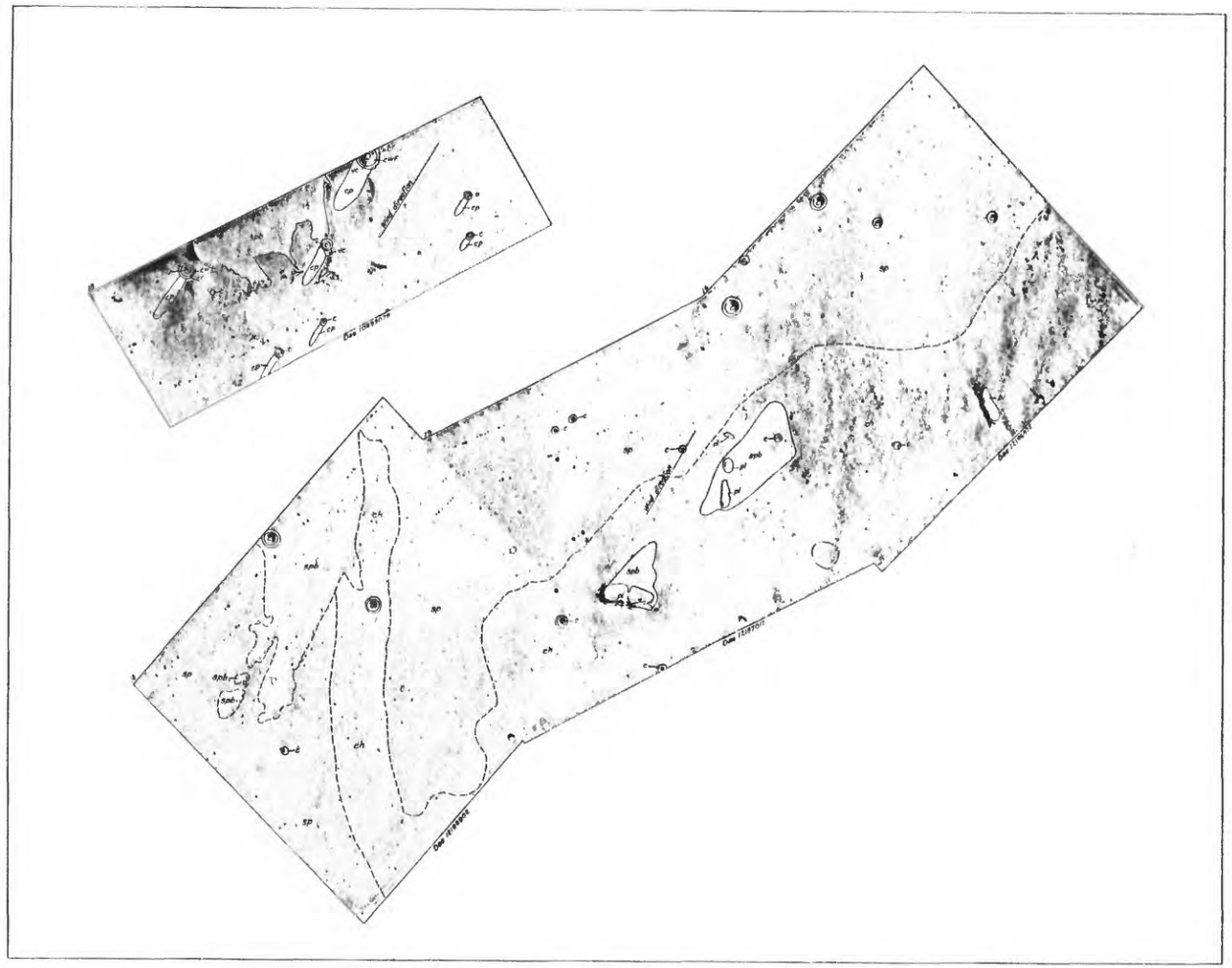

SITE 3 PART OF CHRYSE

Scale 1:250,000

HAROLD MASURSKY AND GEORGE W. COLTON

EXPLANATION

REGIONAL UNITS

sp	smooth plains
sph	smooth plains, bright
ch	channel deposits, smooth
ep	crater plumes, light
pl	plateau material

CRATER UNITS

c	crater material, undifferentiated
cr, cw, cf, ccp, cwf	

cr - rim material
cw - wall material
cf - floor material
ccp - central peak material
cwf - wall & floor material, undifferentiated

VOLCANIC UNITS

vc	volcanic cone (prominent raised rim; obvious central depression)

LINE SYMBOLS

- prominent rim crest
- buried crater
- scarp; barb points down slope
- contact
- shallow, channel-like trough

CANDIDATE VIKING LANDING SITE 4
URANIAE (8°N, 163°W)
1:1,000,000
By Michael H. Carr and Charles E. Meyer

The area lies within the sparsely cratered plains just north of their contact with the densely cratered province. In the northern part of the area, relatively featureless smooth plains predominate. Further south, closer to the boundary with the cratered province, seemingly older plains units occur. To the west of the map area are extensive areas of knobby terrain, characterized by numerous closely spaced equidimensional hills. Some of this terrain also occurs in the western part of the map area.

Knobby terrain is probably the oldest unit in the area. Elsewhere on Mars, it occurs close to the boundary between the densely cratered terrain and the sparsely cratered province. It appears to form by a combination of tectonic and erosional processes as the plains encroach upon the primitive cratered terrain. The next oldest units are the dissected and fractured plains. These are interpreted as volcanic lava plains that have been partly fractured and eroded. Insufficient areas are exposed for meaningful crater counts to allow the units to be dated relative to plains units that occur elsewhere. Similar fractured plains in the Tharsis and Lunae Lacus regions are, however, older than the lobate plains in those regions, and the fractured plains that occur here may be of a similar age. The dissected and fractured nature of the units also suggests a relatively old age for a plains unit. The youngest of the plains units is the smooth plains which complexly embays all the others. It lacks the lobate flow structures and ridges that are common on the volcanic plains around Tharsis. The lack of obvious volcanic structures suggest that the smooth plains here may be largely eolian in origin.

The ellipse, centered at 8°N, 163°W, includes mostly smooth plains. Dissected plains occur around a large crater near the center of the ellipse and fractured plains occur at its northern end. It is recommended that the ellipse be moved approximately 1° to the north or northwest to avoid the rough terrain around the aforementioned crater.

EXPLANATION

dp
Dissected plains

Characteristics
Forms a complexly dissected plain and numerous isolated mesas and buttes at the southern edge of the map. The unit is at a slightly higher elevation than the surrounding smooth plains unit (sp) and the contact is commonly a low escarpment. The dissected plains unit has a lower albedo than the surrounding smooth plains and the complex embayment relations give the area a patterned appearance.

Interpretation
The unit is interpreted as the remnants of a relatively old volcanic plain. Includes some ejecta from a large crater just south of the map area.

fp
Fractured plains

Characteristics
Similar to unit dp but the surface is crossed by numerous closely spaced, NW-SE trending fractures. Albedo lower than surrounding plains. Bounding escarpments less common than with unit dp.

Interpretation
Interpreted as a relatively old volcanic plain similar to unit dp, but intensely fractured.

sp
Smooth plains

Characteristics
Relatively featureless plain that intricately embays units dp, fp, and kt. Superimposed craters generally small and bowl-shaped. Fills the floors of large subdued craters. B-frame coverage indicates that small isolated islands of units kt, fp and dp occur throughout the area included in the unit.

Interpretation
Interpreted as primarily eolian debris.

kt
Knobby terrain

Characteristics
Occurs mainly in the western part of the map area. Surface characterized by numerous closely spaced, equidimensional rounded hills. As the dimensions of the hills become smaller and the spacing between them wider, the unit grades into the smooth plains.

Interpretation
The origin of the unit is uncertain but appears to be related to the breakup of the densely cratered terrain since the unit occurs mostly at the boundary between the densely cratered terrain and the sparsely cratered plains.

c
Crater materials

Characteristics
Materials in and around small bowl-shaped craters.

Interpretation
Interpreted as ejecta, talus, and breccias associated with relatively young impact craters.

cr
Crater rim materials

Characteristics
Forms the rims of several large flat-floored craters. Hummocky surface, embayed by surrounding plains.

Interpretation
Interpreted as ejecta from relatively old impact craters.

0 50 100 200 km

TRANSVERSE MERCATOR PROJECTION
SCALE 1:4,000,000

SITE 4 URANIAE

scale 1:1,000,000

M. H. CARR, C. E. MEYER

EXPLANATION

sp
Smooth plains

kt
Knobby terrain

dp
Dissected plains

fp
Fractured plains

cr
Crater rim

c
Crater

m
Mesa

Contact

Lineation

CANDIDATE VIKING LANDING SITE 4
URANIAE (8°N, 163°W)
1:250,000
By Mareta N. West

Viking site 4, Uraniae, is located southwest of the grooved terrain west of Nix Olympica and east of large areas of knobby terrain. Six B-camera photographs cover the mapped region. The southern group of photographs covers an area in the vicinity of a large crater which is clearly visible at A-frame resolution. Many of the small hummocks and plateaus mapped from those frames are probably associated with this crater. The southern area is well covered by B-frame photographs and clearly appears to be too rough for a landing.

The B-frame farthest north depicts an area which is virtually featureless. If this site is retained, the author suggests that the center be moved to 9°N, 164°W. The area provides a variety of targets for orbital photography. A lander would obtain clues to the origin of the vast Martian plains.

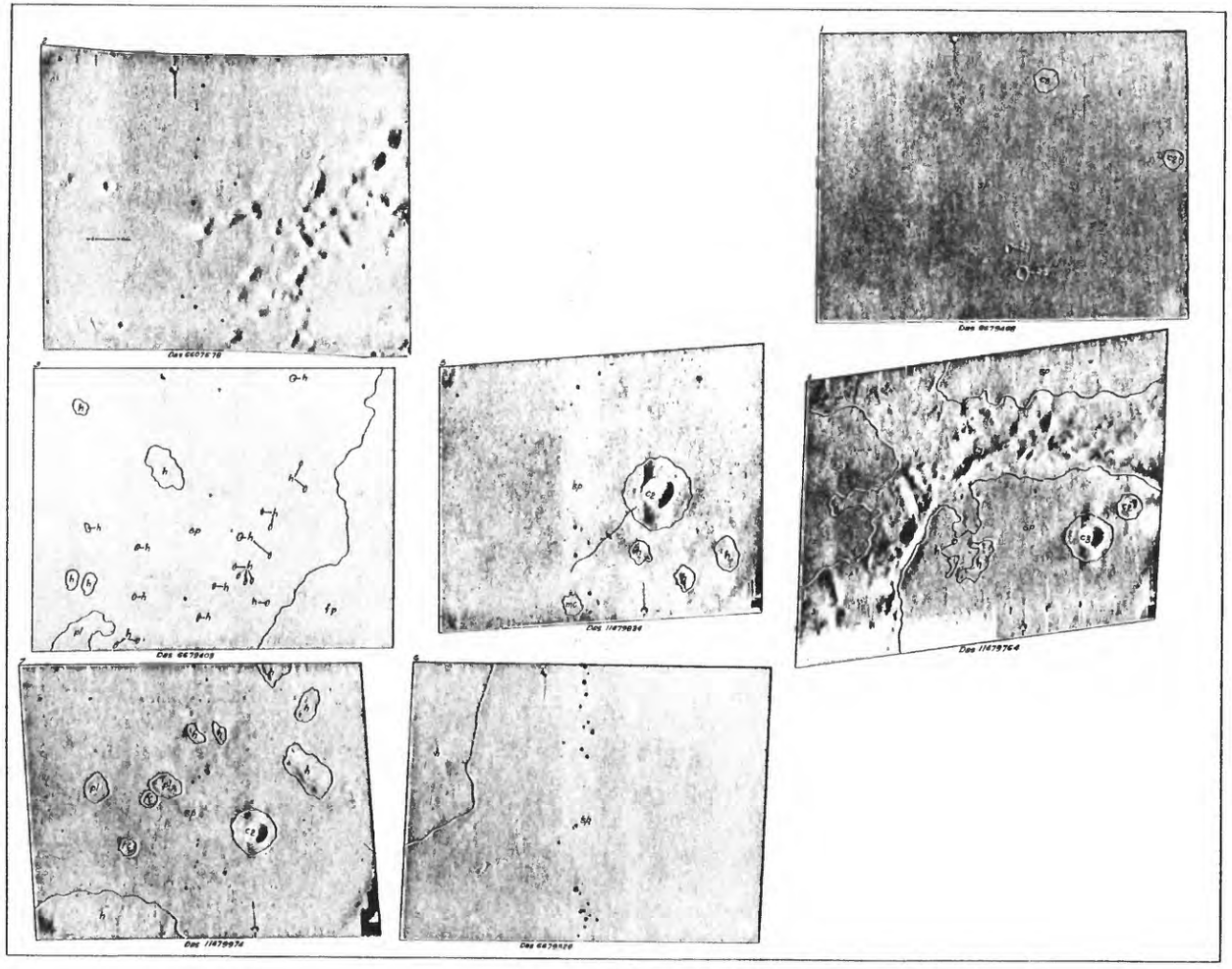

Scale 1:250,000

0 50 km

SITE 4 URANIAE

scale 1:250,000

MARETA WEST

EXPLANATION

cj Crater material

Circular plan; angular raised rim crest

rc Ring crater

Rounded circular rim; central mound in crater floor

mc Mound crater

Low mound with scalloped outline; summit pit

sp Smooth plains-forming material

Relatively level to rolling terrain of low relief

cg Slightly subdued, mostly bowl-shaped

cl Very subdued or incomplete; shallow interior

pl Plateau-forming material

Similar to hummocky material but flat topped

h Hummocky material

Rounded hills; larger ones mapped individually

fp Fractured plains

Contact

Ridge

CANDIDATE VIKING LANDING SITE 5
CANDOR (14.7°N, 79.3°W)
1:1,000,000
By Mareta N. West

Viking site 5 lies within an area of low relief between the largest Martian volcanic constructional features and a broad plain. The plains-forming material (sp) which covers approximately half of the mapped area appears to be smooth at A-camera resolution except for a few widespread craters. Two B-camera photographs in this area depict very subdued lobate materials interpreted as lava flow fronts.

Rolling plains material (rp) is more irregular than the plains unit and occurs in a broad valley. Chaotic material forms a rough surface along the eastern wall of the valley and apparently results from fracturing and dissecting of the slope material. More subdued chaotic terrain occurs in patches within the rolling plains. The western valley wall is subdued and discontinuous, and its contact with plains material is gradational.

Three classes of craters are mapped, c_1 being the oldest and most subdued.

The ellipse centered at 10°N, 80°W includes mostly plains materials, which may be largely volcanic as suggested by the lobate escarpments visible on B-camera photographs. The rolling plains material may be primarily alluvial. Presumably eolian material is ubiquitous on Mars.

The site appears to be relatively free of hazards for approach and landing. However, the center of the ellipse could be moved approximately one degree to the southwest away from the more irregular rolling plains.

EXPLANATION

c_1 c_2 c_3

Crater materials

Material of craters ranging from incomplete or very subdued (c_1) to circular with angular elevated rim crests (c_3). Interpreted as materials of craters mostly of impact origin.

p

Smooth plains-forming material

Forms relatively smooth plain; flow fronts visible on B-frame throughout the area. Also patches occur on some crater floors. Interpreted as volcanic flows where extensive; probably eolian deposits within craters.

rp

Rolling plains

Undulating material occurring in broad valley; western contact gradational with plains unit. Interpreted as alluvial deposits.

cht

Chaotic terrain

Material which is rough and angular where developed on valley wall and more subdued where present within the valley. Interpreted as fractured material older than the plains units.

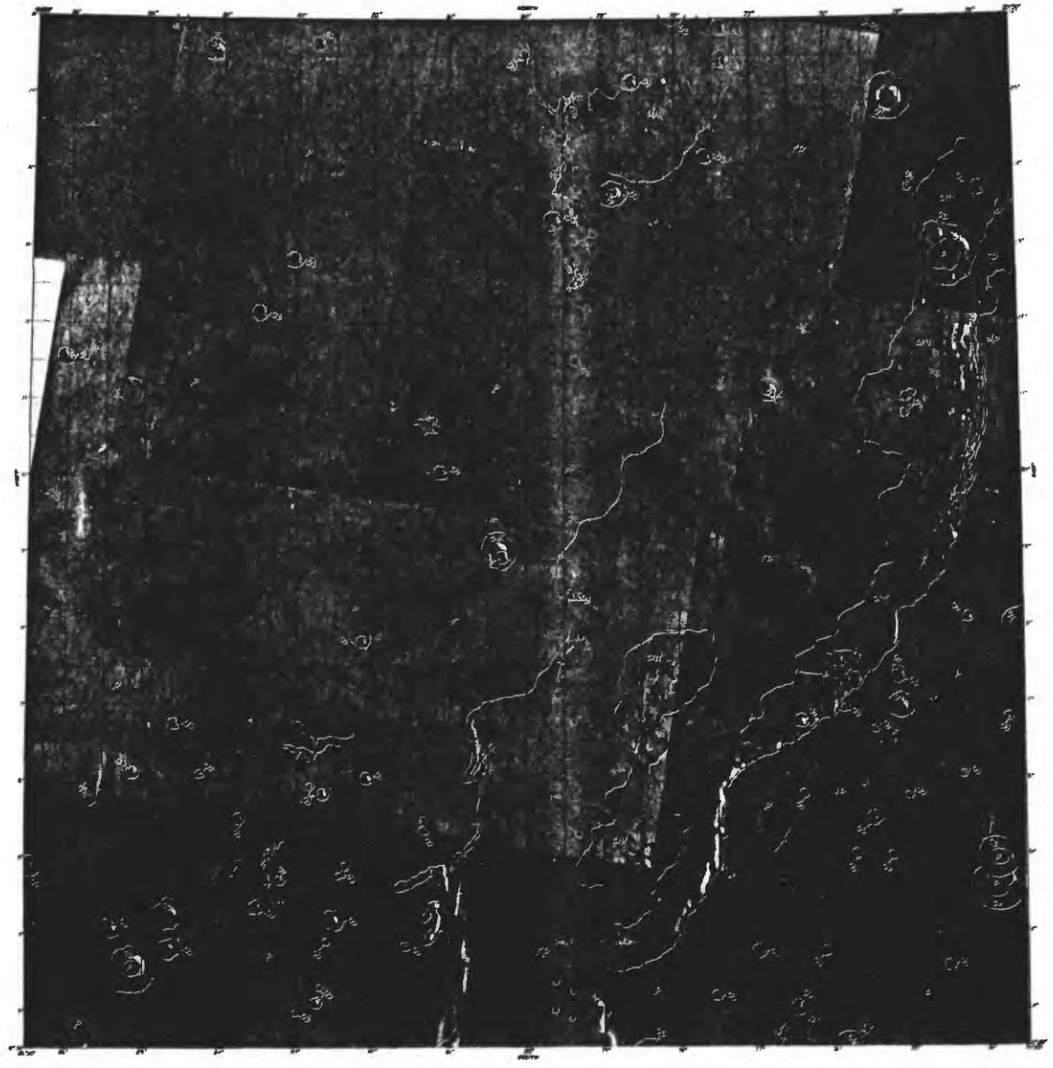

0 50 100 200 km

TRANSVERSE MERCATOR PROJECTION
SCALE 1:4,000,000

SITE 5 CANDOR

Scale 1:1,000,000

MARETA WEST

EXPLANATION

c_3

c_2

Younger craters

Material of craters having circular rim and angular elevated rim crest; bowl shaped interior

c_1

Older crater

Material of incomplete subdued crater; smooth floor, shallow interior

p

Plains-forming material

Relatively smooth material in which flow fronts and braided ridges occur; flow fronts visible on B frame photographs; also includes smooth material in some crater floors

rp

Rolling plains

Material occurring in broad shallow channel; surface more irregular than unit p

cht

Chaotic material

Material of rugged angular blocks; some in channel

Contact

Depression

Ridge

Flow front

CANDIDATE VIKING LANDING SITE 5
CANDOR (14.7°N, 79.3°W)
1:250,000
By Michael H. Carr

The three frames lie just to the west of a north-south trending, flat-floored valley, 100-200 km across and 1,500 km long. To the north the east wall of the valley is complexly embayed and fractured while to the south chaotic terrain occurs at the valley edge. The west wall is discontinuous and generally lower than the east wall. The most northerly of the three frames mapped includes part of the west wall. The other two are in the plains to the west of the valley.

The most northerly (14.7°N, 79.3°W) B-frame includes mostly valley floor. On the floor are numerous low, flat-topped mesas, each bounded by a low escarpment. Also present are some very subdued lobate escarpments, suggestive of flow fronts. The west wall of the valley is marked by some highly fractured terrain, to the west of which are the lobate plains. In the northwest corner is a dark area with a very fine surface texture. This may be a wind scoured surface similar to that occurring just to the north at 17.5°N, 75.8°W (DAS 07327743), or it may be closely spaced dunes.

The other two B-frames are within the lobate plains to the west of the valley. The plains are very sparsely cratered. The most prominent features are a series of very subdued lobate escarpments, interpreted as lava flow fronts. There appears to be a succession of flows one on another, the younger, uppermost flows having sharper relief than the lower flows.

The site appears to present a minimum hazard from a terrain standpoint, provided the ellipse does not overlap the valley. The flow fronts are believed to be very subdued features and the actual fronts themselves constitute a very small fraction of the total area. The ellipse would present less hazard if it were moved 1 degree to the southwest so that it excluded the parts of the valley that presently fall within the northern part of the ellipse. The surface probably resembles lunar maria surfaces, somewhat modified by eolian activity.

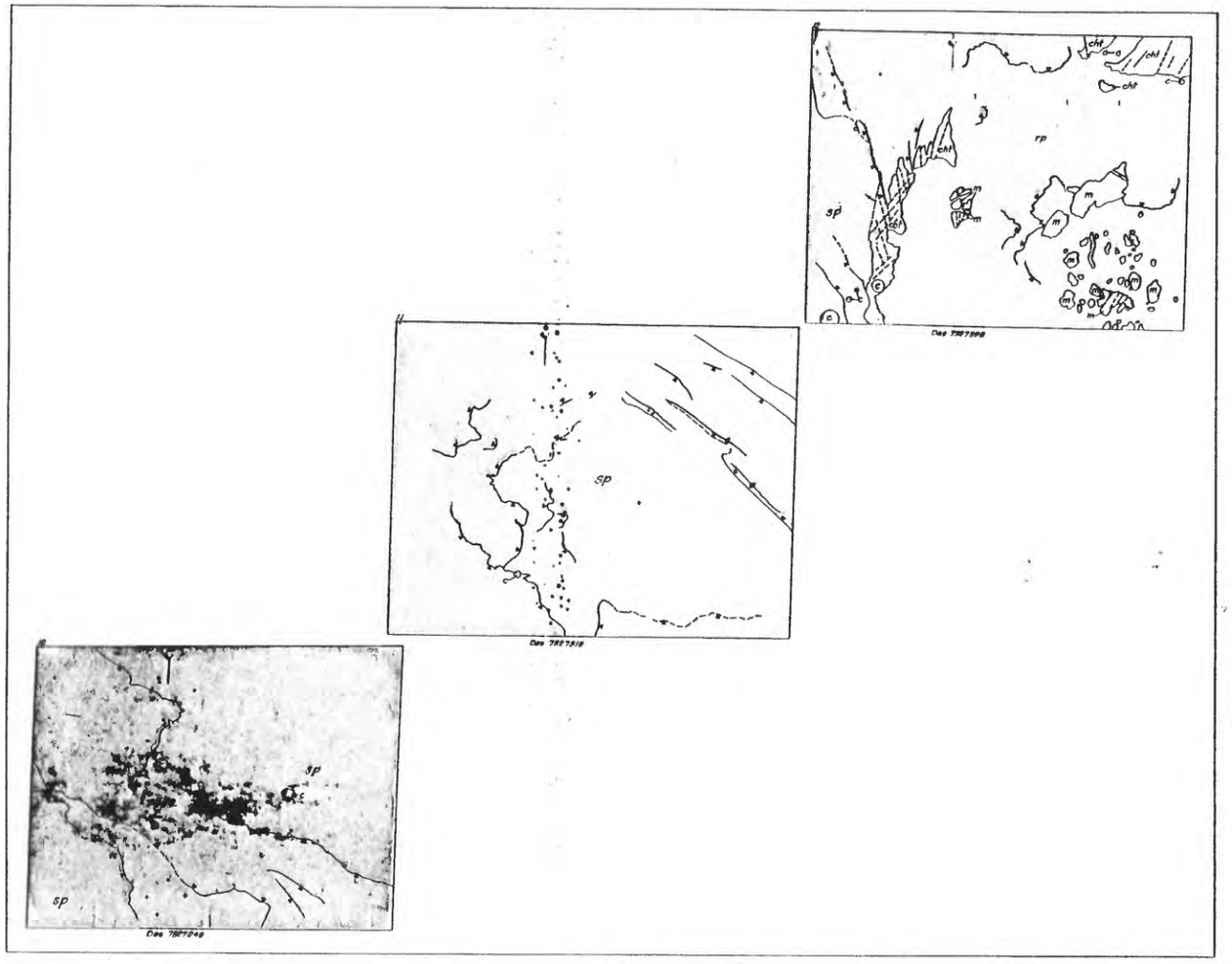

SITE 5 CANDOR

scale 1:250,000

M. H. CARR

EXPLANATION

m
Mesa

sp
Smooth plains-forming material

Relatively smooth material in which flow fronts and braided ridges occur; flow fronts visible on B frame photographs; also includes smooth material in some crater floors

rp
Rolling plains

Material occurring in broad shallow channel; surface more irregular than unit p

cht
Chaotic material

Material of rugged angular blocks; some in channel

c
Crater

Contact

Ridge

Flow front

Lineaments

Fault
Bar and ball on downthrown

CANDIDATE VIKING LANDING SITE 7
AMAZONIS (-2°S, 148°W)
1:1,000,000
By George W. Colton

Landing site 7, Amazonis, is located along the south edge of the Amazonis basin, west of the Tharsis ridge.

Topographically the area is dominated by a broad, shallow, northwest-trending depression which is bordered on the north by a gently asymmetric arch, and on the south by a densely cratered plateau. An abrupt escarpment marks the boundary between the depression and cratered plateau. Many fault scarps on the uplifted arch, small scarps within the depression, and closely spaced, sharply defined ridges and grooves in patches of bedrock beneath the plains unit also trend northwestward.

A deposit of smooth plains material is the dominant stratigraphic unit. Owing to tectonic deformation, the smooth plains unit in this area occurs at a higher elevation than do similar units in the other landing site areas. It appears to be relatively thin and, in some areas covered by B-frames, it is too thin to mask the underlying bedrock.

Materials of the sp unit probably consist of an unconsolidated mixture of igneous rock debris and of shock-metamorphosed and other impact crater debris. All three types of debris have probably undergone one or more earlier cycles of fluvial and eolian erosion and deposition. Eolian transport appears to have occurred dominantly from the northwest to the southeast. In the southern part of the ellipse, fluvial sediments derived from north-flowing channels may be dominant and probably reflect the composition of the cratered plateau region. In the northern part of the ellipse, a higher percentage of igneous rock debris derived from nearby outcrops of bedrock (unit fp) may be included in the surficial material.

EXPLANATION

sp
Smooth plains

Characteristics
Relatively flat and featureless at A-frame resolution. Albedo variable; typically quite high. Occupies most of map area (between the northern broad arch and southern cratered plateau); also floors of large craters.
Interpretation
Eolian material of variable thickness but probably thin in this area. Materials near channel mouth may be predominately fluvial.

fp
Fractured plains

Characteristics
Coarsely textured areas of northwest trending ridges and grooves along the margin of the depression where tectonic uplift has occurred. Finely textured areas occur in the floor of the depression.
Interpretation
Older, densely fractured bedrock, partly exhumed; structural grain accentuated by wind scour. Lobate pattern in some areas suggests lava flows.

cht
Chaotic terrain

Characteristics
Slightly depressed areas within unit cp of irregular hummocks, with intervening valleys, depressions, and sinuous grooves and channels. Associated with channel systems.
Interpretation
Collapsed areas of unit cp resulting from subsurface displacement of fluids.

cp
Cratered plains

Characteristics
Densely cratered, relatively level, plateau. Albedo darker than unit sp. Numerous poorly defined, north-south trending, irregular escarpments. Most craters rimless, flat-floored, and filled with unit sp.
Interpretation
Flat-lying, layered rock, probably scoured and planed by eolian erosion. May represent a thick sequence of old lava flows.

ht
Hilly terrain

Characteristics
Nondescript terrain intermediate in surface expression between units sp and kt.
Interpretation
Occurrence along east edge of map may be due to faulting; occurrences along west edge of map may be related to slumping and eolian erosion of pre-existing terrain along flanks of unit fp.

kt
Knobby terrain

Characteristics
Present as two small patches of numerous closely spaced, rounded hills. Grades into smooth plains (sp).
Interpretation
Origin uncertain; may be erosionally degraded remnants of unit cht.

sch
Smooth channel deposits

Characteristics
Present in bottom of some larger channels. Surface texture generally smooth; gentle smaller-scale channels visible locally.
Interpretation
Fluvial sediments deposited during discharge stage. Not mapped where covered by windblown material of unit sp.

bch
Braided channel deposits

Characteristics
Complexly incised, intersecting. Linear channels that occupy the broader part of the main channel, marginal to unit sch.
Interpretation
Abandoned drainage channels which antedate unit sch; analogous to terrestrial river terrace deposits.

ach
Abandoned channel deposits

Characteristics
Irregular hummocky material in depressed area along west edge of map.
Interpretation
Slumped or collapsed material in abandoned channel system; may have accumulated in response to uplift of unit fp.

vc
Volcanic cone

Characteristics
Low, subdued cones with summit depressions in western map area. Albedo slightly darker than surrounding unit sp.
Interpretation
Probably volcanic cones composed of pyroclastic debris.

c cr cw cwf cf ccp
Crater materials

Characteristics
Smooth to very rough crater wall and floor materials.
c, crater material undivided
cr, crater rim material; smooth to very rough
cw, crater wall material; smooth to very rough
cwf, crater wall and floor material undivided
cf, rough crater floor (smooth floors mapped as sp)
ccp, central peak material

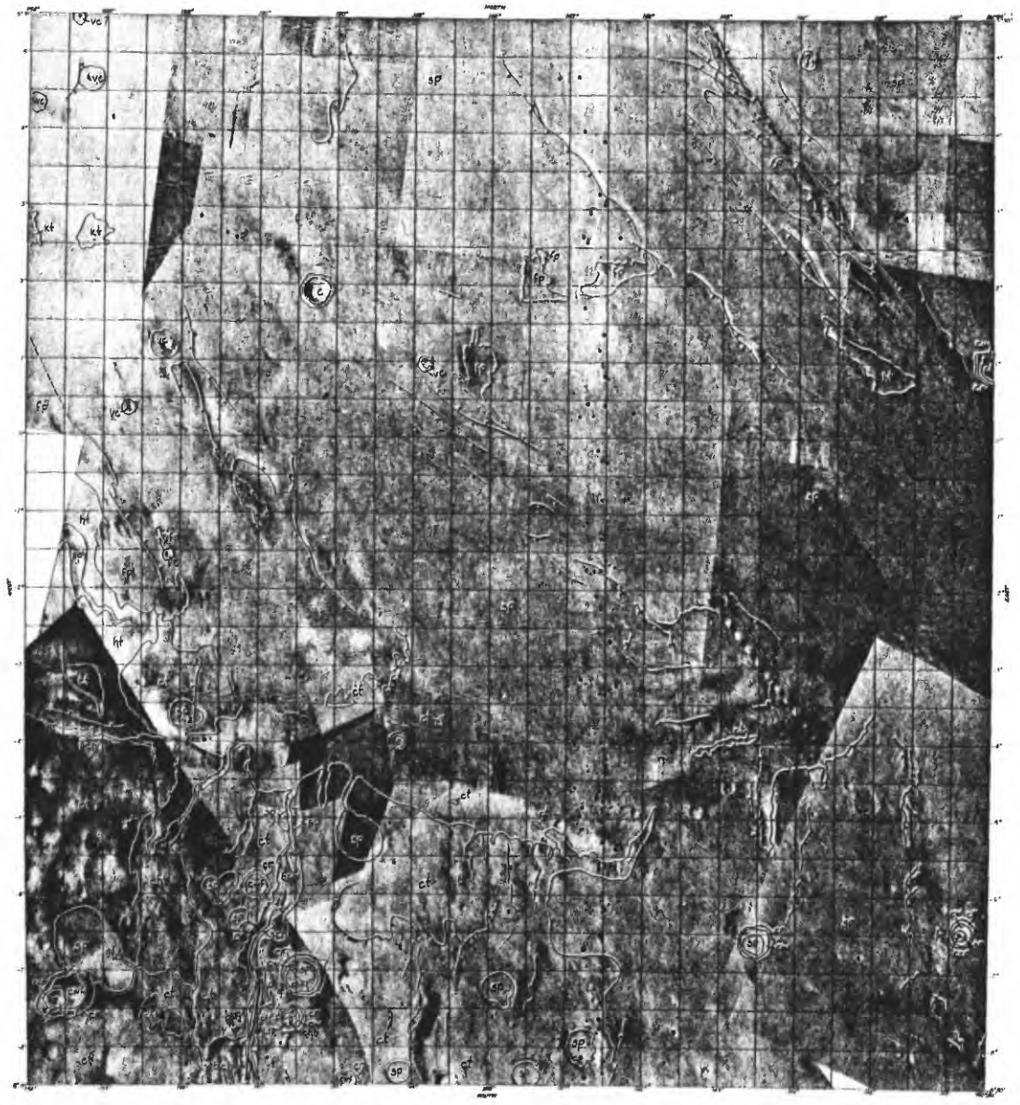

SITE 7 AMAZONIS

Scale 1:1,000,000

G. W. COLTON

EXPLANATION

sp — Smooth plains

fp — Fractured plains

kt — Knobby terrain

ht — Hilly terrain

cf — Cratered terrain

sch — Smooth channel deposits

bch — Braided channel deposits

ach — Abandoned channel deposits

cht — Chaotic terrain

Contact
Dashed where buried or extrapolated

Fault
Ball on downthrown side

Escarpment
Line marks base; barbs point downslope

Prominent crater rimcrest

Narrow channel

CRATER DEPOSITS

c | cr | cw | cwf | cf | ccp

c - crater
cr - crater rim
cw - crater wall
cwf - crater wall and floor, undifferentiated
cf - crater floor
ccp - crater central peak

vc — Volcanic cone

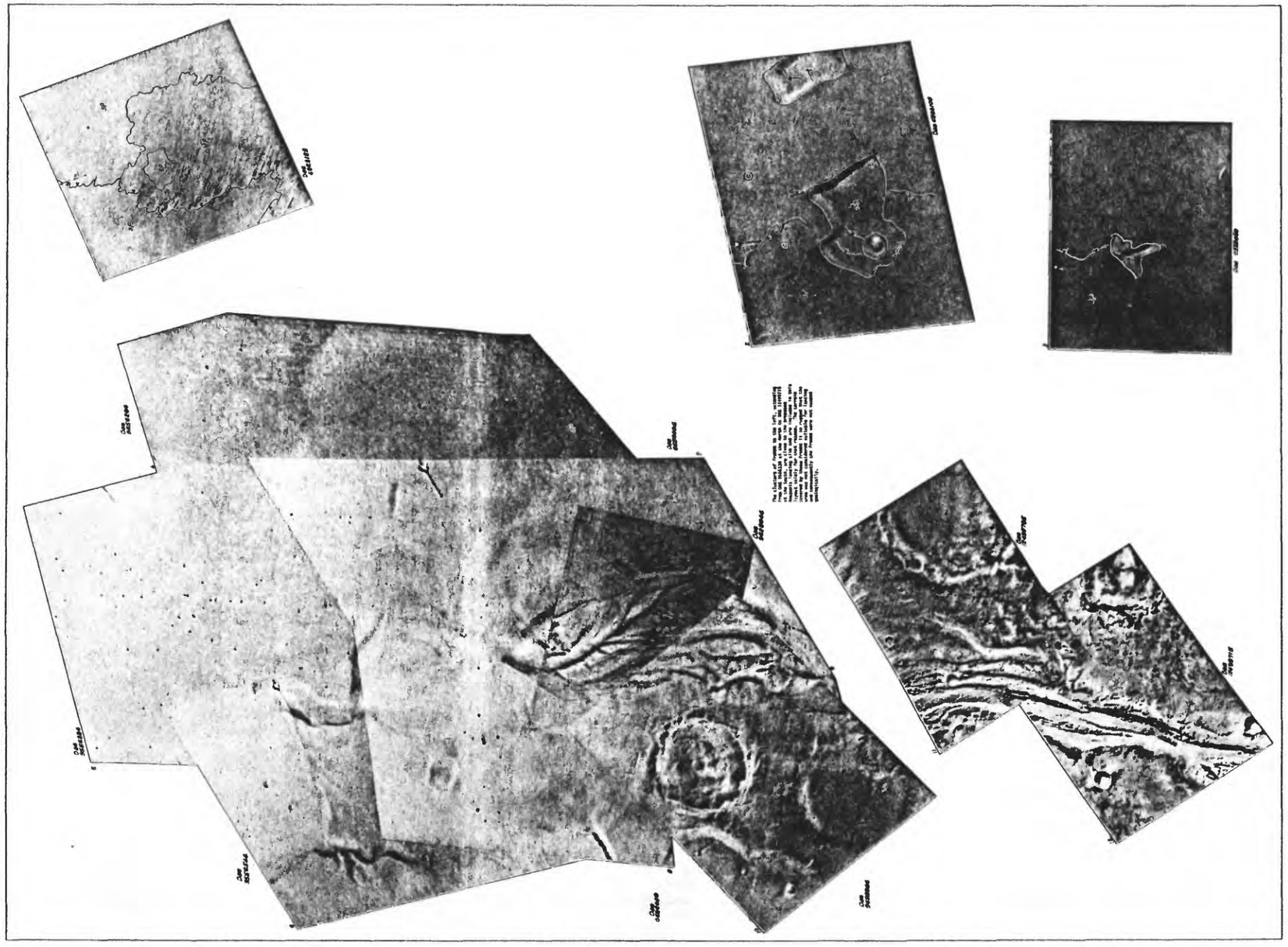

SITE 7 AMAZONIS

Scale 1:250,000

N. J. TRASK

EXPLANATION

SP
Smooth plains

fp
Fractured plains

C
Crater

cf
Cratered terrain

Contact
Dashed where buried
or extrapolated

Escarpment
Line marks base;
barbs point downslope

CANDIDATE VIKING LANDING SITE 8
ZEPHYRIA (2°S, 186°W)
1:1,000,000
By David H. Scott

The landing ellipses (azimuths 7°-57°) traverse smooth plains (sp), knobby (kt), hilly (ht), and rolling (rt) terrain in a low area (-3.8 km) along the Martian equatorial belt (preliminary elevation contour map). B-camera frames near the centers of both ellipses show that the smooth plains at A-camera resolution have rough to uneven surfaces caused in part by massive slumping and incipient slumping and collapse (chaotic terrain). Possibly about 50 percent of the terrain in each landing ellipse could be classified as smooth plains. Dielectric constants and rms slope data are not available. B-camera frames about 7° due west (near 2°S, 193°W) of the ellipse center also indicate that terrain considered to be smooth at A-camera resolution is actually extremely hilly in places. There are no other areas within the map outlines where high resolution (B-camera) control is sufficient to safely warrant consideration of another landing site.

Scientific interest is moderate to high; eolian material and bedrock are about equally exposed. Bedrock may consist of alluvial, volcanic, or differentiated crustal materials. The hilly and rolling terrain are older erosional variants of the knobby terrain.

Landing hazards are relatively high; some terrain now mapped as smooth plains may be considerably rougher at larger scales.

EXPLANATION

sp
Smooth plains material

Characteristics
Flat, featureless at A-frame resolution; B-frames near center of ellipse show subjacent topography--chaotic terrain and incipient chaotic terrain (see 1:250,000 scale map).
Interpretation
Eolian material; thin in places.

lp
Lobate plains

Characteristics
Undulating, smooth to coarse texture, lobate scarps. Appears to be partly covered by smooth plains unit (sp) but embays knobby terrain (kt).
Interpretation
Lava flows and flow fronts; younger than knobby terrain, older than smooth plains.

kt
Knobby terrain

Characteristics
Round to subangular equidimensional knobs; resembles Alpes formation on Moon
Interpretation
Structurally dislocated bedrock in process of erosion.

ht
Hilly terrain

Characteristics
Similar to unit kt but more subdued.
Interpretation
Same as for unit kt but erosion more advanced.

rt
Rolling terrain

Characteristics
Low relief, undulating terrain; resembles smooth plains at a 10 km scale.
Interpretation
Similar to unit ht but erosion and filling by wind very far advanced.

l d
Light and dark materials

Characteristics
Plumose streaks occurring to leeward of crater rims and small hills (kt).
Interpretation
Light material, wind deposits. Dark material, wind deposits of different composition than light material, or areas denuded by wind possibly exposing bedrock.

m
Mesa terrain

Characteristics
Inferior examples of flat-topped prominences well developed elsewhere on Mars.
Interpretation
Remnants of block-faulted bedrock.

c cr cw cp
Crater materials

c, crater material, undivided
cr, crater rim material. Smooth to rough.
cw, crater wall material. Smooth, in places gradational with crater floors (not mapped).
cp, central peak material. Hills and ridges toward center of crater.

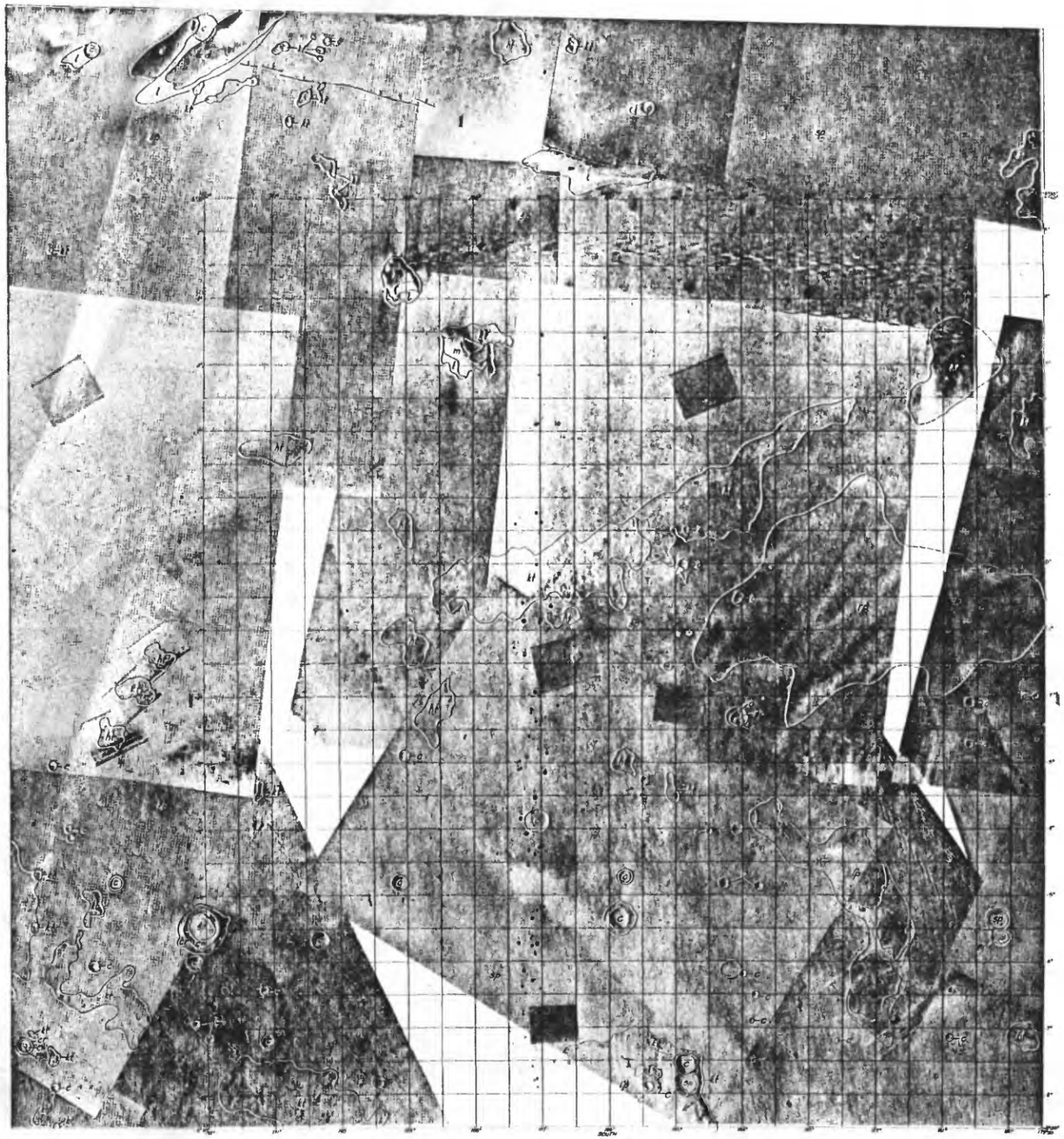

SITE 8 ZEPHYRIA

Scale 1:1,000,000

D. H. SCOTT

EXPLANATION

sp
Smooth plains material

kt
Knobby terrain

lp
Lobate plains

ht
Hilly terrain

rt
Rolling terrain

l | d
Light and dark materials

m
Mesa terrain

c | cr | cw | cp
Crater materials

c-crater
cr-crater rim
cw-crater wall
cp-central peak

Scarp
Barb points downslope

Contact

Dashed where buried
or extrapolated

Fault

Ball on low side

Rimless depression

Prominent rim crest
of crater

Buried crater rim crest

(no page 42)

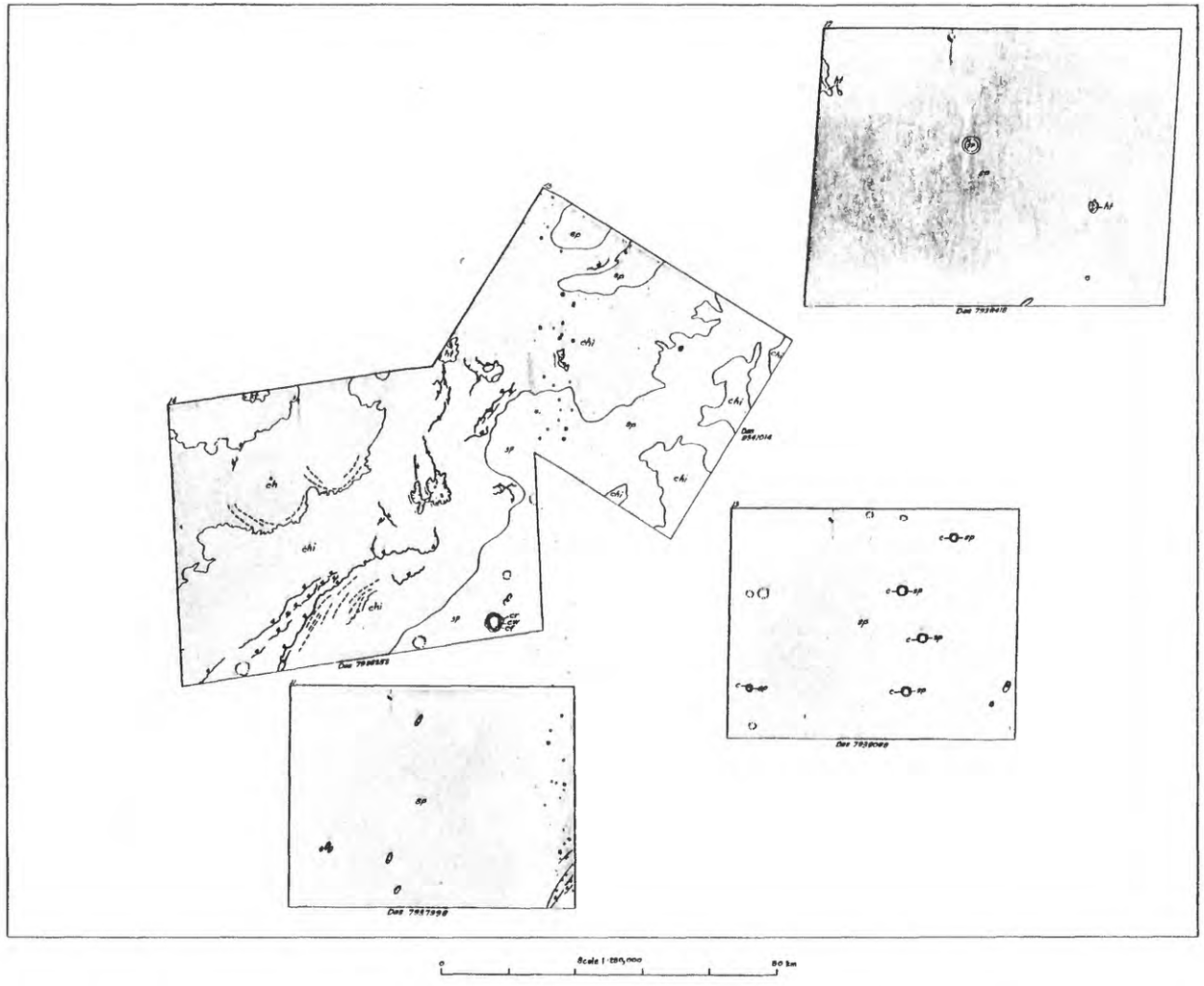

SITE 8 ZEPHYRIA

Scale 1:250,000

G. W. COLTON

EXPLANATION

sp
Smooth plains material

kt
Knobby terrain

ht
Hilly terrain

ch
Chaotic terrain

chi
Incipient chaotic terrain

c | cr | cw | cf
Crater materials

c-crater
cr-crater rim
cw-crater wall
cf-crater floor

Lineament

Channel or trough

Rimless depression

Contact

Dashed where buried or extrapolated

Prominent rim crest of crater

Scarp

Barb points down slope

Buried crater rim crest

CANDIDATE VIKING LANDING SITE 9
MEMNONIA (9°S, 141°W)
1:1,000,000
By Elliot C. Morris

Viking landing site 9 lies on a relatively smooth plain about 1,000 km west of the large volcanic feature known as "south spot." There are two geologic terrain units recognized within the landing site: lobate plains (lp) and cratered terrain (ct). The lobate plains unit is the most extensive unit in the mapped area. The cratered terrain occupies most of the western part of the area but only about 1/6 of the southern part of the three sigma landing ellipse includes this unit. A small patch of cratered terrain also is found southeast of the landing ellipse. An area about 30-40 km wide, extending almost 300 km north from the center of the landing ellipse contains a number of rolling ridges, scarps, subdued craters, and circular depressions. This area is thought to be a ridge or high area of underlying cratered terrain that is thinly mantled by lobate plains material; a subdued expression of the underlying terrain is seen in the lobate plains material.

Of the two geologic terrain units within the landing site, the lobate plains material, as seen at A-camera resolution, presents the least hazards to a Viking spacecraft. The rough rims and walls of a few widely dispersed craters on the lobate plains material are the most hazardous features in the landing site; however, they probably occupy less than one percent of the total area of the landing ellipse. Other hazards are the slopes of escarpments which may be as steep as 30°, but these also occupy less than one percent of the total landing ellipse. The cratered terrain, which occupies about 10 to 15 percent of the southern end of the landing ellipse, is somewhat rougher than the lobate plains; however most craters, which are moderately spaced, are severely degraded and have smooth flat floors. Although this unit contains considerably more crater walls and steep escarpments than the lobate plains, its overall appearance is smooth and rounded. Crater walls and escarpments probably occupy one or two percent of the area of cratered terrain in the landing ellipse.

The area within the landing site covered by the lobate plains material is interpreted to be a basin flooded with basalts which probably flowed into the basin from the northeast. These flows have subsequently been covered by eolian materials. The thickness of this eolian blanket varies from place to place. The source of eolian material is probably the surrounding cratered terrain but a significant percentage of the material may come from the underlying basalt flows. Small craters probably excavate the underlying basalt and bring it to the surface. The highly comminuted and fractured material is then dispersed by eolian processes. Samples of the lobate plains material obtained by the Viking lander would probably comprise a mixture of the materials that make up the cratered terrain and the materials (basalt flows) that underlie the eolian cover in the basin.

EXPLANATION

lp
Lobate plains

Characteristics
Appears to bury, mantle, and overlap all older units. At A-camera resolution the lobate plains show little or no detail except for a few craters, a few subdued lobate and sinuous escarpments and ridges, and complex light and dark streaks. B-frames in the mapped area also show subdued ridges and low lobate scarps.

Interpretation
Unit is interpreted to be a basin filled with lava flows that are covered with eolian material of variable thickness.

ct
Cratered terrain

Characteristics
Consists of undulating plains with flat-floored, severely degraded, moderately spaced craters that are seldom over 30 to 40 km in diameter. North-trending subdued ridges and east-facing scarps are common. Within the mapped area, the unit has a subdued, rounded appearance. The contact of the cratered terrain with the lobate plains unit in the southern part of the mapped area is a scarp; in the northern part it is very indistinct, and the lobate plains unit appears to overlap and bury the cratered terrain. Because of the lack of a distinct boundary, the contact between the two units has been arbitrarily placed.

Interpretation
An ancient cratered terrain subsequently modified by other erosional processes.

c
Crater material undivided

Characteristics
Crater material includes rough rim deposits and wall material which is gradational in places with crater floors. Some craters contain hills and peaks in their centers which are mapped as central peak (cp).

Interpretation
Crater morphologies indicate impact origin.

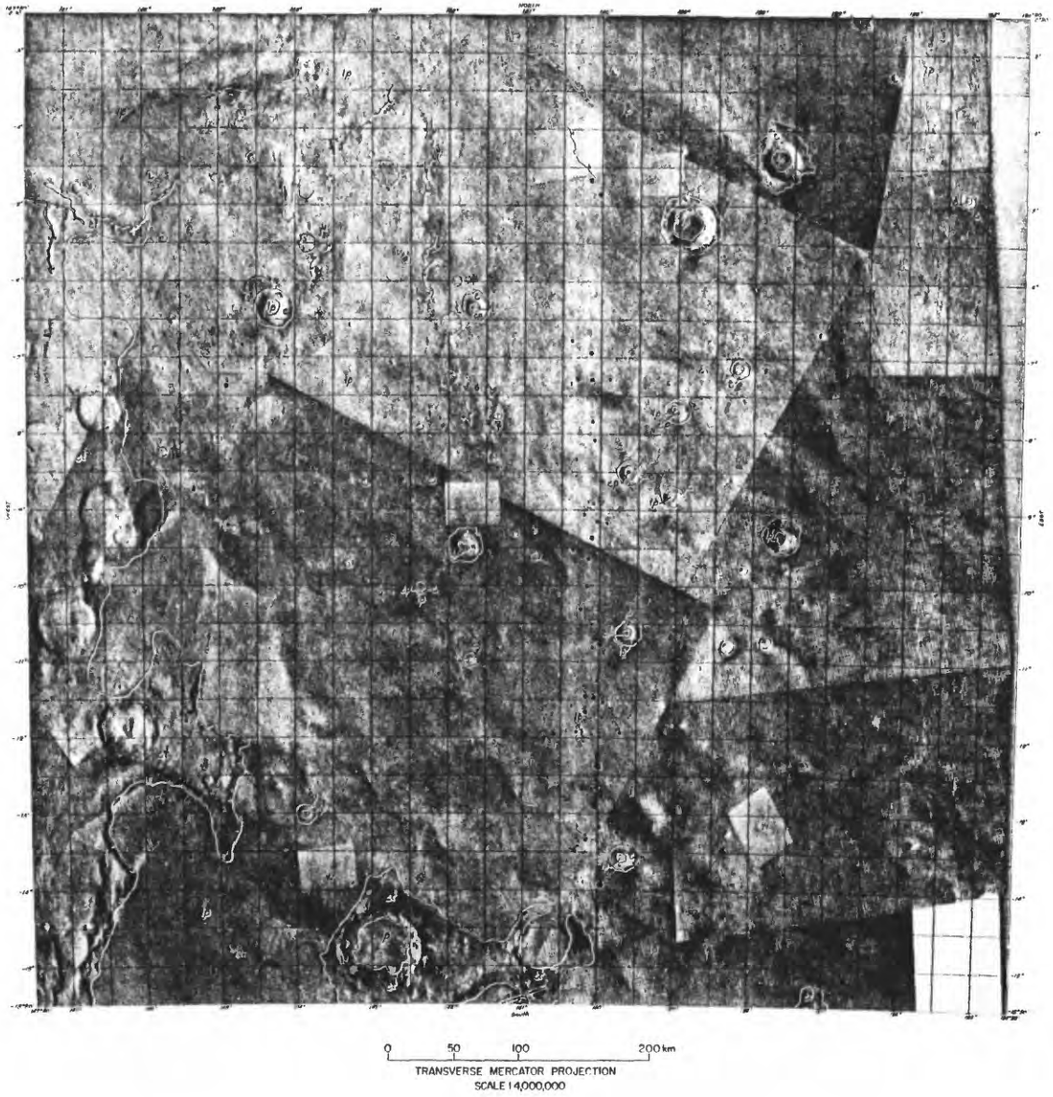

SITE 9 MEMNONIA

Scale 1:1,000,000

E. MORRIS 9

EXPLANATION

lp — Lobate plains

c — Crater material undivided

cp — Central peak

ct — Cratered terrain

Contact

excarpment, arrow point indicates down direction

enclosed basin surrounded by escarpment

Prominent rim crest of crater

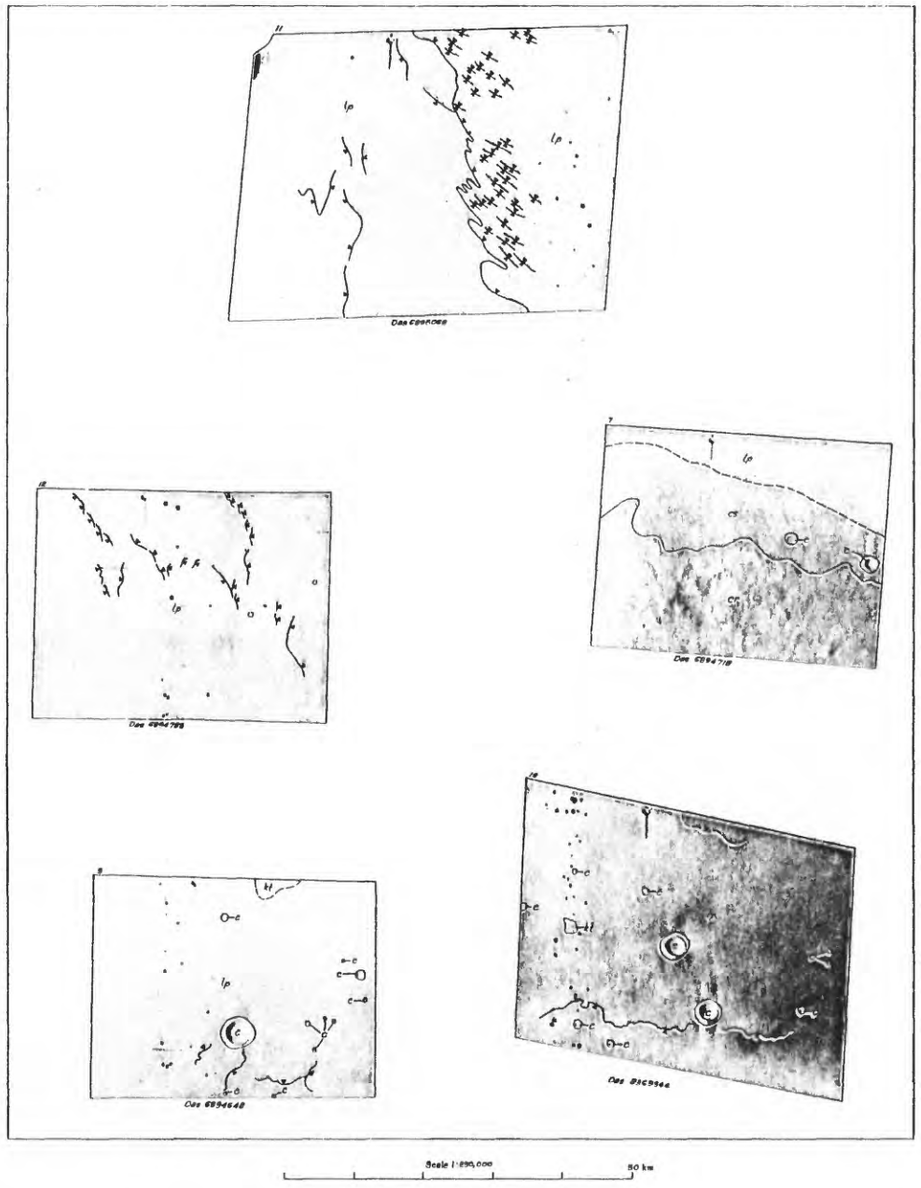

SITE 9 MEMNONIA

Scale 1:250,000

D. E. STUART-ALEXANDER

EXPLANATION

CRATER DEPOSITS

c	cr	cs

c - crater
cr - crater rim
cs - crater secondaries

kf

Knobby terrain

lp

Lobate plains

Contact
Dashed where buried
or extrapolated

Escarpment
Line marks base;
barbs point downslope

Trough

CANDIDATE VIKING LANDING SITE 10
AQUAE APOLLINARES (7.6°S., 177.6° W.)
1:1,000,000
By Daniel J. Milton and Alta S. Walker

Unit sp is believed to consist of a fine-grained eolian deposit or material reworked by wind action. It appears to be completely featureless in a B-frame at 7.6° S., 177.6° W.

The southwest map area contains a large volcanic complex. Volcanic features are progressively less distinct away from the caldera. The area mapped as lava plains probably consists of lava flows; that mapped as lp/sp may be either flows or alluvial deposits. Possibly the lava flows extend into the sp unit as far as the albedo boundary shown on the map, the ridged and grooved terrain (shown in B-frame DAS 06606883) is the edge of the lava plain; if so, the lava plain is unacceptable for landing.

Much of the 1 and 3 ellipses are on darker material like the ambiguous volcanic/sediment classification found at site 9. The 3 ellipse consists of volcanic materials in the southwest portion and a miscellany of raised plains and small craters in the northeast portion; both are probably acceptable if not desirable for landing. The ellipse could easily be adjusted to a safer target point in the sp unit, or to change azimuth for orbital purposes.

No relevant radar data exist for evaluating landing hazards at site 10. The elevation is acceptable. Based on photointerpretation, landing safety is classified as "good" for unit sp or the lower eastern slopes of the caldera, "acceptable" on units rt and rp, and "poor" to "hazardous" on all other map units.

EXPLANATION

rt
Rolling terrain

Characteristics
NE-SW oriented light and dark blotches and streaks.
Interpretation
Smooth plain modified by eolian activity. Large-scale relief probably low; possibly broad sand ridges and deflation basins.

cr
Crater rim

Characteristics
Rough rim of fairly fresh impact crater.

c
Crater

Characteristics
Contact drawn at rim crest, which is usually narrow and raised.

ft
Fretted terrain

Characteristics
Abundant steep sided hills rising from smooth floor.
Interpretation
Eroded terrain, probably originally lava plain, with mesa-like remnants.

lp
Lava plain

Characteristics
Complex crater with radial grooves on outer slope, grading eastward into more featureless surfaces with widely separated scarps.
Interpretation
Old, somewhat eroded volcanic complex, with summit caldera and exterior lava flows. Scarps may be flow fronts or erosional. A well developed regolith probably exists on lower slopes.

sp
Smooth plain

Characteristics
Featureless plain, except for slight vague albedo markings and some small craters.
Interpretation
Alluvium, surface materials probably largely of eolian origin. Dark areas in southwest of plain are probably alluvium of somewhat different mineral composition or coarser particles. As a less likely alternative, dark areas could be lava plains on the distal edge of the volcanic complex.

rp
Raised plain

Characteristics
Includes isolated, internally featureless dark areas bounded by outward-facing low scarps, an area in the northwest with some irregular and (at B-frame scale) complex fracturing, and areas at the south edge of the plain that are apparently gently sloping and show barely resolvable or widely spaced relief features.
Interpretation
Probably similar to smooth plains, but with some exposed bedrock and uplifted and eroded areas.

fp
Fractured plain

Characteristics
Raised areas with close-set parallel lineaments.
Interpretation
Eroded remnants of old terrain with jointing accentuated by wind scour. Probably much bedrock exposed.

ct
Cratered terrain

Characteristics
Abundant large craters, with irregular relief in intercrater areas.
Interpretation
Ancient impact-cratered terrain, surface much modified by subsequent processes.

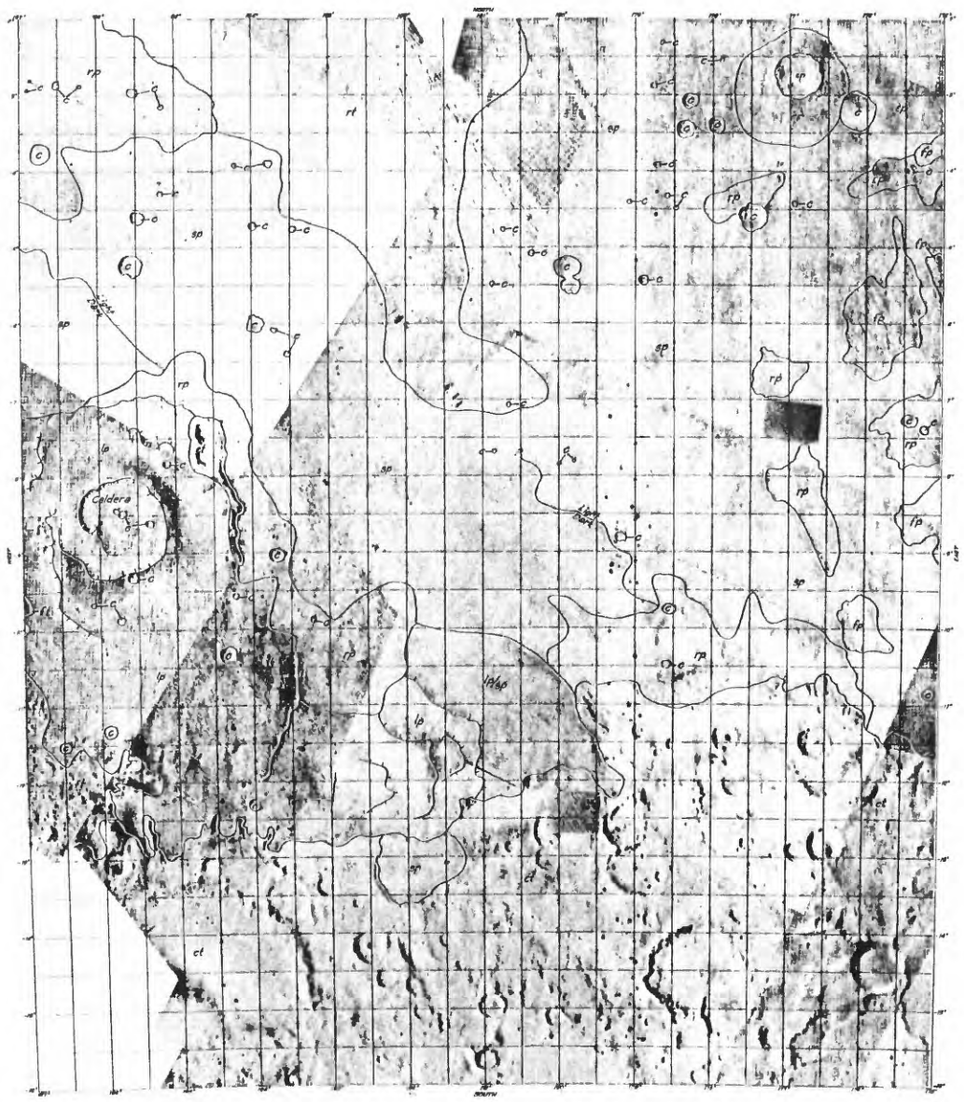

SITE 10 AQUAE APOLLINARES

Scale 1:1,000,000

DANIEL J. MILTON AND ALTA S. WALKER

EXPLANATION

rt
Rolling terrain

cr
Crater rim

c
Crater

ft
Fretted terrain

lp
Lava plain

sp
Smooth plain

rp
Raised plain

fp
Fractured plain

ct
Cratered terrain

Light / Dark
Albedo contrast

Contact

Escarpment
Line drawn at top;
hatchures point downslope

(no page 50)

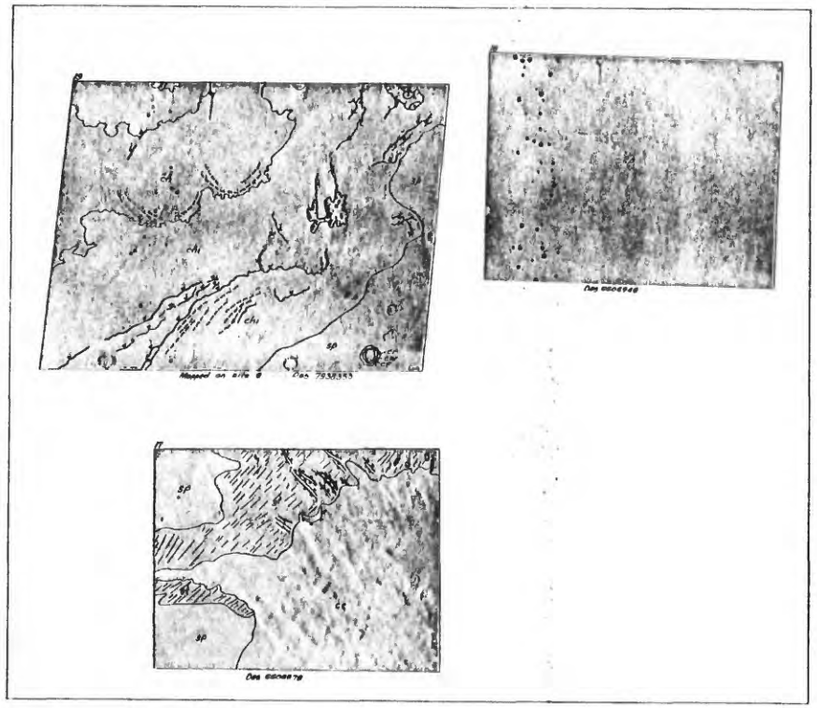

SITE 10 PART OF AQUAE APOLLINARES

Scale 1:250,000

E. C. MORRIS AND GEORGE W. COLTON

EXPLANATION

sp
Smooth plains material

kt
Knobby terrain

ct
Cratered terrain

ch
Chaotic terrain

chi
Incipient chaotic terrain

gt
Grooved terrain

c | cr | cw | cf
Crater materials

c-crater
cr-crater rim
cw-crater wall
cf-crater floor

Contact
Dashed where buried or extrapolated

Scarp
Barb points down slope

Groove or lineation

Small graben

Closed basin

Form line

Slump mass
arrow points in direction of movement

Prominent rim crest of crater

Buried crater rim crest

CANDIDATE VIKING LANDING SITE 12
HESPERIA-"DANDELION" (16°S, 251°W)
1:1,000,000
By Carroll A. Hodges

The ellipse of potential interest is centered at -16°, 251°, northeast of the large volcanic center, "Dandelion". The target material is a level plain (lvp) apparently continuous with lava flows from the volcano. This plain is largely devoid of the wrinkle ridges which dominate the topography of the adjacent plains unit (rgp); the two units appear to be gradational, however, and probably consist of the same, or similar, volcanic materials, emanating from the "Dandelion" center.

To the northeast is a highly cratered terrain (ep), characterized by dendritic channels and short gullies, giving an "etched" appearance to the plain; a low escarpment appears to separate this terrain from the higher lava plains. The marked contrast in crater densities suggests that the volcanic plains are younger, and probably overrode the etched plain, but the original lava escarpment is being dissected.

Light and dark "wind tails" or plumose streaks are prominent on the plains and suggest that the windswept surface may have been partially stripped of regolith material, and eolian sediments redeposited elsewhere. Exposure of bedrock is also suggested by the relatively high dielectric constants of 5.6-6.2 (Haystack radar, 1971) across parts of the volcanic plains. Radar data indicate rms slopes averaging 3.5 for the level plains unit and 3.7-4.3 for the ridged unit, confirming the generally planar character of both units.

Within the landing ellipse, fairly young volcanic material would likely be sampled, with possible components of exotic eolian debris derived primarily from the cratered "highland" terrain.

EXPLANATION

d
Dark materials

Characteristics
Probably residual debris, possibly coarse-grained, concentrated on downwind parts of crater floors and commonly forming "windtails" beyond crater rims.

Interpretation
Interpreted as eolian material or lag gravels, perhaps residual alluvial or impact debris. Bright plumes, eolian debris, are not mapped.

cd
Cratered dome

Characteristics
Dome with irregularly shaped summit depression; radial ridges and valleys, concentric graben.

Interpretation
Interpreted as shield volcano.

lvp
Level plain

Characteristics
Relatively level surface; few craters, sparse wrinkle ridges in contrast to adjacent ridged plains.

Interpretation
Interpreted as volcanic plain.

rgp
Ridged plain

Characteristics
Plain characterized by numerous wrinkle ridges.

Interpretation
Interpreted as volcanic plain gradational with unit lvp.

ep
Etched plain

Characteristics
Cratered terrain adjacent to volcanic plain; network of channels and gullies.

Interpretation
Interpreted as eolian debris.

c
Craters

Characteristics
Rim, wall, and floor materials of all craters. No designation of relative ages.

Interpretation
Interpreted as craters mostly of impact origin.

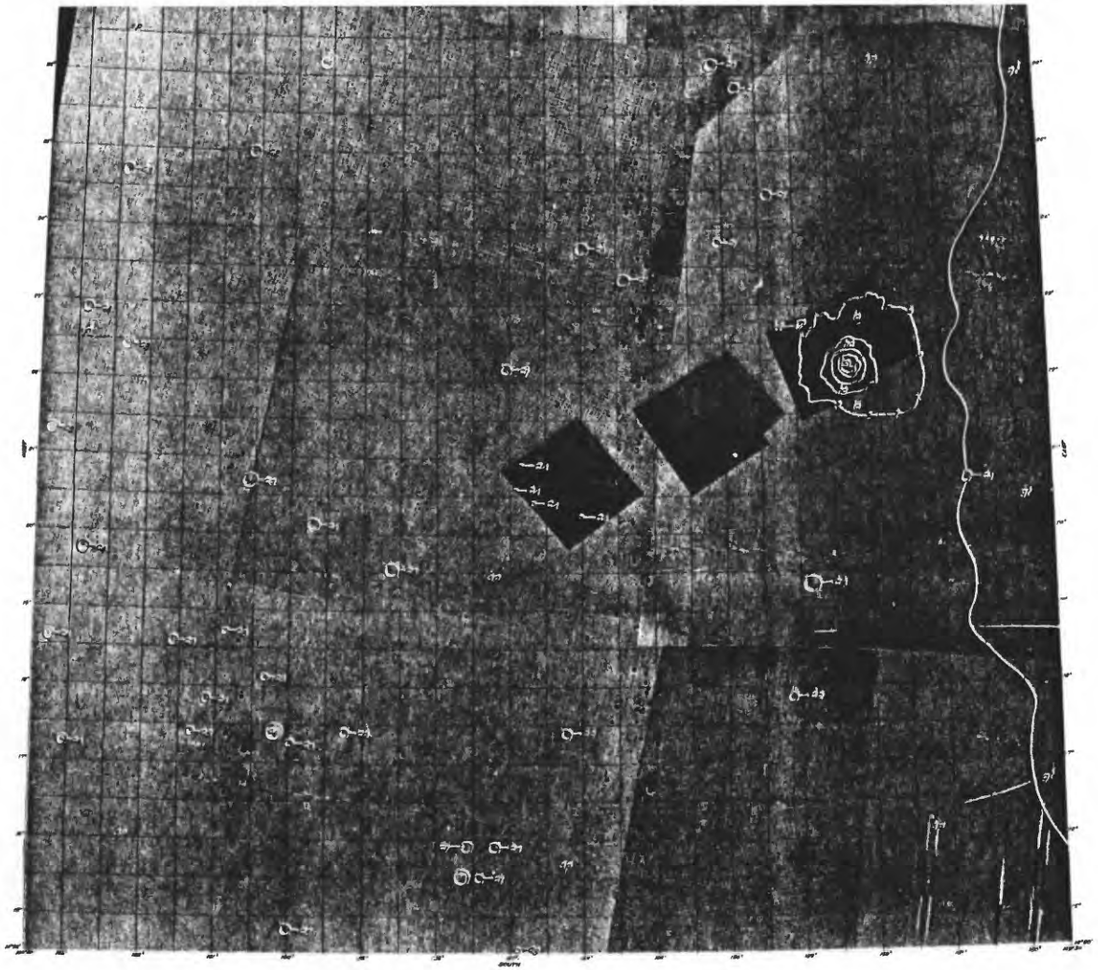

0 50 100 200 km

TRANSVERSE MERCATOR PROJECTION
SCALE 1:4,000,000

SITE 12 HESPERIA

Scale 1:1,000,000

CARROLL ANN HODGES

EXPLANATION

sp — Smooth plain

d — Dark materials

cd — Cratered dome

lvp — Level plain

rgp — Ridged plain

ep — Etched plain

c — Craters

Approximate geologic contact, dotted where buried

Apparent "stream" channel

Rim crest of crater

Narrow graben or structurally controlled furrow

Rim crest of degraded crater with no obvious rim materials

Base of scarp (crest not well defined)

Wrinkle ridge

Crest of prominent scarp

APPENDIX I

SITE CERTIFICATION RATIONALE

The instruments on board the Viking lander are designed to search for signs of past or present life in the fragmental surface materials at the landing site. Therefore the main consideration in nominating candidate landing sites is to select those where the environment is or may have been conducive to the development of life forms. The fundamental requirements for life processes are presence of water and appropriate temperatures. Water may occur in several ways:

1. Areas of production: water and CO_2 are among the products from volcanoes. Prime candidate areas are those near active, or recently active, volcanic centers.

2. Areas of collection: water may be collected in low areas by flowage from surface channels or by undergound flow. Prime candidate sites are basins into which surface or subsurface flow is directed.

3. Areas of storage: water may be stored in the polar caps, in permafrost layers (subsurface frozen water), in subsurface reservoirs, or as water adsorbed on the fragmental surface material. Prime candidate sites are those near the polar cap, or where permafrost or subsurface waters may be available at or near the surface.

The relative importance of these occurrences is hard to evaluate, and the geologists who nominated the candidate landing sites had to base their selections on their understanding of the geologic, geophysical, and geochemical attributes of each site. Other factors, such as an appropriate atmospheric composition and pressure, and seasonal changes in the chemistry and physical composition of the rock and sediment substrate related to the seasonal changes of the planet's atmosphere also had to be considered.

The task was to select two sites which met the constraints imposed by suitable temperature and presence of water, yet which would represent as widely diverse geologic settings as possible. A committee of geologic mappers, chaired by Harold Masursky, divided the sites arbitrarily into two groups and designated a preferred prime and backup site for each group. The viability of these sites was then matched against mission operation constraints, that is, mutual support of one orbiter for the other landing site, et cetera. The final site choice was based on both operational and scientific considerations.

SCENARIO I

The prime A site, Viking candidate site 3, or "Chryse" is an area where several large channels have deposited sediments eroded from the "continental" type rocks of the highlands to the south. This site is an area where water may have collected. Materials available to the sampler may contain organic material formed during an earlier wet period, which would be detectable by the gas chromatograph mass spectrometer. Materials may also show signs of fluvial erosion and shaping.

The prime B site, Viking candidate site 9, or "Memnonia" is an area of lobate plains interpreted as basaltic lava flows thinly mantled by eolian deposits. The low elevation at this locality, and the presumed basaltic composition of the flows suggest that the area may represent "ocean floor" type rocks. The high water content in the atmosphere at the proper season makes this area the most likely to contain signs of life detectable by the biology instruments.

The orbital track for the two missions will be complementary; the track for the A mission covers the canyon region, and that for the B mission covers the volcanic region.

The two backup sites may represent less variation in the anticipated composition of the surface materials. Site 1 is backup for 3 in the A mission; site 10 is backup for 9 in the B mission. The backup sites represent compromises in landing objectives and orbital coverage.

SCENARIO II

The two prime sites are similar to those of Group I, but reversed in order. The prime A site, Viking candidate site 7, or "Amazonis" is in smooth plains at the mouth of several small channels. Close to the channel mouths the material may consist of fluvial debris eroded from the highlands. Farther north the surface materials may be eolian debris. The orbital tracks overfly terrain that may be of somewhat less interest scientifically than those of Group I.

As backup sites, candidate site 4 could be substituted for site 5 in the A mission, and site 8 for site 7 in the B mission. Both backup sites represent compromises similar to those for the backup sites in Group I.

SLOPE ANALYSIS OF THE MARTIAN EQUATORIAL BELT AT 30 KM RESOLUTION

By Richard J. Pike

INTRODUCTION

This report presents a statistical description of part of Mars with respect to slope angle, the most important constituent of surface roughness. The work described here is reminiscent of the terrain program undertaken in preparation for the lunar Surveyor spacecraft landings (McCauley, 1964; Rowan and others, 1971). Because the available Martian data are rather crude for terrain analysis applications, the results are preliminary and highly generalized. M. K. Ko, U.S. Geological Survey Computer Center Division, wrote the program by which the Martian topographic elevations were converted to slopes and then to slope statistics. His assistance is appreciated.

DATA

The statistical description of Mars is based on terrain slopes that have a constant length of about 30 km. The raw data are roughly even-spaced altitudes generated by the Mariner 9 ultraviolet spectrometer experiment (Hord and others, 1972). The UVS elevations are arrayed across the planet in discontinuous, SSW-NNE profiles that vary in length and are roughly 500 km apart in the E-W direction. The horizontal distances between adjacent elevations were calculated by conventional solutions of oblique spherical triangles. Individual slope values are defined arbitrarily by straight lines joining adjacent elevations along a profile. Slope statistics were generated only for profiles which contained at least 33 elevations, none of which were less than 20 km apart or more than 50 km apart. These criteria, which eliminated about 1,300 of the 6,600 original elevations, assured that the remaining data would be of adequate quantity and uniformity for statistical manipulation. Certainly, the slope statistics are only as reliable as the overall quality of the raw UVS measurements. The resulting 104 topographic profiles (map, figure 1), each containing up to 78 elevations and averaging 32 km between adjacent elevations, provide planetwide coverage of Mars within 40° of the equator.

TERRAIN PARAMETERS

The low and variable resolution of the Martian UVS data and the small number of slopes per profile restrict the choice of terrain descriptors to the simplest central tendency and dispersion measures describing two types of slope-frequency distributions (Rowan and others, 1971). For the algebraic distribution, slopes facing west are designated negative and east-facing slopes are positive. This distinction yields a symmetrical, if not perfectly Gaussian, distribution for which meaningful central tendency and dispersion statistics can be computed. Ignoring the plus-minus convention results in an absolute slope-frequency distribution for which only central tendency statistics are appropriate. Seven slope parameters were calculated from frequency distributions that were derived for each profile: (1) absolute mean, (2) absolute median, (3) absolute maximum, (4) algebraic mean, (5) algebraic median, (6) algebraic standard deviation, and (7) dispersion coefficient. Defined as algebraic standard deviation divided by absolute mean, the dispersion coefficient is analogous to a well-known statistic, the coefficient of variation (Croxton and others, 1967) it measures relative dispersion.

DISCUSSION

Statistics describing 20 of the 104 profiles are not very representative because each of the 20 samples crosses two distinctively different terrain types. Most of these polymorphic terrains can be recognized easily from values of the slope dispersion coefficient. Prior analysis of lunar and terrestrial slopes (Pike, 1972a) shows that values of this parameter typically vary between 1.32 and 1.40 for homogeneous terrain samples. Inhomogeneous, or polymorphic, samples have significantly higher dispersion values. According to table 3, most Martian slope dispersion values cluster between 1.20 and 1.49 (fig. 3C-E); higher values tend to be scattered widely between 1.50 and 2.18. Inspection of the map, figure 1, reveals the obviously polymorphic character of the 20 samples exceeding 1.50 in dispersion. Commonly, steep slopes on canyonlands and volcanoes are mixed with much smoother topography of the adjoining plains (figs. 3A, B). This combination yields standard deviations or algebraic slope that are disproportionately large for the value at the absolute mean slope. These 20 samples account for the worst of the scatter in figure 2. Providing the number of slopes per profile is not reduced to an unacceptably low figure, each of these polymorphic samples can be subdivided into two more homogeneous profiles, and the slope statistics recalculated. For example, the mean absolute slope value for the smoother portion of sample 20, which crosses Amazonis Planitia, (fig. 3B) is only 0.47° whereas it is 0.85° for the undivided sample, which includes the southern flank of Olympus Mons. Results of this procedure would show up on the map (fig. 1) as two additional concentrations of smooth samples, located just north and south of the canyonlands region, and including two more of the Viking sites. In addition, the first two smooth areas should be somewhat enlarged. Thus the statistics presented here support photointerpretive conclusions that the candidate landing sites lie in the smoothest regions of Mars.

Predictions of fine-scale surface roughness can be developed from the generalized negative correlation between slope length and those slope statistics which are calculated over a constant base length (McCauley, 1964; Pike, 1969). Figure 4 summarizes current information on the mean absolute slope: base length relation for three planets. The terrestrial envelope is derived from contour map data describing highly contrasting terrain types, and accordingly, is very broad. The range of lunar slope means (0.75 km resolution data from Rowan and others, 1971) lies completely within the terrestrial data; it is more restricted than the terrestrial envelope because of the photometric sampling technique used to obtain the data. The four linear extrapolative models, which were generated from the 0.75 km lunar data, yield reasonable slope predictions at the 1-10 m scale. The Martian UVS data at about 30 km base length bracket these four models with remarkable symmetry. However, the serious discrepancy in figure 4 between the UVS slope data and slope data (Pike, 1972b) calculated from the 1971 Mars radar results (Goldstone data) must be reconciled before reliance can be placed on extrapolations of any Martian topographic data. This discrepancy does not invalidate the relative roughness ranking of Martian profiles described here. Once reasonable mean slope predictions are possible in the absolute sense, entire slope-frequency distributions can be constructed at slope lengths most relevant to problems of spacecraft landing and vehicle maneuverability (Pike, 1969, 1972a).

RESULTS

The seven slope parameters calculated for each of the 104 profiles are listed in table 1 along with the identification number and the sample size. Most absolute values of mean and median algebraic slope are low, indicating that few profiles possess systematic asymmetry or are significantly tilted. Those profiles that are tilted transect large, steep terrain features with a regional slope (such as the south flank of Olympus Mons). Statistically the steepest slope values in each profile covary with absolute mean and median slope and with the algebraic standard deviation. Geographically, steepest slopes coincide with recognizeable terrain features, such as crater rim crests, volcanoes, rilles, and canyonlands terrain. These results all suggest that the UVS data are accurately describing topographic characteristics of Mars.

The relative roughness of the terrain transected by each sample is expressed symbolically in figure 1 by the width and configuration of the profile traces. Figure 2, the basis of the simple roughness classification used in figure 1, is a plot of algebraic standard deviation against absolute mean slope (Rowan and others, 1971). There are, by inspection, six natural breaks in the data in figure 2, yielding seven roughness classes. Table 2 gives summary data on the seven categories. The resulting proportions of rough (15%) and smooth (15%) samples to intermediate samples (70%) are a very reasonable subdivision of a planet into preliminary surface-roughness types; unusually rough and smooth areas stand out well. Most of the rougher profiles (fig. 3A-C) cross volcanoes or the canyonlands. The smoother profiles (fig. 3D, E) are preferentially located, in two clusters. One group lies roughly between 225° and 275°W longitude and between 10° and 40°N latitude; the other is between 150° and 180°W longitude and between 05°S and 20°N latitude. Seven of the ten candidate Viking landing sites under consideration in late 1972 are situated in or near these two smoother areas.

REFERENCES

Croxton, F. E., Cowden, D. J., and Klein, S., 1967, Applied General Statistics, Prentice-Hall, 754 p.

Hord, C. W., Barth, C. A., Stewart, A. I., and Lane, A. L., 1972, Mariner 9 ultraviolet spectrometer experiment: photometry and topography of Mars: Icarus, v. 17, p. 443-456.

McCauley, J. F., 1964, Terrain analysis of the lunar equatorial belt: U.S. Geol. Survey open-file report, 44 p.

Pike, R. J., 1969, Lunar surface geometry, in Lunar terrain and traverse data for lunar roving vehicles design study: Preliminary U.S. Geol. Survey Rept., Sect. B, p. B1-B46.

Pike, R. J., 1972a, Lunar landscape morphometry, Parts I, II, and III; unpublished manuscript, 119 p.

_____, 1972b, Preliminary slope-frequency distributions on Mars: Viking Data Analysis Team (VDAT) Report, 1972.

Rowan, L. C., McCauley, J. F., and Holm, E. A., 1971, Lunar terrain mapping and relative roughness analysis: U.S. Geol. Survey Prof. Paper 599-G, 32 p.

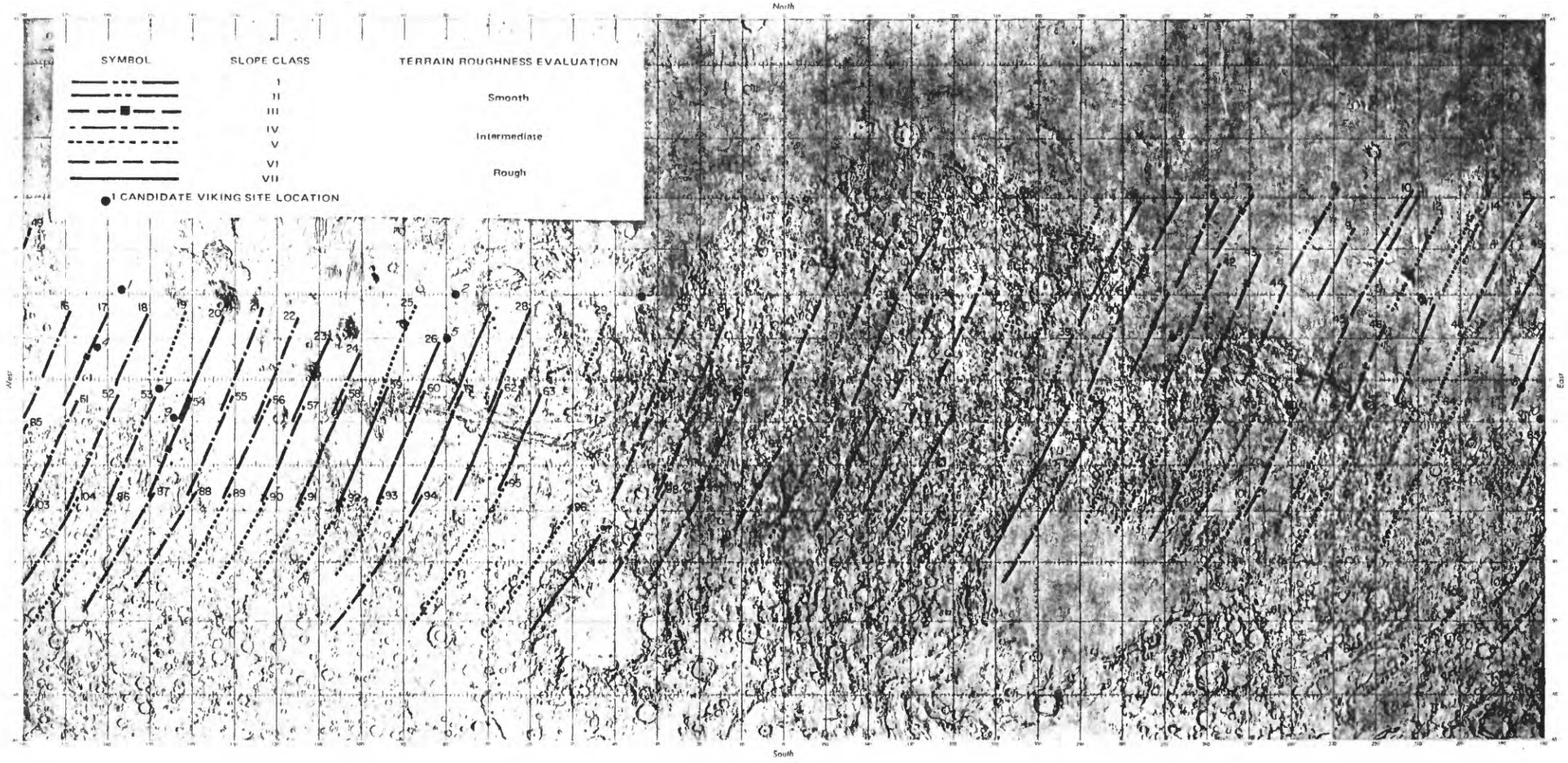

Figure 1. Index map of topographic profiles showing seven classes of terrain roughness

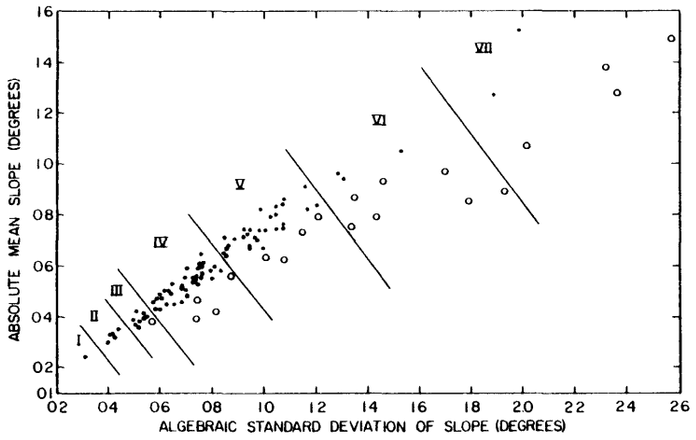

Figure 2. Scatter diagram of terrain profiles

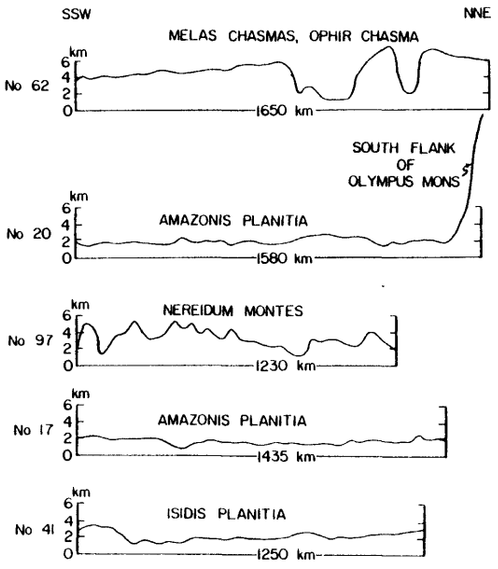

Figure 1. Representative topographic profiles of Mars

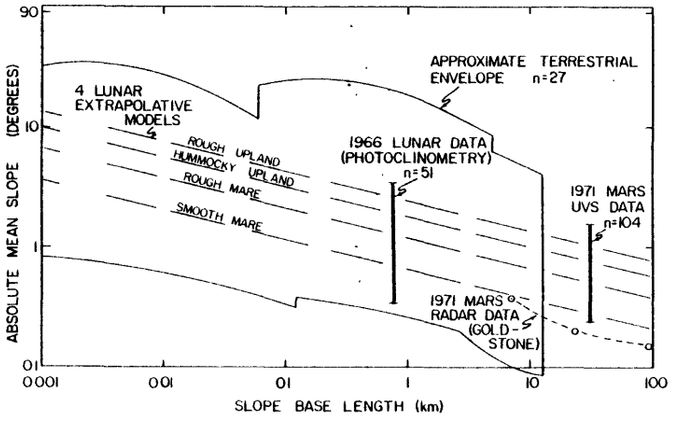

Figure 4. Relation between slope angle and slope length for three planets

Table 1. Martian slope statistics at 30 km resolution

Sample	N	Mean (alg.)	Mean (abs.)	Steepest	Std.dev. (alg.)	Dispersion coeff.	Median (abs.)	Median (alg.)
1	47	-0.082	0.427	2.13	0.587	1.38	0.291	-0.108
2	32	-0.153	0.551	2.29	0.738	1.34	0.403	-0.235
3	74	0.018	0.638	2.80	0.858	1.33	0.483	0.043
4	54	-0.098	0.589	1.55	0.705	1.20	0.572	-0.069
5	43	-0.049	0.376	1.78	0.523	1.39	0.287	-0.024
6	35	-0.068	0.416	3.47	0.815	1.96	0.262	-0.010
7	34	-0.112	0.379	1.97	0.568	1.50	0.216	-0.028
8	36	-0.026	0.244	0.96	0.313	1.28	0.197	-0.020
9	33	0.011	0.386	2.70	0.737	1.91	0.188	0.041
10	32	-0.109	0.474	1.38	0.587	1.24	0.375	-0.090
11	55	-0.046	0.463	2.48	0.689	1.49	0.281	-0.010
12	46	0.121	0.791	4.39	1.213	1.53	0.509	-0.034
13	40	0.081	0.720	2.17	0.939	1.30	0.595	0.061
14	35	0.124	0.714	2.20	0.931	1.30	0.609	0.080
15	54	-0.014	0.557	3.06	0.880	1.58	0.332	0.103
16	54	-0.049	0.346	1.30	0.435	1.26	0.299	0.032
17	48	-0.029	0.409	1.50	0.537	1.32	0.326	0.028
18	36	-0.013	0.329	0.87	0.407	1.24	0.270	-0.001
19	33	-0.020	0.616	5.10	1.075	1.75	0.444	-0.172
20	52	-0.458	0.845	8.28	1.786	2.11	0.313	-0.070
21	51	-0.012	0.485	1.32	0.602	1.24	0.392	-0.108
22	53	0.096	0.491	2.24	0.651	1.33	0.439	0.160
23	42	0.066	1.379	7.94	2.326	1.69	0.661	-0.012
24	32	0.374	0.639	1.89	0.760	1.19	0.457	0.381
25	53	0.423	0.676	5.08	0.954	1.41	0.556	0.270
26	37	0.319	1.489	8.61	2.575	1.73	0.661	0.145
27	53	-0.173	1.284	8.07	2.366	1.84	0.427	-0.048
28	52	-0.006	0.888	10.91	1.927	2.17	0.466	0.129
29	33	0.188	0.763	3.02	1.079	1.41	0.539	0.349
30	52	-0.018	0.462	3.15	0.754	1.63	0.259	0.019
31	51	0.088	0.610	2.14	0.770	1.26	0.477	-0.134
32	32	0.164	0.739	3.52	1.046	1.42	0.458	0.151
33	62	-0.007	0.586	2.55	0.808	1.38	0.420	0.049
34	43	0.091	0.827	2.74	1.046	1.26	0.738	0.281
35	53	0.050	0.395	1.99	0.546	1.38	0.297	0.120
36	52	0.037	0.521	2.26	0.692	1.33	0.441	0.018
37	55	-0.004	0.604	1.97	0.760	1.26	0.456	-0.145
38	49	0.011	0.815	3.33	1.172	1.44	0.492	0.141
39	44	0.130	0.738	2.98	0.987	1.34	0.564	0.239
40	42	0.153	0.454	2.38	0.664	1.46	0.287	0.116
41	41	0.041	0.357	1.81	0.520	1.46	0.241	-0.089
42	66	0.051	0.445	2.84	0.634	1.43	0.319	0.088
43	64	0.108	0.373	1.91	0.511	1.37	0.281	0.162
44	48	-0.016	0.329	0.92	0.426	1.30	0.238	0.023
45	39	0.072	0.428	2.31	0.599	1.40	0.309	0.127
46	42	0.012	0.386	1.32	0.500	1.29	0.321	-0.057
47	47	-0.009	0.502	2.31	0.698	1.39	0.344	0.045
48	42	0.111	0.735	3.29	1.007	1.37	0.587	0.157
49	60	0.011	1.051	4.85	1.531	1.46	0.606	-0.101
50	34	-0.024	0.965	6.44	1.703	1.76	0.462	0.019
51	49	-0.011	0.534	2.59	0.747	1.40	0.406	-0.029
52	50	0.003	0.462	1.33	0.580	1.26	0.403	0.064

Table 1 (continued)

Sample	N	Mean (alg.)	Mean (abs.)	Steepest	Std.dev. (alg.)	Dispersion coeff.	Median (abs.)	Median (alg.)
53	49	0.002	0.303	1.06	0.398	1.31	0.232	-0.017
54	44	-0.011	0.394	1.83	0.538	1.37	0.338	-0.064
55	46	-0.055	0.473	1.90	0.610	1.29	0.407	-0.045
56	45	-0.117	0.594	2.02	0.760	1.28	0.515	-0.106
57	45	-0.190	0.572	2.67	0.765	1.34	0.401	-0.161
58	51	-0.144	0.874	6.48	1.345	1.54	0.540	-0.223
59	54	-0.128	1.270	6.41	1.887	1.49	0.863	0.096
60	49	-0.006	6.751	6.03	1.335	1.78	0.443	-0.054
61	51	-0.119	0.925	4.89	1.461	1.58	0.519	-0.122
62	51	-0.080	1.073	8.20	2.016	1.88	0.338	-0.107
63	45	0.005	0.789	5.61	1.437	1.82	0.352	0.017
64	46	0.003	0.534	2.49	0.743	1.39	0.329	-0.055
65	47	-0.005	0.502	1.44	0.620	1.24	0.446	-0.063
66	45	0.004	0.320	1.20	0.433	1.35	0.232	0.021
67	38	0.036	0.418	1.06	0.507	1.21	0.406	-0.030
68	58	0.003	0.634	4.42	1.006	1.59	0.355	-0.010
69	54	0.015	0.498	1.50	0.638	1.28	0.422	0.077
70	48	0.019	0.483	2.29	0.709	1.47	0.293	0.006
71	55	0.006	0.936	4.73	1.314	1.40	0.678	-0.027
72	57	-0.005	0.743	2.76	0.947	1.27	0.635	-0.133
73	69	-0.045	0.843	2.97	1.080	1.28	0.592	0.038
74	64	-0.056	0.955	3.80	1.287	1.35	0.706	0.063
75	76	-0.057	0.550	2.46	0.756	1.37	0.330	-0.016
76	51	-0.080	0.839	5.13	1.208	1.44	0.628	-0.040
77	56	-0.062	0.738	2.59	0.927	1.26	0.600	-0.087
78	56	-0.026	0.546	1.46	0.698	1.28	0.396	-0.038
79	69	-0.016	0.647	2.87	0.848	1.31	0.500	-0.066
80	48	0.087	0.509	2.37	0.693	1.36	0.360	0.138
81	53	0.093	0.910	2.97	1.155	1.27	0.769	0.288
82	64	0.025	0.705	3.88	0.973	1.38	0.546	0.138
83	51	-0.038	0.858	2.63	1.083	1.26	0.752	-0.134
84	65	0.019	0.799	3.32	1.052	1.32	0.614	-0.176
85	32	-0.023	0.528	1.26	0.645	1.22	0.411	-0.030
86	55	-0.030	0.668	3.22	0.951	1.42	0.419	-0.031
87	49	-0.094	0.556	2.23	0.742	1.34	0.483	-0.090
88	40	0.017	0.544	1.80	0.737	1.35	0.345	0.039
89	35	-0.003	0.696	2.55	0.981	1.41	0.413	-0.119
90	33	-0.013	0.817	2.99	0.993	1.22	0.772	0.307
91	36	-0.069	0.789	2.37	1.032	1.31	0.578	-0.046
92	32	-0.092	0.700	1.95	0.878	1.25	0.603	-0.098
93	34	0.016	0.706	1.85	0.854	1.21	0.621	-0.221
94	55	-0.064	0.581	2.58	0.799	1.38	0.407	0.021
95	58	-0.092	0.679	2.67	0.869	1.28	0.478	-0.184
96	51	-0.022	0.673	3.26	0.995	1.48	0.434	-0.038
97	37	-0.027	1.530	5.87	1.992	1.30	1.207	-0.034
98	38	-0.009	0.594	1.77	0.751	1.26	0.543	-0.042
99	41	-0.036	0.546	2.69	0.814	1.49	0.318	-0.014
100	39	0.099	0.726	4.02	1.151	1.59	0.378	0.039
101	34	-0.005	0.667	1.93	0.858	1.29	0.483	0.010
102	45	-0.172	0.751	3.54	1.079	1.44	0.542	-0.187
103	40	-0.049	0.597	1.93	0.762	1.28	0.501	-0.010
104	57	-0.074	0.581	3.03	0.843	1.45	0.414	-0.104

Table 2. Summary data on seven relative-roughness classes of Martian terrain

Terrain roughness evaluation	slope classes	n	Median of absolute means in Figure 2 (°)	Median of algebraic standard deviations in Figure 2 (°)	Line symbol in Figure 1
	I	1	0.24	0.31	
Smooth	II	5	0.33	0.42	
	III	9	0.39	0.52	
Intermediate	IV	40	0.53	0.74	
	V	33	0.74	1.00	
Rough	VI	10	0.91	1.45	
	VII	6	1.33	2.17	

Table 3. Distribution of dispersion coefficient for slopes from 104 Martian topographic profiles

Values of Dispersion Coefficient*	Frequency	Sample No.
1.20 - 1.24	10	-
1.25 - 1.29	21	-
1.30 - 1.34	16	-
1.35 - 1.39	16	-
1.40 - 1.44	12	-
1.45 - 1.49	9	-
1.50 - 1.54	3	7, 12, 58
1.55 - 1.59	4	15, 61, 68, 100
1.60 - 1.64	1	30
1.65 - 1.69	1	23
1.70 - 1.74	1	26
1.75 - 1.79	3	19, 50, 60
1.80 - 1.84	2	27, 63
1.85 - 1.89	1	62
1.90 - 1.94	1	9
1.95 - 1.99	1	6
2.00 - 2.04	0	-
2.05 - 2.09	0	-
2.10 - 2.14	1	20
2.15 - 2.18	1	28

*Defined as algebraic standard deviation of slope divided by the absolute mean slope.

INFRARED CHARACTERIZATION OF MARTIAN SURFACE

By Joseph T. O'Connor

ABSTRACT

Mariner 6 and 7 infrared reflectivities have been correlated with Mariner 9 photogeological units with good internal consistency. Laboratory measurements of infrared reflectivities are not inconsistent with a model of fine windblown feldspathic deposits comprising the bright areas while coarser grained basaltic materials comprise (some) dark areas. Semitone areas may be fine grained deposits of mixed reflectivity.

INTRODUCTION

In order to provide effective planning for the impending Viking lander it is desirable to have a pre-knowledge of the nature of the surface on which the landers will descend. Many methods are being used to investigate this surface, including photogeology, radar-reflectivity, ultraviolet reflectivity, and infrared emission from the Mariner 9 IRIS. It is most likely that no one of these techniques will give a unique characterization of the surface of Mars. Hopefully, together, they will provide information on which a rational decision can be made as to the pertinent surface properties of the desired locations.

To the previously listed techniques we would add infrared reflectivity as determined from the Mariner 6 and 7 traverses of the Martian surface. In utilizing infrared reflectivity it must be noted that there are many factors which contribute to the reflectivity of the surface. The complexity of these factors is further complicated when a planetary surface is observed through an atmosphere which contains variable amounts of suspended particulate matter. Among factors affecting the infrared reflectivity are the geometry of the observation, temperature of the surface, the grain size of the surface, the packing of the grains on the surface, the composition of the surface material, the temperature gradient within the surface material, the composition of the atmosphere, the temperature of the atmosphere, the composition of particulate material suspended in the atmosphere, the grain size of the material suspended in the atmosphere, and the temperature of the material suspended in the atmosphere. Many of these factors operate independently of each other, or in some intricate and unknown relation to each other. Most of them are only poorly known for the surface or the atmosphere at any given reflection point. Accordingly we have not attempted to define the reflectivity of the Martian surface in the infrared on a theoretical or detailed parametric basis. We have instead attempted to correlate infrared reflectivity obtained from Mariners 6 and 7 with photogeology obtained from the Mariner 9 photographs. We feel that by geologic interpretation of photographs and correlation of these interpretations with infrared reflectivities we may be able to deduce general physical properties of the geologic features observed.

DETAILS OF TECHNIQUE

Most of the geological units confined to this study were obtained from Mars Chart MC-19, the geology of which was mapped (in a generalized fashion) by the author and R. S. Saunders during the preliminary Viking-Lander site-selection exercise conducted under the auspices of the U.S. Geological Survey. This quadrangle is crossed by three paths of Mariner 6 and two paths of Mariner 7. It shows a great diversity of geological types including bright plains, dark plains, hilly terrain with abundant drainage patterns, chaotic terrain, canyonlands, mountainous terrain features, bright basins, and the ubiquitous craters. In addition to MC-19 information was obtained from MC-10, MC-11, MC-18, MC-20, MC-26, MC-27, and MC-28. Two main properties were looked for in the data relating to geological units. The first was the normal albedo of the surface unit, the second was the deviation of that unit from a Lambert surface. Since the two are not completely distinct, they will be discussed together in this report.

The locations of the Mariner 6 and 7 infrared spectra were obtained from Pimentel and Herr (1970). These locations were plotted on uncontrolled photomosaic prepared by the U.S. Geological Survey from Mariner 9 data. It is realized that locations of specific points on these charts may be off by a degree or so. Since the area covered by the spectrometer is generally three degrees normal to the path and a half a degree or so parallel to the path, this small location error should not be too serious.

In his article on lunar photometry (Minnaert, 1941) suggests a simple but useful function which relates the scattering of a real surface to that of a Lambert surface. This function, referred to as the "Minnaert Law," is:

$$B \cos \varepsilon = B_0 (\cos i \cos \varepsilon)^k$$

B = apparent reflectivity
B_0 = normal reflectivity
i = angle of incidence
ε = angle of emergence
k = limb darkening parameter

As described in Young and Collins (1971), an optically thin scattering atmosphere over a black planet would give cosine limb darkening (i.e. $k = 0$). The moon with no limb effect has $k = 0.5$; a Lambert surface (full cosine darkening) will give $k = 1.0$; and a specular-reflector corresponds to $k \to \infty$. In the visible part of the spectrum, measurements of $k = 0.7$ are common for observations of Mars. The value of k is obtained by plotting on log-log paper $(B \cos \varepsilon)$ v $(\cos i \cos \varepsilon) = 1$. Measurements of dark granular materials (Young and Collins, 1971), or those of hydrated iron oxide mixtures (3,4), have given values for B similar to those of Mars. We have measured the reflectivity of Mars at 4450 cm^{-1} using the Mariner 6 and 7 infrared spectrometers and made Minnaert plots of the data, isolating the points according to geologic units outlined above. These plots are presented in figure 1 and table 1. The following features are immediately apparent: most of the data for single geological units fall on or near straight lines when plotted in this fashion. These straight lines appear to define the different units having different normal albedos. Most of the unit plots have nearly the same slope for the Minnaert Law.

This slope of the Minnaert plots is steeper than observed in the visible spectrum, close to 1.0 for many of the units examined (table 1). Only the dark plains material showed an obvious deviation from the steep slope. This deviation in slope may be followed by hilly material with which the dark plains material is intimately associated.

From the Mariner 9 photographs we have reason to believe that some of the bright plains in the north of Thymiamata and the floor of Hellas are probably eolian in character. The similarity of slopes of the Minnaert plot may then imply a similarity in physical state for much of the Martian surface. Variations in albedo could be assigned to variations in composition of the surface. This variation could result largely from the selective winnowing out of certain components of the surface materials with respect to others. On the other hand, the lower slope and normal albedo of the dark plains material, and perhaps the hilly material as well, may indicate coarsening grain size in these units. Hoping to shed more light on this subject, we made laboratory measurements of the reflectivity of different materials at differing angles of incidence and emergence with a laboratory goniometer spectrometer kindly loaned to us for this purpose by K. Coulson, University of California at Davis. The results of this experiment are as follows:

The goniometer spectrometer was not set up to operate at 4450 cm^{-1}. Instead we made our measurements at 0.9 microns (11,100 cm^{-1}). Three materials were used as sample materials for this examination. The first was a basalt ash (lapilli size to fine-grained ash) occurring naturally in the Sunset Crater area near Flagstaff, Arizona. The second material was a very fine basalt ground to 250 to 400 mesh. The third material was the feldspar andesine ground to the same size as the fine basalt. Reflectivities were measured at two phase angles--50° and 84°--corresponding to two of the major phase angle measurements from the Mariner 6 and 7 data.

The reflectivities of these surfaces were very much as expected. The coarse basalt ash had a very low reflectivity. The fine basalt had a slightly higher reflectivity, and the andesine had the highest reflectivity. Plotting the laboratory data on Minnaert plots, we discovered a dependency of the slope of the curve on phase angle, something which was not noticed in the plots of the Mariner 6 and 7 data. For the two materials which showed good reciprocity, the slope at phase angle = 50° was lower than the slope at phase angle = 84°. There was a regular difference observed between the materials in the Minnaert plot as well (fig. 2). The coarse basalt ash showed the lowest apparent slopes as well as the largest divergence between slopes at different phase angles. The andesine showed the steepest slopes and the smaller difference between slopes at different phase angles. The fine basalt showed a Minnaert plot slope (at 50° phase angle) which was similar to that of the coarse basalt ash (at 84° phase angle). The specimen did not show reciprocity at 84° phase angle and the data at this phase angle were not included.

Comparing the measurements from Hellas Basin with those of the andesine from the laboratory, it is noticed that the slopes are fairly comparable. Both of these groups of measurements were the brightest obtained for their respective experiments. Unfortunately, we cannot make direct comparisons between the reflectivities of the laboratory samples and the Martian surfaces measured since no mutual calibration of the two instruments has been accomplished. If we assume from the television photographs of the Hellas Basin that this area is covered with a wind-drifted layer of wind winnowed basalt weathering products, we can construct a model of the Martian surface which is compatible with the results we have observed here. This model would owe its brightness (in Hellas) to the removal of the dark components of basalt over eons of weathering by the weathering process itself. The residuum would be largely feldspathic, of fine grain size (ten to one hundred microns), and deposited on the surface of the planet.

At the opposite end of the terrain spectrum would be the dark plains units (and possibly associated hilly units) of the equatorial zone. The surfaces here would be more comparable with the coarse basalt ash of the laboratory experiments. One could postulate either weaker or stronger winds to effect either less winnowing or more thorough removal of fines, but the resulting material apparently is coarser and more "rock-like" than that of the basins. Between these two extremes we have a number of semitone areas such as Pandorae Fretum wherein the albedo is lower than that of Hellas but the slope of the Minnaert plot is relatively steep. To the writer this suggests that the area is a mixture of windblown material, some derived by long weathering of surfaces, the other derived from younger fresher areas.

We have not mentioned intermediate rock types in this report because there is no evidence, in the Mariner 6 and 7 studies, of the presence of intermediate rocks (Herr and others, in prep.).

Much more work is necessary on this concept before all the loose ends can be tied together. This report is a rough draft prepared hurriedly for this particular conference. We hope to have a firmer consolidation of the study available by the middle of January.

CONCLUSIONS

Infrared reflectivities of geologic units on Mars have sufficient intraunit consistency and interunit difference to permit some interpretation of the characteristics of the units.

Terrestrial measurements of infrared reflectivities are consistent with an interpretation of Hellas (and other bright plains) as wind-drifted, fine-grained (10-100 μ), feldspathic weathering products of basalt. The measurements are also consistent with the dark plains being comprised of coarser basaltic ash (or rubble?).

More terrestrial materials should be examined at wave lengths closer to those of the Mariners 6 and 7 data before these conclusions are finally accepted.

REFERENCES

Dollfus, A., 1966, Contribution au colloque Caltech-JPD sur la lune et les planetes: Mars, in Proceedings of the Caltech-JPL Lunar and Planetary Science Conference, Sept. 13-18, 1965: JPL Tech. Mem. 33-267, p. 288-305.

Minnaert, M., 1941, The Reciprocity Principle in lunar photometry: Astrophys. Jour., v. 93, p. 403-410.

Pimentel, G. C., and Herr, K. C., 1970, Data format report: Final report for JPL contract 951722, University of California, Space Sciences Laboratory Series 11, Issue 44.

Young, A. T., and Collins, S. A., 1971, Photometric properties of the Mariner cameras and of selected regions on Mars: Jour. Geophys. Res., v. 75, no. 2, p. 432-437.

Table 1. Infrared reflectivity properties for Martian geologic units and terrestrial laboratory materials.

Unit or material	Phase angle (°)	Relative reflectivity	k	cm^{-1}
1. Hellas	83.6	40.1	1.086	4450
2. Eolian plains (Mariner 7)	48.3	34.9	1.021	4450
3. Pandorae Fretum (Mariner 7)	83.6	30.9	1.011	4450
4. Composite bright plains	85.9			
	83.6			
	55.6			
	39.2	26.7	0.954	4450
5. Dark plains	83.9			
	55.5	14.3	0.745	4450
6. Andesine (fine)	84	--	1.112	11100
7. Andesine (fine)	50	--	0.948	11100
8. Basalt (fine)	50	--	0.863	11100
9. Basalt ash (coarse)	84	--	0.843	11100
10. Basalt ash (coarse)	50	--	0.489	11100

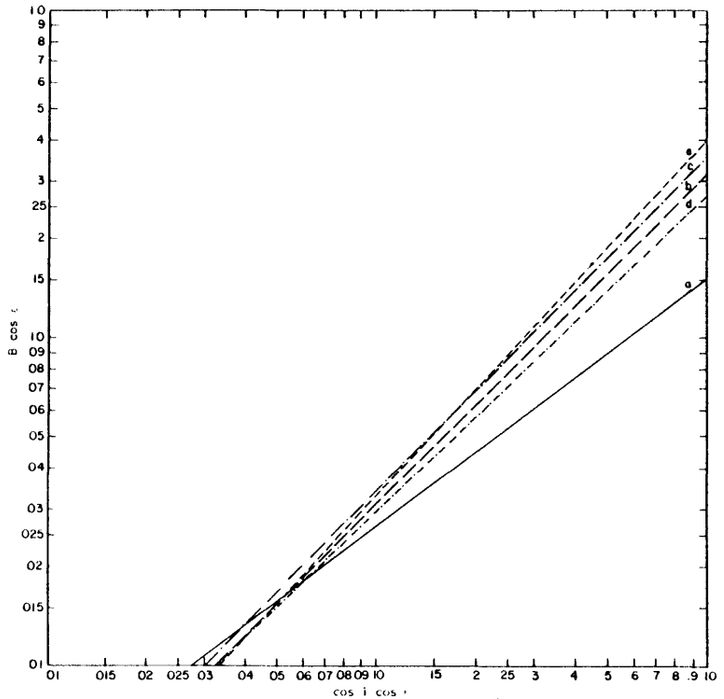

Figure 1. Minnaert plots of Martian infrared (4450 cm^{-1}) reflectivities for various geologic units
a. Dark plains (mainly Margaritifer Sinus)
b. Composite bright plains (Thymiamata, Aeyre, Deucalionis)
c. Pandorae Fretum
d. Eolian Plains (Eden-Thymiamata)
e. Hellas
x. Roughly hilly terrain with distinct drainages

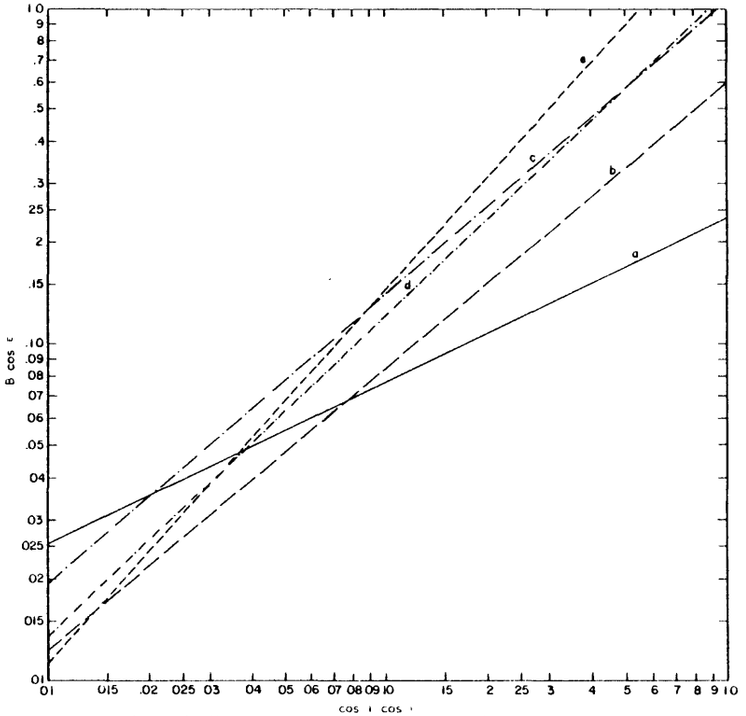

Figure 2. Minnaert plots of infrared (11,100 cm^{-1}) reflectivity of selected terrestrial materials
a. Basalt ash (coarse) 50° phase angle
b. Basalt ash (coarse) 84° phase angle
c. Basalt ash (fine) 84° phase angle
d. Andesine 50° phase angle
e. Andesine 84° phase angle

Root-mean-square slopes estimated from Doppler-spread and time-delay in the radar echos are an estimate of surface roughness at scale-lengths of 10 to 100 wavelength of the radar (38 to 380 cm for Haystack Radar). These rms slopes are approximately equivalent to the estimated algebraic standard deviations above and will be taken as equivalent later. Although such a procedure has inherent uncertainties, the sophistication of the analyses of radar data do not warrant closer correlations. For examples, some lunar results suggest that the radar scale-length may be larger than predicted and radar slopes are unidirectional (traverse slopes), whereas maximum components of slopes (landing slopes) are of interest to the spacecraft. Root-mean-square slopes for the landing case are about [illegible] times larger than those for the unidirectional or traverse case. In any event, roughness properly estimated by 3.8 cm radar should be reasonably close to the scale-length of the spacecraft.

Tolerances arising from the physical properties of the Martian surface materials must be viewed from two points of view: (1) the lander and (2) the sampler. For the lander to land, smooth cohesive surfaces are acceptable. If the cohesion is very low like lunar materials, and touchdown velocities are large, the Viking Lander may penetrate to its triangular base. The results of footpad penetration tests (Martin Marietta Corp., 1971; Clark, 1971) are shown on the third graph where it may be seen that the Viking spacecraft will penetrate more than 22 cm into a lunar nominal soil with a density near 1.36 g/cm3 if the velocity at touchdown is 3.48 m/sec, the pressure is 5 mb, and a three point landing is made. Here, no allowance has been made for gravitational effects which might cause penetration to be 10 percent greater. Estimated dielectric constants for basaltic granular materials are correlated with density on the upper abscissa. For a bulk density of 1.3 g/cm3 the dielectric constant is near 2.5. For nominal velocities, of 2.44 m/sec a lunar nominal soil with a dielectric consfant near 2.5 is quite acceptable. If the dielectric constant is near 2.0, penetration will be too great. It should be noted here that dielectric constants may be correlated with the bulk density of the surface materials, moisture content, and composition; the material may be cohesive or cohesionless. Dielectric constants are discussed further below.

TOPOGRAPHY OF THE MARTIAN SURFACE

Surfaces of Mars, like those of the Earth and Moon, are heterogeneous so that mapping at small and large scales may be used to delineate terrain units. Terrains on Mars may be grouped into six major groups at 1 to 25 million scale which have been previously described (Langley Research Center, 1972). They are:

A. Tablelands: (1) smooth, (2) lineated, (3) cratered, (4) ridged, and (5) patterned.
B. Plains: (1) smooth, (2) hummocky, (3) lineated, (4) patterned, (5) ridged, and (6) cratered.
C. Cratered terrain: (1) flat, (2) undivided, (3) patterned, (4) ridged, and (5) large craters.
D. Irregular terrain: (1) rugged, mountainous.
E. Canyonlands: (1) reticulate, (2) dendritic, (3) chaotic, and (4) flat.
F. Domes: (1) undivided.

FINE-SCALE TOPOGRAPHY AND NEAR-SURFACE MATERIALS OF MARS

By Henry J. Moore

The fine-scale topography and physical properties of the near-surface materials of Mars vary significantly from place to place. Variations are so extreme that the chances for a successful Viking Lander mission can be seriously reduced in certain regions. Three independent sources of information demonstrate the variable nature of topography and near-surface materials: (1) Mariner 9 (McCauley and others, 1972), (2) analysis of quasi-specular radar echos from the surface Mars (Rogers and others, 1970; and Pettengill, 1972, unpublished data), and (3) microwave radiometry of Mars from USSR's Mars 2 and 3 Orbiters (Basharinov and others, 1972). Such variations were also anticipated prior to Mariner 9 (Langley Research Center, 1970, Section II-C) and loess, sand deposits, lag gravels, and bare rock were expected on theoretical and experimental grounds (Sagan and Pollack, 1967; Rogers and others, 1970). Subsequent information substantiates pre-Mariner 9 expectations. Mariner 9 obtained images of fields of sand dunes, wind-swept plains, pedestal craters whose flanks probably represent coarse lag gravels, smooth, bland-appearing plains probably underlain by loess, and vast regions of deep dust deposits extending from the poles outward.

Additionally, Mariner 9 spectral instruments detected atmospheric dust, and the Martian surface was obscured by atmospheric dust early in the Mariner 9 mission. Implications of the above for the near-surface materials of Mars are clear--a wide range of physical properties of materials can occur. The implications for topography at the fine scale are also clear--smooth loessial plains, rough dune fields, rough blocky areas, and smooth to rough outcrops should be present on Mars.

As a result of variable surface and near-surface properties, several questions arise: (1) what tolerances in topography and near-surface properties are acceptable for the Viking Lander?, (2) where are the suitable landing areas on Mars and how may they be identified?, (3) where are the unsuitable landing areas on Mars and how may they be identified?, and (4) are the current Viking landing sites acceptable?

VIKING LANDER TOLERANCES

The Viking Lander must land safely and collect a sample in order to achieve its scientific goals. Surface slopes in excess of 19° at the scale-length of the spacecraft (or larger) are too steep. The surface materials must have enough strength so that the spacecraft does not penetrate and stroke more than about 20 cm. Rocks 10-15 cm across are excessively hazardous and may rupture the base of the spacecraft after leg stroking. Additionally, the surface sampler must collect a sample. Thus, a rock surface, a deep coarse gravel, and some cohesive materials are undesirable. Thus, for a complete Viking Lander success a rather narrow range of surfaces and underlying materials are desired.

In order to achieve a probability of success greater than 0.003 by virtue of slope, the algebraic standard deviation for a slope-frequency distribution at the scale-length of the spacecraft should be near 3.8° or less. This is shown in the accompanying two graphs (figs. 1 and 2), where slope-frequency distributions are assumed to be exponential in form, and the algebraic standard deviation is estimated as that value of slope including 68.26 percent of the sample. Then, the frequency of slopes 19° and larger represents the probability of failure and the frequency of slopes less than 19° represents the probability of success.

Some of these terrain units are clearly rougher than others at slope lengths near the resolution of the Mariner 9 A camera resolution (~1-2 km). Terrain units such as the mountainous, rugged irregular terrain and much of the Canyonlands appear so rough that they are unsuitable landing sites for Viking. Within any terrain unit, local areas and features, such as craters, channels, and sand dunes, exist which are rougher appearing than average while local areas which are smoother than average also exist.

Changes of surface roughness with decreasing slope length present a significant problem to the Viking Lander. Mariner 9 A-camera imagery shows many extensive rugged areas, such as Coprates Canyon and the rugged region at the southern edge of Isidis Planitia. For a landing ellipse about 100 km by 650 km, these areas are statistically rough at slope lengths of 1 km and will remain rough or become rougher at smaller slope lengths. B-frame camera images (~200 m resolution) of Mars are scattered but show that some apparently smooth areas on A-camera resolution appear much rougher at this higher resolution. A good example of this is illustrated by a dune field in a crater (Langley Research Center, 1972). Other areas appear smooth at both A and B frame resolutions. Thus, it appears that surface roughness of some areas increases at a different rate than in others. Such a result is found for Earth and the Moon (see for example, Howard and Tyler, 1972).

Surface roughness at slope lengths of 0.10 to 10 m is of critical importance to the Viking Lander. This is well below the resolution of the Mariner 9 B-frame camera (~200 m) which give only scattered coverage of the surface. Thus, it seems reasonable to explore other potential methods of estimating fine-scale surface roughness. Results of interpretations of terrestrial radar echos are considered below.

TERRESTRIAL RADAR ECHOS

Terrestrial-based radar echos offer a possible solution to the problem of fine-scale roughness on Mars, and may yield information on the nature of the near-surface materials. Although results to date for Mars are highly speculative and controversial, the historical background of results for the Moon indicates that interpretations of quasi-specular echos of terrestrial radar are valid. Such echos for Mars should be carefully studied and considered. Such a detailed, careful study by a team of radar astronomers under the direction of G. L. Tyler at Stanford University is currently in progress.

Estimates of lunar slopes and dielectric constants using terrestrial radar date back well before 1960 and precede spacecraft data such as Ranger (1964) and Surveyor (1966). These pre-mission estimates, which are confined to the central lunar disk because the Moon faces Earth, are in remarkable agreement with current results. For example, Pettengill and Henry (1962) argued that only 9 percent of the lunar surface was responsible for diffuse scattering and the remainder was specular and near normal incidence. Then from measured values of radar cross section they calculated relative dielectric constants near 2.8 to 3.0. Similar results were obtained by Evans (1962) who concluded average lunar slopes were near 1 to 10 (~5.7). Later lunar studies using the Hagfor's scattering law gave similar results for the central lunar disk: a rms slope of 7° to 9° and a dielectric constant near 2.8.

Results from the Apollo Bi-static Radar experiment are consistent with earlier results. Here, specular echos from various surfaces of the Moon are being sampled rather than the central disk. Tyler (1972) states:

> "Surface reflectivity shows marked wave length dependences. At 0.13 m reflectivity data are consistent with scattering from a uniform dielectric half-space with a dielectric constant near 3. At 1.16 m no such simple relationship holds and the data must be interpreted in terms of local variations in surface reflectivity, most likely associated with the depth of the regolith."
>
> "Root-mean-square slopes on the scale of 20 to 200 m in length vary between 1 and 8°. In the mare areas observed thus far, the 200 m rms slopes are roughly one-half those obtained at 20 m. In highland areas the 200 m and 20 m slopes are nearly equal, albeit they have markedly different slope frequency distribution."

Good correlation of Apollo 14 bi-static radar data on rms slopes with imagery are shown by Howard and Tyler (1972).

Studies of lunar fines returned by Apollo are difficult to interpret because the soil is disturbed. Gold and others (1970) found that dielectric constants of lunar samples of regolith agreed well with experimental data on terrestrial powders (Campbell and Ulrich, 1969). They obtained the following results, approximately:

Dielectric constant	Density g/cm^3
1.8	1.0
2.0	1.25
2.5	1.6
3.0	1.9
3.5	2.2

The density of the in situ lunar regolith is a problem since it is disturbed during collection. However, estimates of in situ densities for Apollo 15 range between 1.36 and 2.15 g/cm^3, and the average is near 1.7 g/cm^3. Thus, lunar surface data are in good agreement with the terrestrial-based radar and Apollo bi-static radar results.

Terrestrial-based radar estimates of rms slopes for the fine-scale topography of Mars are generally consistent with the expectations for any planetary surface. In particular, surface roughness at the fine-scale (slope lengths near 38 cm to 10 m) varies widely. Radar estimates of dielectric constants are also consistent with the expectations for a wind-swept planet. In particular, the porosity of surface materials would vary widely from dense rock surfaces to low density loess. Although analyses of the radar echos are controversial, it is clear that the radar reflectivity of Mars at both 3.8 cm and 70 cm wavelength varies markedly from place to place and that reflectivities of both Haystack and Goldstone radar vary in essentially the same way in magnitude and location.

There is also a general correlation between terrain units on Mars and the Haystack radar estimates of rms slopes (fig. 4). Ranges of averages of rms slopes have been plotted for the various terrain units. The averages clearly show that, on the fine-scale, visually rough terrain units at large slope lengths also appear rough to the radar (i.e. Canyonlands(Cl), Irregular terrain (Ir), Domes (Dc), and Craters (Cr)). Smooth tableland (Ts) which appears smooth in the imagery is also smooth appearing to the radar. Thus, there is a correlation between imagery and the radar.

Parts of some other terrain units have a substantial number of values of rms slope less than 3.8° and are acceptable for Viking, but other parts are too rough. Selection of landing sites in a terrain unit, for example, Smooth plains (Ps), may be too rough for Viking on a scale-length of a meter or so, and this scale-length is well below Mariner 9 B-camera resolution.

Some estimates of algebraic standard deviations for the Moon have been included in figure 4 for reference purposes. Additionally, more detailed breakdown of averaged rms slopes for various terrain units have appeared elsewhere (Langley Research Center, 1972).

Low estimates of dielectric constants are indicated for the Smooth plains (Ps) terrain unit whereas those of terrain units such as Cratered plains (Pc) and Cratered terrain (CTf, CT, CTp) are quite large. Low values less than 2.5 are probably undesirable for Viking and large ones higher than 3.5 could represent rocks and rocky areas. Thus, if these values are correct and Martian surface materials are dry, some areas are unsuitable for Viking, and landing sites must be selected with care.

Estimates of dielectric constants for the Moon and terrestrial laboratory measurements of dielectric constants have been included in figure 5 for reference purposes. More detailed averages of dielectric constants have appeared elsewhere (Langley Research Center, 1972).

LANDING SITES

As part of the landing site exercise, values of rms slopes and dielectric constants estimated by Haystack radar nearest the chosen landing sites were tabulated and averaged. These values are listed below (table I) where it is shown that only a few selected areas within various landing sites have suitable values of both rms slope and dielectric constant. Here rms slopes near 4 or less and dielectric constants from 3.5 to 2.5 are considered acceptable.

RUSSIA'S MICROWAVE RADIOMETER

Observed brightness temperatures due to planetary thermal emission in two orthogonal polarizations as a function of position on Mars were obtained by 3.4 cm wavelength radiometers aboard Mars 2 and 3 (Basharinov and others, 1972). Limited published results yield large variations of dielectric constants similar to those obtained by terrestrial radar and ranges of near 2 to 5 were obtained.

SUMMARY

The combined evidence from Mariner 9, terrestrial radar, and microwave radiometry indicates both the topography and properties of the Martian surface and near-surface materials vary widely from place to place.

Although radar results are preliminary and subject to controversy, the surface of Mars could present serious problems for the Viking Lander at most of the landing sites if the numbers are correct.

Current re-analyses of the terrestrial-based radar data, which are in progress, are an appropriate and desirable activity.

REFERENCES

Basharinov, A. E., Drozdowskaya, I. B., Egorev, S. T., Galaktionov, V. N., Kolosov, M. A., Krotikov, V. D., Kroupenio, M. N., Kuzmin, A. D., Lodygin, V. A., Malafeev, L. I., Omelchenko, E. I., Schuka, O. B., Shapirovskaya, N. Y., Shutka, A. M., Troitsky, V. S., and Vetukhnovskaya, Yu. N., 1972, Microwave radiometry of Mars from the Mars 2 and 3 Orbiters (Preliminary Results): Icarus, v. 17, p. 540-542.

Clark, L. V., 1971, Effect of ambient pressure on Viking Lander footpad penetration in nominal lunar soil: Memo to I. W. Ransay, Jr., dated Oct. 12, 1971, 11 p.

Evans, J. V., 1962, Radio echo studies of the Moon, in Kopal, Z., ed., Physics and Astronomy of the Moon: Academic Press, New York, p. 429-479.

Gold, T., Cambell, M. J., O'Leary, B. T., 1970, Optical and high-frequency electrical properties of the lunar sample: Science, v. 167, no. 3918, p. 707-709.

Howard, H. T., and Tyler, G. L., 1972, Bistatic-radar investigation: Apollo 15 Preliminary Science Report, NASA SP-290, sec. 23, p. 1-10.

Langley Research Center, 1970, Mars Engineering Model: Natl. Aeronautics and Space Admin., Langley Research Center, Viking Project Office.

Langley Research Center, 1972, Viking Data Analysis Team Report: Natl. Aeronautics and Space Admin., Langley Research Center, Viking Project Office, Viking 75 Project (Preliminary) Document M 75-144-0, 190 p., 8 maps.

Martin Marietta Corp., 1971, Footpad soil penetration tests, Part I, Data Summary: VER-188, 12 Nov. 1971, 24 p. plus figures.

McCauley, J. F., Carr, M. H., Cutts, J. A., Hartmann, W. K., Masursky, Harold, Milton, D. J., Sharp, R. P., and Wilhelms, D. E., 1972, Preliminary Mariner 9 report on the geology of Mars: Icarus, v. 17, no. 2, p. 289-327.

Pettingill, G. H., and Henry, J. C., 1962, Radar measurements of the lunar surface, in Kopal and Mikhailov, eds.: The Moon, Symposium 14 of IAU held at Pulkovo Obs. near Leningrad USSR, Dec. 1960, p. 519-525.

Rogers, A. E. E., Pettingill, G. H., Shapiro, I. I., Ash, M. E., and Counselman, C. C., 1970, Radar studies of Mars: Final Report, Lincoln Lab. M.I.T., Jan. 15, 1970, Contract NAS 9-7830, 79 p.

Sagan, C., and Pollack, J. B., 1967, A windblown dust model of Martian surface features and seasonal changes: Smithsonian Astrophysical Observatory Special Report 255, 44 p.

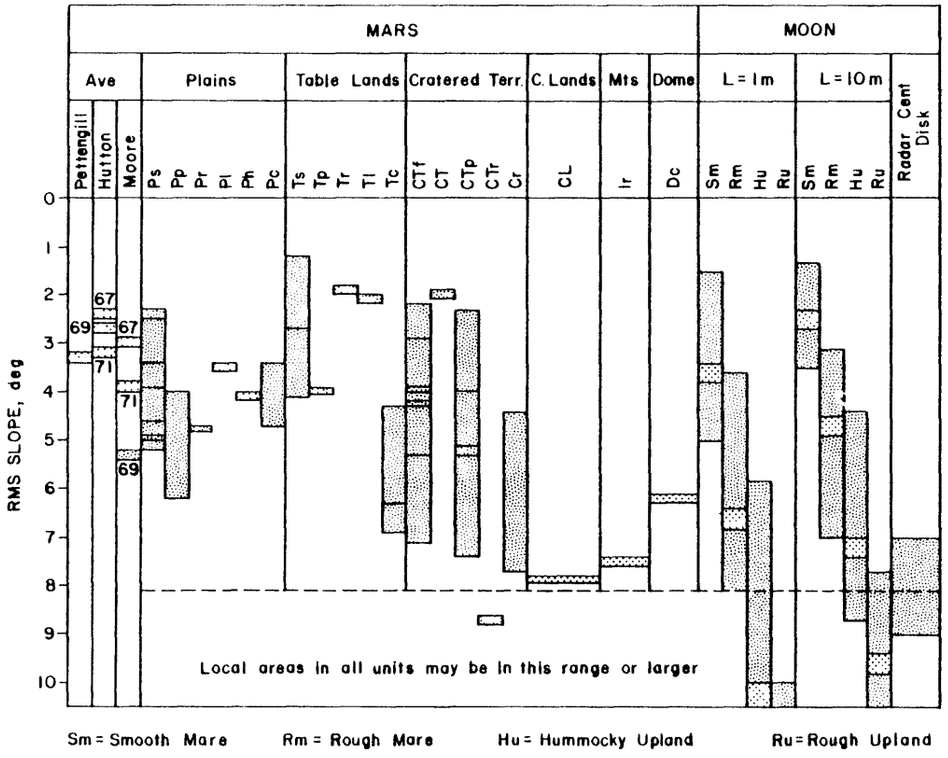

Figure 4. Correlation of Mars radar rms slope with the various Martian terrain units

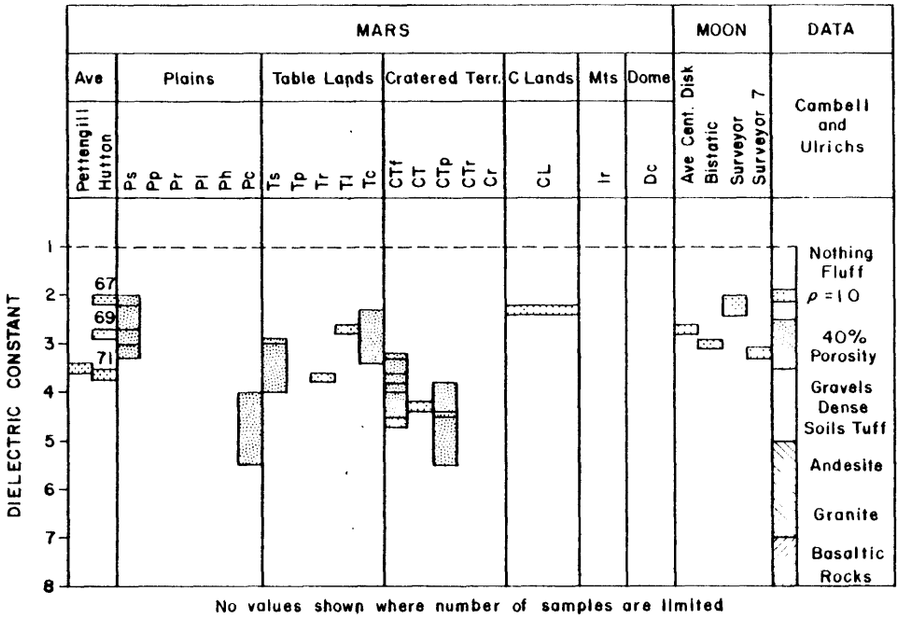

Figure 5. Correlation of Mars radar dielectric constant values with the various Martian terrain units

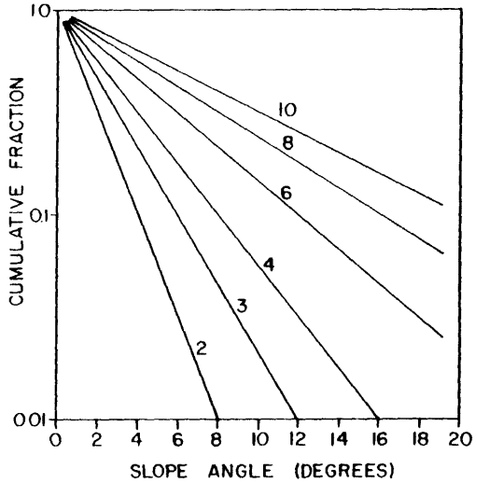

Figure 1. Slope-frequency distributions with estimated algebraic standard deviations of 2, 3, 4, 6, 8, and 10 degrees

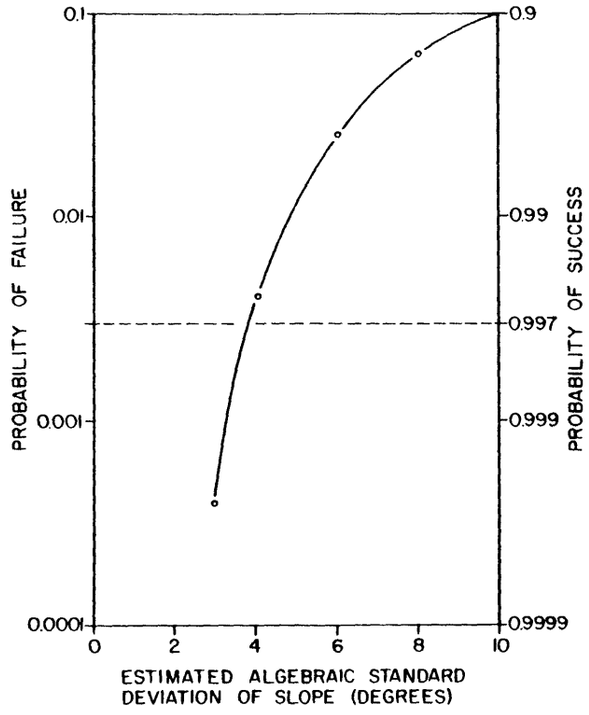

Figure 2. Probability of success or failure as a function of estimated algebraic standard deviation of slope

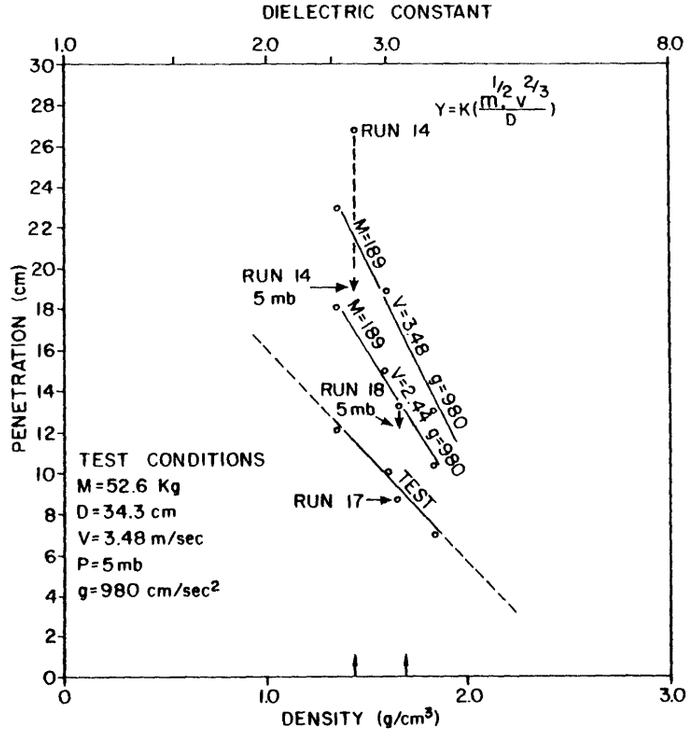

Figure 3. Penetration of Viking Lander in lunar nominal soil

Table I. Haystack radar estimates of Viking landing sites.

Site 1 21°N, 157°W Eumenides

Longitude (°W)	Latitude (°N)	Dielectric constant	rms slope
153.80	23.94	---	8.1°
153.97	20.74	1.6	0.8°
159.34	20.74	3.0	4.0°
161.34	19.82	1.8	0.8°
162.01	23.45	1.4	0.8°
Average		2.0	2.9°

Only acceptable value is 3.0 and 4.0 at 159.34°W ,20.7°N

Site 2 20°N, 77°W Lunae Palus

Longitude (°W)	Latitude (°N)	Dielectric constant	rms slope
71.94	23.93	1.7	2.7°
73.05	21.71	2.4	4.0°
88.84	20.72	1.8	2.7°
Average		2.0	3.1°

Only acceptable value is 2.4 and 4.0 at 73.05°W ,21.71°N

Site 3 19.5°N, 34°W Chryse

Longitude (°W)	Latitude (°N)	Dielectric constant	rms slope
30.20	21.70	1.9	1.3°
32.95	22.36	---	8.1°
35.49	21.70	---	8.1°
38.32	22.36	2.4	4.0°
38.76	24.00	---	8.1°
Average		2.2	5.9°

Only acceptable value is 2.4 and 4.0 at 38.32°W ,22.36°N

Site 4 88°N, 163°W Uraniae

Longitude (°W)	Latitude (°N)	Dielectric constant	rms slope
164.4	3.7	---	8.1°
164.6	6.6	1.7	1.3°
164.0	7.1	---	8.1°
160.5	9.5	---	8.1°
164.6	9.5	---	8.1°
166.2	9.7	1.7	0.8°
Average		1.7	5.8°

No acceptable values.

Site 5 14.7°N, 79.3°W Candor

Longitude (°W)	Latitude (°N)	Dielectric constant	rms slope
75.0	12.5	---	8.1°
75.8	11.5	---	8.1°
75.8	12.1	1.5	1.2°
77.0	11.2	---	8.1°
78.2	11.2	1.5	0.8°
78.5	12.0	---	8.1°
80.3	11.5	1.8	2.0°
81.2	10.8	2.3	4.0°
82.5	11.1	---	8.1°
82.8	11.1	3.1	4.0°
84.5	10.9	---	8.1°
Average		2.0	5.5°

Only acceptable value is 3.1 and 4.0 at 82.8°W, 11.1°N

Site 6 10°N, 269°W Nepenthes

Longitude (°W)	Latitude (°N)	Dielectric constant	rms slope
265.2	8.0	---	8.1°
265.8	9.5	---	8.1°
267.3	7.2	---	8.1°
268.0	11.9	4.1	4.0°
268.1	12.0	4.0	4.0°
269.6	7.9	---	8.1°
271.7	7.1	---	8.1°
272.3	11.9	3.5	4.0°
272.8	9.6	1.9	1.6°
274.0	7.9	---	8.1°
Average		3.4	6.2°

Only acceptable value is 3.5 and 4.0 at 272.3°W ,11.9°N

Site 7 2°S, 148°W Amazonis

No radar estimates in 2°S latitude band.

Site 8 2°S, 186°W Zephyria

No radar estimates in this latitude band.

Site 9 9°S, 144°W Memnonia

Average values nearest radar estimates (139°W to 149°W along 15°S) are 2.3 for dielectric constant and 1.9° for rms slope. Ten of thirty-five values of dielectric constant are 2.4 to 3.6. Five of thirty-six values of rms slope exceed 4.0°

Site 10 9°S, 178°W Appollinares

Nearby Haystack radar estimates are limited but nearest ones are:

Longitude (°W)	Latitude (°S)	Dielectric constant	rms slope
175	12	1.7	0.7
183	11	---	10.5

Site 11a 20°N, 253°W Amenthes

Longitude (°W)	Latitude (°N)	Dielectric constant	rms slope
232.82	22.96	1.5	0.8°
235.01	19.85	5.6	4.0°
238.43	22.97	1.8	0.8°
240.38	19.85	3.6	4.0°
244.04	22.97	5.6	4.0°
245.75	19.86	---	8.0°
246.10	23.47	4.6	2.6°
251.11	19.86	4.5	4.0°
251.95	23.47	3.3	1.3°
256.48	19.86	3.2	2.7°
257.80	23.47	5.2	4.0°
Average		3.9	3.3°

Best values are 3.3 and 1.3° at 251.95°W, 23.47°N and
3.2 and 2.7° at 256.48°W, 19.86°N

Site 12 16.0°S, 251.0°W "Dandelion"

Longitude (°W)	Latitude (°S)	Dielectric constant	rms slope
251.38	17.89	---	6.6°
252.39	17.89	3.9	4.7°
248.06	17.88	---	8.1°
251.68	17.88	---	10.5°
252.68	17.88	---	10.5°
248.17	17.87	6.4	5.7°
251.81	17.87	3.2	2.9°
252.79	17.87	3.7	3.3°
248.67	15.88	3.7	2.9°
251.38	15.88	---	6.6°
252.08	15.88	8.8	5.7°
249.26	15.78	---	6.6°
249.94	15.78	---	6.6°
252.65	15.78	5.0	4.7°
253.37	15.78	8.9	5.7°
250.34	15.69	6.7	4.0°
251.02	15.69	6.5	4.0°
253.74	15.69	8.2	4.7°
249.57	15.23	1.9	2.9°
252.74	15.23	1.3	1.0°
Average		5.2	5.4°

Acceptable value is 3.2 and 2.9° at 251.81°W, 17.87°S

CORRELATIONS OF SELECTED B FRAME PHOTOGRAPHS WITH HAYSTACK RADAR DATA, 1971
By Carroll A. Hodges

Acceptable limits:
Root mean square slope (rms) - less than 4.0±
Dielectric constant (DEC) more than 2.5 - less than 3.5±

Photo Number	DAS	Lat./Long. (Center)	Map unit	Avg. rms slope (individual values)	n*	Avg. DEC (individual values)	Comments
1	07110603	-18/119	lp	1.3 (1.4, 1.4, 1.4, 1.0)	4	2.7 (2.7, 2.8, 2.3, 2.8)	Acceptable; unit similar to that at sites 5, 9, and 7
2	07038573	-19/128	lp	1.7 (1.0, 1.0, 1.4, 2.0, 2.0, 1.4, 2.9)	7	3.2 (2.3, 2.3, 1.7, 4.3 4.2, 2.5, 5.2	Acceptable; unit similar to that at sites 5, 9, and 7
3	07110673	-14/117	lp	3.1 (1.4, 1.4, 2.9, 2.9, 2.9, 2.9, 1.4, 4.1, 10.5, 1.0, 3.3, 2.0)	12/11	2.1 (1.7, 2.8, 1.5, 2.4, 2.5, 1.6, 2.2, 3.0, 1.5, 2.0, 2.0)	Low DEC
4	09880579	-14/304	sp	3.5	24/22	2.5	Acceptable; plains in floor of large crater, probably similar to eolian and alluvial plains in site area
5	11656125	-19/142	lp & sp	2.1 (1.4, 2.9, 2.0, 2.0)	4	2.5 (1.7, 2.5, 3.1, 2.8)	Acceptable; similar to units at sites 5, 9, and 7
6	08873419	-14/76	lvp & rgp	2.0 - 3.3	18-21 / 18	2.5 - 2.7	Acceptable; similar to units at site 12
7	07038643	-14/126	sp	3.8 (6.6, 2.0, 2.9, 2.0, 2.0, 0.7, 10.5)	7/5	1.7 (1.9, 2.3, 1.7, 1.6, 1.2)	DEC too low, possibly as result of sub-resolution "micro-dunes"
8	08369349	-13/138	sp	3.5 (0.7, 2.9, 10.5, 10.5, 2.0, 6.6, 1.4, 1.0, 1.0, 1.4, 1.0)	11/8	1.6 (1.8, 1.8, 1.5, 1.6 1.6, 1.5, 1.5, 1.7)	DEC too low
9	06966683	-12/134	lp & sp	1.8 (2.9, 0.7, 0.7, 1.4, 2.9, 1.0, 2.9)	7	1.7 (2.6, 1.2, 1.7, 1.4, 2.0, 1.5, 1.8)	DEC too low

*Number of values averaged over 5 degree interval; rms/DEC, if different.

SUMMARY OF ELEVATION DATA ON CANDIDATE LANDING SITES

Site No.	Latitude	W.Long.	Prelim Elevation Contour Map	M 9	Haystack 1969	UVS	IRIS	Haystack 1971	Earth-based CO_2 and other (Wells)
1	21 N	157	-4.2	(-5.3)	-3.5	2.3			-2.9
2	20 N	77	-1.0		+1.0	4.3			-3.3
3	19.5 N	34	-4.8		-3.0	-1.7			-4.0
4	8 N	163	-4.0	(-4)	-2.8	0.9			-3.5
5	10 N	80	-1.1		+1.0	3.5	1.2		0.8
6	10 N	269	-4.0		-1.5	-1.6	-4.3		-2.5
7	2 S	148	-1.0			0.6	-1.1		-3.0
8	2 S	186	-3.7			-0.7	-1.9		-3.8
9	9 S	144	-0.2			1.6	0.0		-3.5
10	9 S	181	-3.0			0.1	-1.0	-2.6	-2.8

All elevations (except Haystack 1969) adjusted to be referenced to level where pressure is 4.8 mb.
Numbers in ( ) are data Kilore has said are not good.
Underlined digits are uncertain.